

国立病院機構鹿児島医療センター

研究業績集 第23号

令和4年4月～令和5年3月(2022年4月～2023年3月)

国立病院機構鹿児島医療センター

臨床研究部

はじめに

鹿児島医療センター研究業績集第23号の発刊にあたって

令和4年度(2022年度)研究業績集第23号を発刊する運びとなりました。平成11年(1999年)に始まり、23冊目となります。今回の論文数は総説を含めて38編(英文25編、和文13編)、学会報告107件(国3件、国内101件)でした。ほぼ昨年同様の実績ですが、学会発表は増加傾向で今後論文等が増加することを期待しています。

2023年5月に新型コロナウイルス感染症も5類となり、さまざまな活動が再開し、コロナ禍前に戻りつつあります。医学研究活動も、再開され、当院の職員も国内外の発表が始まってきました。喜ばしいことです。ただ新型コロナウイルス感染症の負の影響は大きく、そこから復活するにはもう少し時間が必要ですし、かなりのエネルギーを要することでしょう。ただ、医学の未解決なことはコロナ感染症とは無関係ですので、今まで温めてきた、自分の研究を発表し、論文作成まで行ってもらいたいものです。

現在若者の知的欲求が低下している印象も受けます。コロナ感染症や働き方改革でより拍車がかかったようにも見受けられます。些細な事でも疑問に感じたことをまずは調べてみてはどうでしょうか。単に日常の臨床に追われるだけの生活では、何か物足りなさを感じます。その隙間を埋める一つ的手段として研究があると思っています。眼の前の現象を観察し、疑問を抱き、極めたいと言うこだわりを持つことが、研究のきっかけになるでしょう。さらに極めていくとますます研究に対する面白みや喜びが生まれてくると思っています。

鹿児島医療センターの研究部門が新型コロナウイルス感染症以前にも優る活動を行う事を期待したいと思います。若手のこだわりを期待します。小さなことに感動し、大きな成功を収めてもらいたいと思います。

独立行政法人国立病院機構鹿児島医療センター

田中康博

目次

はじめに

1. 臨床研究部の組織概要	1
2. 臨床研究と治験	
① 臨床研究	4
② 治験実績	11
3. 業績報告	
① 英文原著論文等	15
② 和文原著・著書等	18
③ 学会発表	20
④ 研究会	29
⑤ 学術講演会	30
4. 論文	34

1. 臨床研究部の組織概要

1. 名称・所在地

独立行政法人国立病院機構鹿児島医療センター臨床研究部

鹿児島県鹿児島市城山町8-1

2. 沿革

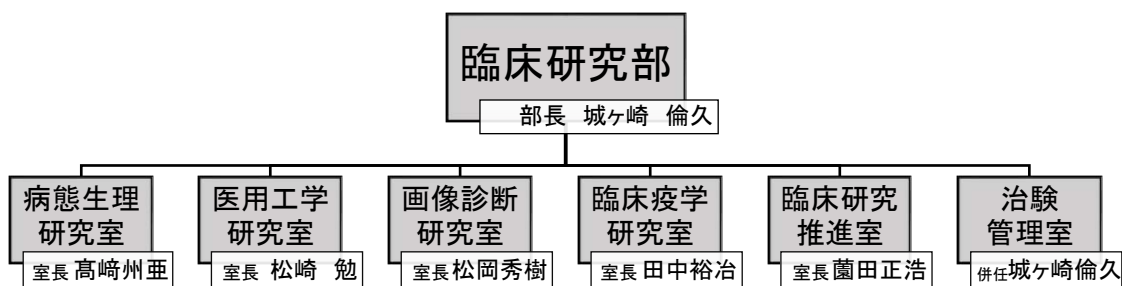
臨床研究部は1999年10月に設置されました。当初は病態生理研究室、医用工学研究室、画像診断研究室、臨床疫学研究室、治療評価研究室の5室で運営されていましたが、2007年に治療評価研究室を臨床研究推進室と名称変更を行い、さらに2013年からは治験管理室を加え、現在1部6室で活動しています。2006年からは東病棟8階に臨床研究部・治験管理室がありましたが、2018年4月の通信病院機能移転に伴い、2017年11月に臨床研究部は旧更衣棟に、治験管理室は事務棟に移転しました。

3. 組織構成

臨床研究部長の総括のもとに以下の研究室を設置しています。

1. 病態生理研究室
2. 医用工学研究室
3. 画像診断研究室
4. 臨床疫学研究室
5. 臨床研究推進室
6. 治験管理室

令和2年度の臨床研究部の各室の体制は以下に示す通りです。



4. 鹿児島大学大学院医歯学総合研究科

当院は平成21年より、鹿児島大学の連携大学院となっており、先進医療学講座(連携講座)生理活性物質制御学を開講しています。

これまでに5人の学生が臨床研究部で研究を行い、鹿児島大学大学院医歯学総合研究科の大学院博士号を取得しました。

5. 臨床研究部の活動

1) 臨床研究

NHO 共同研究として自己免疫性疾患特異的 iPS 細胞を国立病院機構弘前病院に提供し、共同研究を行っています。

本部主導大規模臨床研究(EBM 研究)としては 5 件の課題に参加しています。内訳としては外科 2 件、血液内科 1 件、糖尿病・内分泌内科 1 件、循環器内科 1 件でした。

NHO ネットワーク研究にも積極的に参加しており 11 件の課題があります。内訳としては血液内科が 5 件、糖尿病・内分泌内科、外科、病理診断科、臨床研究部主導、歯科口腔外科、脳血管内科が各 1 件でした。

NHO が主導する研究以外でも、各診療科、コメディカル、看護部、看護学校で独自の研究が行われており、研究課題数は全部で 97 課題ありました。

2) 競争的研究費

日本学術振興会科学研究費を歯科口腔外科の中村先生が主任研究者として 1 件、分担研究者として 1 件獲得しています。

厚生労働省科学研究費を小児科が 2 件、日本医療開発研究機構研究費を皮膚腫瘍科・皮膚科が 3 件、脳血管内科外 1 件をいずれも分担研究者として獲得しています。

民間セクターからの寄付金は 6 件あり、心臓血管外科が 2 件、消化器内科、皮膚腫瘍科・皮膚科、不整脈治療科、放射線室が各 1 件でした。

3) 治験・製造販売後調査

2022 年度(令和 4 年度)は新規治験が 1 件ありました。継続契約の治験は第Ⅱ相が 2 件でした。そのうち医薬品の治験が 1 件、再生医療の治験が 1 件ありました。診療科の内訳としては脳血管内科が 2 件、循環器内科が 1 件でした。

2022 年度に終了した治験としては契約件数が 1 件であり、契約症例 4 件のうち実施症例が 4 件であり実施率としては 100%でした。

製造販売後調査については、今年度新規登録のあった課題が 17 件ありました。内訳としては脳血管内科が 4 件、血液内科が 3 件、循環器内科が 6 件、皮膚腫瘍科・皮膚科が 2 件、心臓血管外科、糖尿病・内分泌内科、臨床研究部が各々 1 件でした。

2022 年度の受託研究請求額は 1294 万円でした。

4) 倫理審査委員会・治験審査委員会・研究倫理教育

2022 年度に倫理審査委員会は 9 回、治験審査委員会は 12 回開催しました。両審査委員会の外部委員として、元南日本新聞の有川賢司先生と元小学校校長の江口恵子先生に引き続きご協力いただいています。

臨床研究を行う上での倫理教育について国立病院機構では臨床研究に関わる全ての職員に研究倫理教育 eラーニングプログラムである eAPRIN の受講を行っています。臨床研究部では鹿児島医療センターの eAPRIN の受講登録・管理・受講支援を行っています。今年度は 342 名が受講修了しました。

5)学会発表・論文発表（当院所属として機構本部が認めたもの）

学会発表については、国内学会が 104 題、国際学会が 3 題でした。論文については、英語論文は 25 編、そのうち当院職員が筆頭者になっている英文原著論文は 3 編でした。和文原著・総説は 13 編、そのうち当院職員が筆頭者になっているものは 12 編でした。

<業績発表、独自研究>

WoS／PubMed 掲載英文論文		
英文原著論文(筆頭筆者)	3	本
英文原著論文(筆頭筆者以外)	15	本
英文原著論文以外(筆頭筆者)	3	本
英文原著論文以外(筆頭筆者以外)	4	本
和文原著論文等(筆頭筆者)	12	本
和文原著論文等(筆頭筆者以外)	1	本
国際学会発表(演者のみ)	3	回
国内学会発表(演者のみ) * 総会、地方会、シンポジウム、一般演題含む	104	回

6)日本学術振興会科学研究費申請

日本学術振興会科学研究費の申請にあたって「研究機関における公的研究費の管理・監査のガイドライン(実施基準)」に基づく「体制整備等自己評価チェックリスト」および、「研究活動における不正行為への対応等に関するガイドラインに基づく取組状況に係るチェックリスト」を提出する必要があります。臨床研究部では、毎年この2つのチェックリストを文部科学省に提出しています。また「体制整備等自己評価チェックリスト」については厚生労働省にも提出しています。

研究費の不正使用防止に向けた取り組みとして、公的研究費を使用されているすべての医師、事務職員、管理者に対してコンプライアンス教育のための動画を作成し、視聴後に誓約書を提出していただいています。

7)鹿児島市医報学術への寄稿

当院は毎年2回春と秋に鹿児島市医報の「学術」コーナーに寄稿しています。

今年度は第 61 巻 9 号に麻酔科の今林先生の「ED チューブの留置時にポータブル X 線撮影装置を自ら操作することで透視法に近い方法となり得た症例の経験」が、第 62 巻 3 号には救急科の田中先生の「急性期肺塞栓症に対する当院の治療選択の現状と将来の展望」が掲載されました。

2. 臨床研究と治験

① 臨床研究

(ア) NHO 指定臨床研究

種別	研究責任医師	研究課題名
NHO 共同研究	城ヶ崎倫久	自己炎症性疾患特異的 iPSC 細胞の培養ストックの作成及び分化誘導

(イ) EBM 研究

領域・課題番号	研究責任医師	研究課題名
特定臨床研究 H26-EBM(介入)-03	菰方輝夫	睥がん切除後の補助化学療法における S-1 単独療法と S-1 とメトホルミンの併用療法の非盲検ランダム化第 II 相比較試験 (ASMET 研究)
H26-遺伝子-02	大塚真紀	未治療多発性骨髄腫における遺伝子解析による治療感受性・予後予測因子の探索的研究(NGSMM 研究)
H26-遺伝子-03	郡山暢之	日本人の肥満症の発症と治療効果・抵抗性に関連する遺伝素因の探索 -オーダーメイド医療の確立-(G-FORCE 研究)
特定臨床研究 H27-EBM(介入)-01	塗木健介	免疫抑制患者に対する 13 価蛋白結合型肺炎球菌ワクチンと 23 価莢膜多糖体型肺炎球菌ワクチンの連続摂取と 23 価莢膜多糖体型肺炎球菌ワクチン単独摂取の有効性の比較 -二重盲検無作為化比較試験-(CPI Study)
H29-EBM(観察)-02	中島 均	我が国における左冠動脈主幹部インターベンションに対するコホート研究(LM-JANHO)

(ウ) NHO ネットワーク共同研究

領域	研究責任医師	研究課題名
H28-NHO(血液)-02	大塚真紀	成人初発未治療びまん性大細胞型 B 細胞リンパ腫における RCHOP 単独治療と放射線併用療法の治療成績、QOL、費用、費用対効果の多施設共同前向きコホート研究
H30-NHO(血液)-01	大塚真紀	高齢者移植非適応再発・難治末梢性 T 細胞リンパ腫に対する ゲムシタビン、デキサメサゾン、シスプラチン(GDP)療法+ロミデプシン療法の第 II 相試験(PTCL-GDPR)
H30-NHO(糖尿病)-01	郡山暢之	多面的管理達成者の糖尿病性腎臓病(DKD)予後改善効果評価法の確立と、効果予測のための非侵襲的指標の確立(DKDrem-2 研究)
H30-NHO(外科)-01	塗木健介	本邦における成人鼠経ヘルニア術後慢性疼痛の実態調査とそのリスク因子解析 -多施設共同前向きコホート研究- (ヘルニアスタディ)
H31-NHO(血液)-01	大塚真紀	未治療濾胞性リンパ腫における Obinutuzumab の治療成績、QOL、費用対効果、予後に関する多施設前向きコホート研究 (PEACE-FL)
H31-NHO(血液)-02	大塚真紀	B 細胞性急性リンパ性白血病におけるターゲットキャプチャー RNA-seq を用いたサブタイプ診断の実行可能性に関する研究

領域	研究責任医師	研究課題名
H31-NHO(多共)-02	野元三治	メトトレキサート(MTX)関連リンパ増殖性疾患の遺伝子変異プロファイルの解析
R2-NHO(心脳)-04	城ヶ崎倫久	がん化学療法関連心筋症の予測、早期発見、早期治療 ～心臓超音波検査 speckle tracking 法、タイチン truncating 変異の検出、尿中タイチン N フラグメント測定、血中心筋トロポニン I 高感度測定の比較検討～
R3-NHO(血液)-01	大塚真紀	レジストリーデータを利用した AYA 世代 DLBCL の臨床的・生物学的特性を明らかにする観察研究(NHO-DLBCL-AYA 研究)
R3-NHO(他研)-01	中村康典	DOAC 服用患者における抜歯の安全性の確立に関する研究:ガイドライン確立のための多施設共同前向き研究
R4-NHO(心脳)-01	松岡秀樹	急性期 BAD 型脳梗塞に対する抗血栓療法の種類と神経学的予後に関する前向き探索研究

(工) 競争的研究費等

I. 公費臨床試験

財源	課題名	研究者名	金額(円)
厚生労働省 厚生労働科学研究費補助金	小児から成人期発症遺伝性 QT 延長症候群の突然死予防に関する研究	分担研究者 吉永正夫	100,000
厚生労働省 厚生労働科学研究費補助金	特発性心筋症に関する調査研究	分担研究者 吉永正夫	300,000
日本医療研究開発機構研究費	進行性悪性黒色腫治療における抗 PD-1 抗体との TM5614 の安全性・有効性を検討する第 II 相試験	分担研究者 松下茂人	257,374
日本医療研究開発機構研究費	頭頸部基底細胞癌縮小マージン切除による新たな低侵襲標準治療の開発	分担研究者 松下茂人	1,300,000
日本医療研究開発機構研究費	爪部悪性黒色腫への指趾骨温存切除による新たな低侵襲標準治療の開発	分担研究者 松下茂人	650,000
日本医療研究開発機構研究費	ロメリジン塩酸塩による CADASIL 患者に対する脳虚血イベント再発抑制	分担研究者 松岡秀樹	520,000
文部科学省 科学研究費助成事業 基盤研究(C)	心臓弁膜症術後合併症制御に対する医学管理における系統的口腔管理の構築	主任研究者 中村康典	910,000
文部科学省 科学研究費助成事業 基盤研究(C)	心臓弁膜症術後合併症制御に対する医学管理における系統的口腔管理の構築	分担研究者 城ヶ崎 倫久	39,000
文部科学省 科学研究費助成事業 基盤研究(C)	心臓弁膜症術後合併症制御に対する医学管理における系統的口腔管理の構築	分担研究者 金城玉洋	39,000
文部科学省 科学研究費助成事業 基盤研究(C)	心臓弁膜症術後合併症制御に対する医学管理における系統的口腔管理の構築	分担研究者 片岡哲郎	39,000
文部科学省 科学研究費助成事業 基盤研究(C)	心臓弁膜症術後合併症制御に対する医学管理における系統的口腔管理の構築	分担研究者 平峯聖久	39,000

II. 民間セクターからの寄付金

課題名/依頼業者名	研究者名	金額(円)
肝細胞がんに対する肝動脈塞栓療法に関する研究	櫻井 一宏	100,000
高齢者の血管疾患に対する外科治療の研究	金城 玉洋	600,000
wound hygiene コンセプトに基づいた創傷ケア下での筋線維芽細胞の形態ダイナミクスとアウトカム解析	松下 茂人	200,000
201T1 心筋シンチにおける心筋外集積抑制手法の検討	宮島 隆一	500,000
教育研究の助成	塗木 健介	100,000
教育研究の助成	金城 玉洋	100,000

(オ) 臨床研究課題

	研究内容・課題名	部署・研究者名
1	深部静脈血栓症及び肺血栓症の治療及び再発抑制に対するリバー口キサパンの有効性及び安全性に関する登録観察研究(Jxactly Study)	第1循環器内科 中島 均
2	大動脈瘤/大動脈解離患者の実態調査および予後に関する前向き観察研究	第1循環器内科 中島 均
3	動脈硬化を基盤とした虚血性心臓病における新規血液マーカーの確立	第1循環器内科 中島 均
4	2 管球 CT を用いた冠動脈狭窄、心筋虚血、心筋線維化の総合的評価に関する多施設研究(AMPLIFIED)	第1循環器内科 中島 均
5	エベロリムス溶出性コバルトクロムステント(CoCr-EES[XIENCE])留置後のDAPT 投与期間を1か月に短縮することの安全性を評価する多施設前向きオープンラベル無作為化比較試験(ShorT and Optimal duration of Dual AntiPlatelet Therapy study-2(STOPDAPT-2))	第1循環器内科 中島 均
6	実施臨床におけるエベロリムス溶出性ステント(XIENCE V™)とシロリムス溶出性ステント(CYPHER SELECTTM+ステント)の有効性及び安全性についての多施設前向き無作為化オープンラベル比較試験:長期追跡試験(RESET Extended Follow-up Study)	第1循環器内科 中島 均
7	高尿酸血症に対するキサテンオキシダーゼ阻害剤フェブキソスタットの血管障害予防効果に関する多施設共同ランダム化比較試験(PRIZE study)	第1循環器内科 中島 均
8	SGLT2 阻害薬による動脈硬化予防の多施設共同ランダム化比較試験(PROTECT)	第1循環器内科 中島 均
9	実地臨床におけるバイオリムス溶出性ステント(BES)とエベロリムス溶出性ステント(EES)の有効性及び安全性についての多施設前向き無作為化オープンラベル比較試験(NEXT)	第1循環器内科 中島 均
10	至適な血管内超音波ガイド経皮的冠動脈インターベンションの複雑性病変における臨床経過を評価する前向き観察研究(OPTIVUS)	第1循環器内科
11	破裂性腹部大動脈瘤に対する開腹手術とステントグラフト内挿術の治療選択に関する全国多施設観察研究	心臓血管外科 川津祥和
12	非弁膜症性心房細動とアテローム血栓症を合併する脳梗塞例の二次予防における最適な抗血栓療法に関する多施設共同ランダム化比較試験(Optimal Antithrombotic Therapy in Ischemic Stroke Patients with Non-Valvular Atrial Fibrillation and Atherothrombosis: ATIS-NVAF)	脳血管内科 松岡秀樹

	研究内容・課題名	部署・研究者名
13	虚血性脳卒中患者における脳微小出血進展への抗血栓薬関与に関する研究	脳血管内科 松岡秀樹
14	K-RESOLVE Network 研究	脳血管内科 松岡秀樹
15	機械的血栓回収療法による再開通後の脳循環時間と再灌流障害との関連についての研究	脳血管内科 濱田祐樹
16	レセプト等情報を用いた脳卒中・脳神経外科医療疫学調査(J-ASPECT study : Nationwide survey of Acute Stroke care capacity for Proper designation of Comprehensive stroke CenTer in Japan)	脳血管内科 松岡秀樹
17	血管モデルを用いた有効な血栓回収療法手技の確立に関する研究	脳血管内科 濱田祐樹
18	ロメリジン塩酸塩による CADASIL 患者に対する脳虚血イベント再発抑制	脳血管内科 松岡秀樹
19	急性期 BAD 型脳梗塞に対する抗血栓療法の種類と神経学的予後に関する前向き探索研究	脳血管内科 松岡秀樹
20	脳梗塞再発のリスク因子を有する急性期アテローム血栓性脳梗塞及びハイリスク TIA 患者を対象としたプラスグレルのクロピドグレルとの血小板凝集能の比較臨床研究	脳血管内科 松岡秀樹
21	くも膜下出血アウトカム評価ツールの日本語版開発(SAHOT-J)	脳神経外科 久保文克
22	脳卒中患者の長期予後追跡のための QOL データ収集システムの開発 (PROP-J)	脳神経外科 久保文克
23	Double-Layer Carotid Stent の治療	脳神経外科 久保文克
24	未破裂脳動脈瘤に対する脳血管内治療	脳神経外科 久保文克
25	特発性心筋症に関する調査研究	小児科 吉永正夫
26	小児から成人期発症遺伝性 QT 延長症候群の突然死予防に関する研究	小児科 吉永正夫
27	レジストリーデータを利用した AYA 世代 DLBCL の臨床的・生物学的特性を明らかにする観察研究	血液内科 大塚眞紀
28	未治療 CCR4 陽性高齢者 ATL に対するモガムリズマブ併用 CHOP-14 の第 II 相試験	血液内科 大塚眞紀
29	骨髄増殖性腫瘍の実態と遺伝子変異検索	血液内科 大塚眞紀
30	未治療濾胞性リンパ腫における Obinutuzumab の治療成績、QOL、費用対効果、予後に関する多施設前向きコホート研究	血液内科 大塚眞紀
31	B 細胞性急性リンパ性白血病におけるターゲットキャプチャー-RNA-seq を用いたサブタイプ診断の実行可能性に関する研究	血液内科 大塚眞紀
32	成人 T 細胞白血病リンパ腫における CCR4 遺伝子変異と予後の検討	血液内科 大塚眞紀
33	血小板減少を呈する患者における酵素測定法によるゴーシェ病スクリーニング	血液内科 大塚眞紀
34	免疫抑制患者を対象とした PCV13/PPSV23 と PPSV23 の予防効果の比較試験	外科 塗木健介

	研究内容・課題名	部署・研究者名
35	本邦における成人鼠径ヘルニア術後慢性疼痛の実態調査とそのリスク因子解析 -多施設共同前向きコホート研究-	外科 塗木健介
36	CIN に対するレーザー蒸散術の治療成績	婦人科 神尾真樹
37	婦人科悪性腫瘍に関連した脳血管障害の検討	婦人科 徳留明夫
38	PFAPA 症候群における口蓋扁桃摘出術の効果検討と他施設との連携	耳鼻咽喉科 伊藤小都子
39	頭頸部がん再発症例に対する光免疫療法の導入と効果判定について	耳鼻咽喉科 西元謙吾
40	Experience of radiotherapy during the nosocomial cluster of coronavirus disease-19 in a regional core hospital	放射線科 上山友子
41	放射線治療の治療効果評価法・合併症低減法	放射線科
42	オクトレオスキャン症例の解析	放射線科
43	骨転移のある前立腺癌に対する塩化ラジウム治療	放射線科
44	塩化ラジウム治療における MRI の評価	放射線科
45	ブルーリ潰瘍(M.ulcerans 感染症)における無痛性病態メカニズムの解明	病理診断科 後藤正道
46	呼吸上皮腺腫様過誤腫の病理学的特徴と疫学に関する研究	病理診断科 後藤正道
47	メトトレキサート(MTX)関連リンパ増殖性疾患の病態解明のための多施設共同研究 H28-NHO(多共)-02	病理診断科 野元三治
48	メトトレキサート(MTX)関連リンパ増殖性疾患の遺伝子変異プロファイルの解析 H31-NHO(多共)-02	病理診断科 野元三治
49	心臓弁膜症術後合併症制御に対する医学管理における系統的口腔管理の構築	歯科口腔外科 中村康典
50	摂食機能評価に基づいた栄養食事指導の有効性と体組成改善への影響の検討	歯科口腔外科 中村康典
51	爪部悪性黒色腫への指趾骨温存切除による新たな低侵襲標準治療の開発	皮膚腫瘍科・皮膚科 松下茂人
52	頭頸部基底細胞癌縮小マージン切除による新たな低侵襲標準治療の開発	皮膚腫瘍科・皮膚科 松下茂人
53	進行性悪性黒色腫治療における抗 PD-1 抗体との TM5614 の安全性・有効性を検討する第 II 相試験	皮膚腫瘍科・皮膚科 松下茂人
54	メラノサイト系の悪性腫瘍に関する角層解析の有用性	皮膚腫瘍科・皮膚科 松下茂人
55	wound hygiene コンセプトに基づいた創傷ケア下での筋線維芽細胞の形態ダイナミクスとアウトカム解析	皮膚腫瘍科・皮膚科 松下茂人
56	皮膚腫瘍における免疫応答解析に基づくがん免疫療法予測診断法の確立	皮膚腫瘍科・皮膚科 松下茂人
57	JCOG1309 病期 II 期および III 期皮膚悪性黒色腫に対するインターフェロン β 局所投与による術後補助療法のランダム化比較第 III 相試験	皮膚腫瘍科・皮膚科 松下茂人

	研究内容・課題名	部署・研究者名
58	JCOG1605: パクリタキセル既治療原発性皮膚血管肉腫に対するパゾパニブ療法の非ランダム化検証的試験	皮膚腫瘍科・皮膚科 松下茂人
59	ニボルマブ+イピリムマブで治療される悪性黒色腫患者における腸内細菌代謝産物の臨床的意義に関する前向き観察研究	皮膚腫瘍科・皮膚科 松下茂人
60	進行期悪性黒色腫疾患に対する術後補助療法後に関する観察研究	皮膚腫瘍科・皮膚科 松下茂人
61	粘膜炎/末端黒子型メラノーマにおけるニボルマブ+イピリムマブ併用療法の一次治療と抗 PD-1 抗体単剤療法の一次治療(無効後ニボルマブ+イピリムマブを含む)の効果に関する多施設共同後ろ向き研究	皮膚腫瘍科・皮膚科 松下茂人
62	結合組織性皮膚疾患における病態解明	皮膚腫瘍科・皮膚科 松下茂人
63	悪性黒色腫における免疫チェックポイント阻害薬効果に対する HLA CLASS II の影響	皮膚腫瘍科・皮膚科 松下茂人
64	完全奏効(CR)患者における抗 PD-1 抗体治療中止後の効果持続についての後方視的研究	皮膚腫瘍科・皮膚科 松下茂人
65	進行期悪性黒色腫に対するニボルマブ・イピリムマブ併用療法の効果についての後ろ向き観察研究	皮膚腫瘍科・皮膚科 松下茂人
66	皮膚疾患画像ナショナルデータベースの構築とAI活用診療支援システムの開発	皮膚腫瘍科・皮膚科 松下茂人
67	BRAF 陽性悪性黒色腫に対する BRAF・MEK 阻害薬および免疫チェックポイント阻害薬の臨床効果に関する多機関共同後ろ向き観察研究	皮膚腫瘍科・皮膚科 松下茂人
68	本邦における皮膚血管肉腫に対するタキサン系抗がん剤使用成績の検討: 多施設共同観察研究	皮膚腫瘍科・皮膚科 松下茂人
69	悪性黒色腫のリンパ節郭清範囲に関する多施設共同観察研究	皮膚腫瘍科・皮膚科 松下茂人
70	乳房外パジェット病に対する S-1・ドセタキセル併用療法の効果についての後ろ向き観察研究	皮膚腫瘍科・皮膚科 松下茂人
71	露光部(非粘膜炎/非末端黒子型)メラノーマにおけるニボルマブ+イピリムマブ併用療法の一次治療と抗 PD-1 抗体単剤療法の一次治療(無効後ニボルマブ+イピリムマブを含む)の効果に関する多施設共同後ろ向き研究	皮膚腫瘍科・皮膚科 松下茂人
72	超高齢者の有棘細胞癌の再発率に対する観察研究	皮膚腫瘍科・皮膚科 佐々木奈津子
73	基底細胞癌のスクリーニング効果に対する観察研究	皮膚腫瘍科・皮膚科 青木恵美
74	毛巣洞の外科的治療に関する多施設共同後ろ向き研究	皮膚腫瘍科・皮膚科 松下茂人
75	汗孔癌の予後および再発に関する観察研究	皮膚腫瘍科・皮膚科 松下茂人
76	NUT adnexal carcinoma ?	皮膚腫瘍科・皮膚科 佐々木奈津子
77	apocrine carcinoma with sebaceous differentiation の一例	皮膚腫瘍科・皮膚科 松下茂人
78	Cryo AF グローバルレジストリ研究	不整脈治療科 塗木徳人
79	カテーテルアブレーション症例全例登録プロジェクト(J-AB レジストリ)	不整脈治療科 塗木徳人

	研究内容・課題名	部署・研究者名
80	リード抜去症例の実態調査(J-LEX レジストリ)	不整脈治療科 塗木徳人
81	Micra Acute Performance (MAP) AV Japan Registry	不整脈治療科 塗木徳人
82	SARS-CoV-2 検査の評価研究	臨床検査科 梅橋功征
83	鼻腔拭い液及び唾液検体を用いた「ケミルミ SARS-CoV-2Ag」による SARS-CoV-2 感染の臨床性能の検証	臨床検査科 梅橋功征
84	TI 心筋血流シンチグラフィ検査における心外集積低減法の検討	診療放射線科 上野 凌
85	心筋血流 SPECT 検査と冠動脈 CT 検査を用いた Fusion ソフトウェアの開発	診療放射線科 宮島隆一
86	医療被ばく線量の実態調査と Japan DRLs 2020 との比較	診療放射線科 宮島隆一
87	冠動脈撮影プロトコルの被写体配置による線量変化についての基礎的検討	診療放射線科 安武翼
88	冠動脈撮影における寝台配置位置による撮影線量変化について	診療放射線科
89	経皮的カテーテル心筋焼灼術における被ばく線量の推移	診療放射線科 久木野豊
90	心臓カテーテル検査における線量最適化の取り組み	診療放射線科 下新原壱成
91	Driving Surf Protocol 導入後の栄養管理に対する看護師の意識と行動変容 ～適切な栄養管理を目指して～	東 5 階 田原えり奈
92	ハイパフォーマーなジェネラリスト看護師のワーエンゲージメントに影響する因子	看護師長 今吉弥生
93	当院看護師の自ら学ぶ意欲に関する一考察	副看護師長 川畑博美
94	クラスターが発生した病棟の看護師が看護師長に求める支援について	看護師長 中本 恵
95	看護学生の臨床判断能力を育むために効果的と感じる指導方法の検討	看護学校 石川志保
96	ARCS モデルを活用した学習活動による自己教育力と主体性への影響	看護学校 濱崎友実
97	看護学生の小児看護学実習経験が及ぼす倫理的感受性への影響	看護学校 澁谷幸子

② 治験実績

以下に 2022 年度の治験の実績を示す。

2022 年度(令和 4 年度)治験内容

2022.4～2023.3

	医薬品		医療機器		再生医療		合計
	新規契約	継続契約	新規契約	継続契約	新規契約	継続契約	
治験 第Ⅱ相	0(1)	1(1)	0(0)	0(0)	0(0)	1(1)	2(3)
治験 第Ⅲ相	1(0)	0(3)	0(0)	0(0)	0(0)	0(0)	1(3)
合計	1(1)	1(4)	0(0)	0(0)	0(0)	1(1)	3(6)

()内は昨年の実数

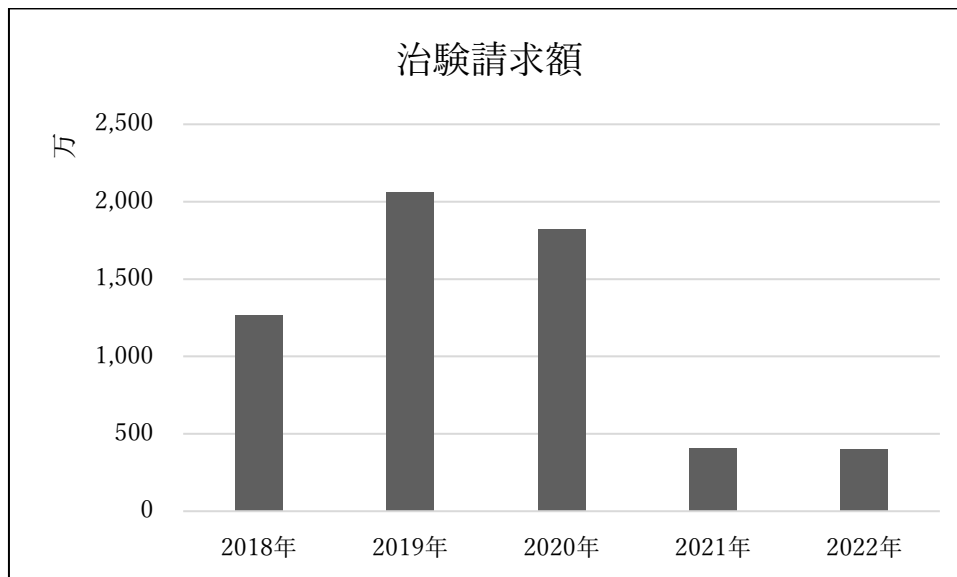
Ⅱ/Ⅲ相試験はⅡ相の項目に記載

実施率(2022 年度に終了した治験)

	契約件数(件)	契約症例・調査数	実施症例・調査票	実施率(%)
治験	1(4)	4(10)	4(10)	100(100)

()内は昨年の実数

治験請求額推移



治験の細目

研究課題名	研究依頼者	責任医師
Elezanumab の前期第Ⅱ相試験	Abbvie 合同会社	松岡秀樹
株式会社ヘリオスの依頼による脳梗塞患者を対象とした HLCM051 の第Ⅱ/Ⅲ相試験	株式会社ヘリオス	松岡秀樹
心房細動患者を対象とした治験	バイエル薬品株式会社	藺田正浩

(ア) 製造販売後調査

研究課題名	研究依頼者	責任医師
アデムパス錠 使用成績調査(慢性血栓塞栓性肺高血圧症)	バイエル薬品株式会社	蔡 榮鴻
ゼルボラフ錠 240mg 特定使用成績調査(全例調査)	中外製薬株式会社	松下茂人
ゼルボラフ錠 240mg 特定使用成績調査(全例調査)	中外製薬株式会社	魚住公治
献血グロベニン-I静注用 使用成績調査(再審査用)「スティーブンス・ジョンソン症候群及び中毒性表皮壊死症」	武田薬品工業株式会社	松下茂人
ビプリブ®点滴静注用 400 単位 使用成績調査	武田薬品工業株式会社	大塚真紀
ジャカビ®錠 5mg 特定使用成績調査(真性多血症)	ノバルティスファーマ株式会社	大塚真紀
ジャカビ®錠 5mg 特定使用成績調査(真性多血症)	ノバルティスファーマ株式会社	魚住公治
アイノフロー吸入用 800ppm 使用成績調査	エア・ウォーター株式会社	金城玉洋
ベンテイビス吸入液 10 µg 使用成績調査(肺動脈性肺高血圧症)	バイエル薬品株式会社	蔡 榮鴻
オプジーボ特定使用成績調査[再発又は難治性の古典的ホジキンリンパ腫]	小野薬品工業株式会社	大塚真紀
自家培養表皮ジェイスの先天性巨大色素性母斑に対する使用成績調査	(株)ジャパン・ティッシュ・エンジニアリング	松下茂人
サデルガカプセル 100mg 特定使用成績調査	サノフィ株式会社	大塚真紀
バベンチオ点滴静注 200mg 特定使用成績調査 (根治切除不能なメルケル細胞癌)	メルクバイオファーマ株式会社(IQVIA サービスーズジャパン株式会社)	松下茂人
ウプトラビ錠 0.2mg, 0.4mg 特定使用成績調査「長期使用に関する調査」	日本新薬株式会社	田中裕治
ベスボンサ®点滴静注用 1mg 特定使用成績調査	ファイザー株式会社	原口浩一
ラパリムスゲル 0.2% 一般使用成績調査(全例調査)-結節性硬化症に伴う皮膚病変-	ノーベルファーマ株式会社	松下茂人
レボレード錠 特定使用成績調査 (再生不良性貧血)	ノバルティスファーマ株式会社	大塚真紀
イストダックス®点滴静注用 10mg 使用成績調査「再発又は難治性の末梢性 T 細胞リンパ腫」	ブリistol・マイヤーズスクイブ株式会社	大塚真紀
トラディアンス配合錠 特定使用成績調査(長期使用に関する調査)	日本ベーリンガーインゲルハイム株式会社	郡山暢之

研究課題名	研究依頼者	責任医師
ビラフトビ®・メクトビ®併用療法 特定使用成績調査〔BRAF 遺伝子変異を有する根治切除不能な悪性黒色腫〕	小野薬品工業株式会社	松下茂人
ゾスパタ錠 一般使用成績調査〔プロトコル No.XSP001〕	アステラス製薬株式会社	大塚真紀
ヴァンフリタ錠 一般使用成績調査	第一三共株式会社	大塚真紀
レパーサ皮下注 特定使用成績調査(長期使用)	アムジェン株式会社	片岡哲郎
レパーサ皮下注 特定使用成績調査(長期使用)	アムジェン株式会社	東 健作
デファイテリオ静注 200mg 一般使用成績調査	日本新薬株式会社	大塚真紀
ジフォルタ®注射液 20 mg 使用成績調査	ムンディファーマ株式会社	大塚真紀
ベレキシブル®錠 特定 使用成績調査 再発又は難治性の中枢神経系原発リンパ腫(PCNSL)	小野薬品工業株式会社	魚住公治
サピエン 3(TAV in SAV)使用成績調査	エドワーズライフサイエンス株式会社	片岡哲郎
サピエン 3(TAV in SAV) 使用成績調査	エドワーズライフサイエンス株式会社	平峯聖久
コラン®特定使用成績調査(洞調律かつ投与開始時の安静時心拍数が75回/分以上の慢性心不全:ただし、β遮断薬を含む慢性心不全の標準的な治療を受けている患者に限る。)	小野薬品工業株式会社	中島 均
コラン® 特定使用成績調査 (洞調律かつ投与開始時の安静時心拍数が75回/分以上の慢性心不全:ただし、β遮断薬を含む慢性心不全の標準的な治療を受けている患者に限る。)	小野薬品工業株式会社	東 健作
ビンダケルカプセル 特定使用成績調査 ~トランスサイレチン型心アミロイドーシス患者に対する調査~ (プロトコル№B3461064)	ファイザー株式会社	藺田正浩
エドルミズ® 特定使用成績調査 [がん悪液質:非小細胞肺癌、胃癌、膵癌、大腸癌]	小野薬品工業株式会社	魚住公治
ポライビー®点滴静注用 30 mg、同 140 mg 一般使用成績調査(全例調査)-再発又は難治性のびまん性大細胞型 B 細胞リンパ腫-	中外製薬株式会社	大塚真紀
ポライビー®点滴静注用 30 mg、同 140 mg 一般使用成績調査(全例調査)-再発又は難治性のびまん性大細胞型 B 細胞リンパ腫-	中外製薬株式会社	魚住公治
Penumbra アスピレーションシステム 使用実態調査	株式会社メディコスヒラタ	濱田祐樹
ダラキューロ配合皮下注 ベルケイド注射用 3mg 全身性 AL アミロイドーシス患者を対象とした特定使用成績調査	ヤンセンファーマ株式会社	大塚真紀
ハイヤスタ錠®10mg 再発または難治性の成人 T 細胞白血病リンパ腫(ATL)患者における一般使用成績調査(全例調査)	Meiji Seika ファルマ株式会社	大塚真紀
ジャディアンズ®錠 特定使用成績調査(慢性心不全患者を対象とした長期使用に関する調査)	日本ベリンガーインゲルハイム株式会社	中島 均
ジャディアンズ®錠 特定使用成績調査(慢性心不全患者を対象とした長期使用に関する調査)	日本ベリンガーインゲルハイム株式会社	東 健作
オンデキサ®静注用 200mg 一般使用成績調査	アストラゼネカ株式会社	城ヶ崎倫久
エフィエント錠特定使用成績調査-脳梗塞発症リスクが高い虚血性脳血管障害患者-	第一三共株式会社	松岡秀樹
レプラミド®カプセル一般使用成績調査〔再発又は難治性の FL 及び MZL〕	ブリistol・マイヤーズスクイブ株式会社	大塚真紀
ハイヤスタ錠 10mg 再発又は難治性の末梢性 T 細胞リンパ腫 (PTCL)患者における一般使用成績調査(全例調査)	MeijiSeika ファルマ株式会社	大塚真紀
タケキャブ錠 副作用・感染症調査	大塚製薬株式会社	大野文也

研究課題名	研究依頼者	責任医師
メトレキサート錠 2mg「タナベ」 副作用・感染症報告	田辺三菱製薬株式会社	大渡五月
タフィンラーカプセル・メキニスト錠 「有害事象詳細調査」	ノバルティスファーマ株式会社	佐々木奈津子
ダラキューロ配合皮下注の副作用・ 感染症等詳細調査(ヤンセン 症例管理番号:J 22064667)	ヤンセンファーマ株式会社	鎌田勇平
ウブレチド錠 5mg 副作用・感染症調査	鳥居薬品株式会社	中藺省太
ソグルーヤ®皮下注 5mg, 10mg 特定使用成績調査 「ソグルーヤ®長期使用に関する特定使用成績調査」	ノボ ノルディスクファーマ株式会社	郡山暢之
「レイポー錠 100 mg」に関する副作用詳細調査	第一三共株式会社	山下悠亮
「リクシアナ OD 錠 15 mg」に関する副作用詳細調査	第一三共株式会社	濱田祐樹
フォシーガ錠 副作用・感染症詳細調査	アストラゼネカ株式会社	牧野美和
アキシャルックス点滴静注 250 mg一般使用成績調査(全例調査)切除 不能な局所進行又は局所再発の頭頸部癌	楽天メディカル株式会社	西元謙吾

3. 業績報告

① 英文原著論文等

※2022 年度中に Epub(online で公開)された論文も含まれます。また、実際に印刷された年度に再掲載しています。

■ 第1循環器内科

Michallek F, Nakamura S, Kurita T, Ota H, Nishimiya K, Ogawa R, Shizuka T, **Nakashima H**, Wang Y, Ito T, Sakuma H, Dewey M, Kitagawa K.

Fractal Analysis of Dynamic Stress CT-Perfusion Imaging for Detection of Hemodynamically Relevant Coronary Artery Disease.

JACC Cardiovasc Imaging. 2022; 15(9): 1591-1601. (Epub 2022 May 11)

■ 第2循環器内科・婦人科

Karakida N, Yanazume S, Tokudome A, **Sonoda M**, Kobayashi H.

Successful Treatment of a Life-Threatening Pulmonary Embolism Following Retroperitoneal Tumor Surgery.

Cureus. 2022; 14(11): e31501.

■ 不整脈治療科・小児科

Mori H, Sumitomo N, Tsutsui K, Fukunaga H, Hayashi H, Nakajima H, Muraji S, Nabeshima T, Kawano D, Ikeda Y, Asano S, Nitta J, Watanabe S, Hokosaki T, Sato S, Chisaka T, Higaki T, Nakajima T, Tamura S, Kaneko Y, Ikeda K, Okada A, Kobayashi H, Motoki H, Minamiguchi H, Imamura T, Shizuta S, Kawamura M, Munetsugu Y, Suzuki T, Murakami T, Horigome H, Wada T, Takamuro M, Ozawa J, Suzuki H, Izumi D, Otsuki S, Chinushi M, Kato K, Miura M, Maeda J, Fukunaga M, Kondo H, Takahashi N, Tobiume T, Morishima I, Kuraishi K, Nakamura K, Hayashi H, Suzuki H, Yoshida Y, Fukamizu S, Hojo R, **Nuruki N**, **Yoshinaga M**, Hayashi K, Fukaya H, Kishihara J, Kobayashi T, Kato R.

Efficacy of Subcutaneous implantable cardioverter-defibrillators in ≤18 year-old CHILDREN: SAVE-CHILDREN registry.

Int J Cardiol. 2023; 371: 204-210. (Epub 2022 Sep 8)

■ 脳血管内科

Hamada Y, Shigehisa A, Kanda Y, **Ikeda M**, **Takaguchi G**, **Matsuoka H**, Takashima H.

Enhancement of the Ivy Sign during an Ischemic Event in Moyamoya Disease.

Intern Med. 2023; 62(4): 617-621. (Epub 2022 Jul 29)

Hamada Y, **Ikeda M**, **Shimotakahara S**, **Tahara S**, **Onobuchi N**, **Kanda Y**, **Takaguchi G**, **Matsuoka H**.

Plaque Protrusion in a Patient with Left Common Carotid Artery Stenting after Radiation Therapy: A Case Report

J Neuroendovasc Ther.2022; 16(10): 503-509

Hamada Y, **Matsuoka H**, Takashima H.

Development of Ivy Sign and Infarction in the Lateral Part of the Hemisphere or the Middle Cerebral Artery Territory in Association with Steno-occlusive Involvement of the Posterior Cerebral Artery in Moyamoya Disease.

Intern Med. 2023; 62(11): 1703-1704. (Epub 2022 Oct 19)

■小児科

Ozawa J, Ohno S, Melgari D, Wang Q, Fukuyama M, Toyoda F, Makiyama T, **Yoshinaga M**, Suzuki H, Saitoh A, Ai T, Horie M.

Increased CaV1.2 late current by a CACNA1C p.R412M variant causes an atypical Timothy syndrome without syndactyly.

Sci Rep. 2022; 12(1): 18984.

Yoshinaga M, Takahashi H, Ito Y, Aoki M, Miyazaki A, Kubo T, Shinomiya M, Horigome H, Tokuda M, Lin L, Ogata H, Nagashima M.

Developmental trajectories at a high risk for childhood overweight/obesity.

Pediatr Int. 2023; 65(1): e15425.

Kamimura M, Nishikawa T, Takahashi Y, Nagahama J, Nakagawa S, **Ninomiya Y**, **Yoshinaga M**, Okamoto Y.

Anthracyclines for acute promyelocytic leukemia in a female with congenital long QT syndrome.

Pediatr Blood Cancer. 2023; e30323. Epub ahead of print.

Fukuyama M, Horie M, Aoki H, Ozawa J, Kato K, Sawayama Y, Tanaka-Mizuno S, Makiyama T, **Yoshinaga M**, Nakagawa Y, Ohno S.

School-based routine screenings of electrocardiograms for the diagnosis of long QT syndrome.

Europace. 2022; 24(9): 1496-1503.

■血液内科・腫瘍内科

Owatari S, Tokunaga M, Nakamura D, **Uozumi K**, Sagara Y, Nakamura H, **Haraguchi K**, Nakano N, Yoshimitsu M, Ito Y, Utsunomiya A, **Otsuka M**, **Hanada S**, Iwanaga M, Ishitsuka K.

A decrease in newly diagnosed patients with adult T-cell leukemia/lymphoma in Kagoshima, a highly endemic area of HTLV-1 in southwestern Japan.

Leuk Lymphoma. 2023; 64(4): 865-873. (Epub 2023 Feb 10)

Arai A, Yoshimitsu M, **Otsuka M**, Ito Y, Miyazono T, Nakano N, Obama K, Nakashima H, **Hanada S**, **Owatari S**, Nakamura D, Tokunaga M, Kamada Y, Utsunomiya A, **Haraguchi K**, Hayashida M, **Fujino S**, Odawara J, Tabuchi T, Suzuki S, Hamada H, Kawamoto Y, Uchida Y, Hachiman M, Ishitsuka K.

Identification of putative noncanonical driver mutations in patients with essential thrombocythemia.

Eur J Haematol. 2023; 110(6): 639-647. (Epub 2023 Mar 14)

■消化器内科

Kumagai K, Mawatari S, **Moriuchi A**, Oda K, Takikawa Y, Kato N, Oda S, Inoue K, Terai S, Genda T, Shimizu M, Sakaida I, Mochida S, Ido A.

Early-phase prothrombin time-international normalized ratio in acute liver injury indicates the timing of therapeutic intervention and predicts prognostic improvement.

Hepatol Res. 2023; 53(2): 160-171. (Epub 2022 Nov 10)

Mawatari S, Tamai T, Kumagai K, Saisyoji A, Muromachi K, Toyodome A, Taniyama O, Sakae H, Ijuin S, Tabu K, Oda K, Hiramine Y, **Moriuchi A**, **Sakurai K**, Kanmura S, Ido A.

Clinical Effect of Lenvatinib Re-Administration after Transcatheter Arterial Chemoembolization in Patients with Intermediate Stage Hepatocellular Carcinoma.

Cancers (Basel). 2022; 14(24): 6139.

■病理診断科・耳鼻咽喉科

Goto M, **Nishimoto K**, **Jougasaki Y**, **Matsuzaki T**, **Nomoto M**.

Respiratory epithelial adenomatoid hamartomas of the sinonasal tract: A histopathological analysis of 50 patients.

Pathol Int. 2022; 72(11): 541-549. (Epub 2022 Sep 14).

■腫瘍内科

Suzuki S, Hourai S, **Uozumi K**, Uchida Y, Yoshimitsu M, Miho H, Arima N, Ueno SI, Ishitsuka K. Gamma-secretase inhibitor does not induce cytotoxicity in adult T-cell leukemia cell lines despite NOTCH1 expression. *BMC Cancer*. 2022; 22(1): 1065.

■歯科口腔外科

Yoshimura T, Suzuki H, Takayama H, Higashi S, Hirano Y, Tezuka M, Ishida T, Ishihata K, Amitani M, Amitani H, Nishi Y, **Nakamura Y**, Imamura Y, Nozoe E, Inui A, Nakamura N. Prognostic value of inflammatory biomarkers in aged patients with oral squamous cell carcinoma. *Front Pharmacol*. 2022; 13: 996757.

Nishi Y, Seto K, Murakami M, Harada K, Ishii M, Kamashita Y, Kawamoto S, Hamano T, Yoshimura T, Kurono A, **Nakamura Y**, Nishimura M. Effects of Denture Cleaning Regimens on the Quantity of Candida on Dentures: A Cross-Sectional Survey on Nursing Home Residents. *Int J Environ Res Public Health*. 2022; 19(23): 15805.

■皮膚腫瘍科・皮膚科

Kamimura A, Nakamura Y, Takenouchi T, **Matsushita S**, Omodaka T, Yamamura K, Uchi H, Yoshikawa S, Yanagisawa H, Ito T, Kiyohara Y, Nakamura Y, Aoki M, Ishizuki S, Oashi K, Miyagawa T, Maeda T, Ogata D, Hatta N, Ohe S, Isei T, Takahashi A, Umeda Y, Yamaguchi B, Ishikawa M, Horimoto K, Fujisawa Y, Uehara J, Shibayama Y, Kiniwa Y, Kawahara Y, Matsuya T, Uhara H, Kato J, Nakamura Y, Murakami T, Namikawa K, Yoshino K, Funakoshi T, Takatsuka S, Matsui Y, Sasaki J, Koga H, Yokota K, Komori T, Fukushima S, Yamazaki N. Concordance in judgment of clinical borders of basal cell carcinomas in Japanese patients: A preliminary study of JCOG2005 (J-BASE-MARGIN). *J Dermatol*. 2022; 49(9): 837-844. (Epub 2022 May 5)

Kato J, Namikawa K, Uehara J, Nomura M, Nakamura Y, Uhara H, Uchi H, Yoshikawa S, Kiniwa Y, Nakamura Y, Miyagawa T, **Matsushita S**, Takenouchi T, Hatta N, Ohno F, Maeda T, Fukushima S, Yamazaki N. Prognoses of patients with melanoma who continue/discontinue anti-programmed death-1 therapy after achieving a complete response in a real-world setting: a multicentre retrospective study. *Br J Dermatol*. 2022; 187(4): 594-596. (Epub 2022 Jun 7)

Baba N, Kato H, Nakamura M, **Matsushita S**, **Aoki M**, Fujimoto N, Kato T, Iino S, Saito S, Yasuda M, Asai J, Ishikawa M, Yatsushiro H, Kawahara Y, Matsuya T, Araki R, Teramoto Y, Hasegawa M, Tokunaga T, Nakamura Y. Narrower clinical margin in high or very high-risk squamous cell carcinoma: a retrospective, multicenter study of 1,000 patients. *J Dtsch Dermatol Ges*. 2022; 20(8): 1088-1099. (Epub 2022 Aug 4)

Muto Y, Kambayashi Y, Kato H, Fukushima S, Ito T, Maekawa T, Fujisawa Y, Yoshino K, Uchi H, **Matsushita S**, Yamamoto Y, Amagai R, Ohuchi K, Hashimoto A, Fujimura T. Adjuvant Anti-PD-1 Antibody Therapy for Advanced Melanoma: A Multicentre Study of 78 Japanese Cases. *Acta Derm Venereol*. 2022; 102: 678. (Epub 2022 Jun 2)

Nakamura Y, Namikawa K, Kiniwa Y, Kato H, Yamasaki O, Yoshikawa S, Maekawa T, **Matsushita S**, Takenouchi T, Inozume T, Nakai Y, Fukushima S, Saito S, Otsuka A, Fujimoto N, Isei T, Baba N, Matsuya T, Tanaka R, Kaneko T, Onishi M, Kuwatsuka Y, Nagase K, Onuma T, Nomura M, Umeda Y, Yamazaki N.

Efficacy comparison between anti-PD-1 antibody monotherapy and anti-PD-1 plus anti-CTLA-4 combination therapy as first-line immunotherapy for advanced acral melanoma: A retrospective, multicenter study of 254 Japanese patients.

Eur J Cancer. 2022; 176: 78-87. (Epub 2022 Oct 1)

Sasaki-Saito N, Yamamura K, **Hitaka T**, **Hirano Y**, **Nishihara K**, **Aoki M**, **Matsushita S**. BRAF N581S and NRAS Q61R-mutated malignant melanoma and sensitivity to BRAF/MEK inhibitors.

J Dermatol. 2023; 50(1): e28-e29. (Epub 2022 Oct 11)

Fujimura T, Maekawa T, Kato H, Ito T, **Matsushita S**, Yoshino K, Fujisawa Y, Ishizuki S, Segawa K, Yamamoto J, Hashimoto A, Kambayashi Y, Asano Y.

Treatment for taxane-resistant cutaneous angiosarcoma: A multicenter study of 50 Japanese cases.

J Dermatol. 2023 Mar 20. Epub ahead of print.

Fujimura T, Furudate S, Maekawa T, Kato H, Ito T, **Matsushita S**, Yoshino K, Hashimoto A, Muto Y, Ohuchi K, Amagai R, Kambayashi Y, Fujisawa Y.

Cutaneous angiosarcoma treated with taxane-based chemoradiotherapy: A multicenter study of 90 Japanese cases.

Skin Health Dis.2022; 3(1): e180.

■ 救急科

Matsushita C, **Inatsu M**, **Tanaka H**.

3D-rendered computed tomography imaging support the diagnosis and strategic decision-making: a rare case of acute pulmonary thromboembolism presenting with thrombus straddling a patent foramen ovale.

Eur Heart J. 2023; 44(13): 1189.

■ 薬剤部

Fujimoto A, Koutake Y, Hisamatsu D, Ookubo N, Yabuuchi Y, Kamimura G, Kai T, Kozono A, Ootsu T, Suzuki H, Matsuo K, Kuwahara K, Oiwane Y, Nagata Y, **Tanimoto K**, Sato E, Suenaga M, Uehara T, Ikari A, Endo S, Hiraki Y, Kawamata Y.

Risk factors indicating immune-related adverse events with combination chemotherapy with immune checkpoint inhibitors and platinum agents in patients with non-small cell lung cancer: a multicenter retrospective study.

Cancer Immunol Immunother. 2023. Epub ahead of print.

② 和文原著・著書等

高崎州壱

ACHD(成人先天性心疾患)とフレイル
循環器系と健康長寿・フレイル対策: 40, 2022 年 10 月

川津祥和、伊藤由加、今田 涼、大野文也、山下雄史、永富修二、立石直毅、金城玉洋
心臓手術における陰圧切開創治療システム
胸部外科; 76(2): 99-103, 2023 年 2 月

大野文也、永富修二、寺園和哉、立石直毅、向原公介、金城玉洋
腹部人工血管置換術後に対麻痺を発症した腎動脈下腹部大動脈瘤の1例
日本血管外科学会雑誌; 31(6): 343-346

今田 涼、永富修二、金城玉洋、大野文也、立石直毅、川津祥和
ウシ心嚢弁を使用した僧帽弁置換術中にカフリークを認めた1例
胸部外科; 75(13): 1112-1116, 2022年12月

森内昭博
肝疾患診療における医療費助成制度「肝がん・重度肝硬変治療研究促進事業」について
鹿児島県内科医会報; (54):30-31, 2023年1月

高取寛之、塗木健介、小田原晃、菰方輝夫
脳塞栓症・心房内血栓症・直腸癌に対する集学的治療を行った1例
鹿児島市医報; 61(6): 51-52, 2022年6月

甲斐美帆、吉永浩介、牧瀬裕恵、徳留明夫、野元三治、神尾真樹
CA125が異常高値を呈した卵巣低異型度漿液性癌の一例
鹿児島地方部会雑誌; 31: 36-40

喜山敏志、井内寛之、伊東小都子、西元謙吾、松崎 勉、山下勝
黄色肉芽腫性唾液腺炎の5例
耳鼻咽喉科臨床; 115(4): 315-321, 2022年4月

安藤由実、喜山敏志、西元謙吾、松崎 勉
小児咬筋内血管腫例
耳鼻咽喉科臨床; 115(9): 805-809, 2022年9月

甲斐美帆、牧瀬裕恵、徳留明夫、野元三治、神尾真樹
CA125が異常高値を呈した卵巣低異型度漿液性癌の一例
鹿児島産科婦人科学会雑誌; 31: 36-40, 2023年3月

今林 徹、島内美奈、内田陽治、内田明子、東 亮子、砂永仁子、米谷 新、二木貴弘、下野謙慎、垣花泰之、山口英明、井手上淳一
EDチューブの留置時にポータブルX線撮影装置を自ら操作することで透視法に近い方法となり得た症例の経験
鹿児島市医報; 61(9): 22-27, 2022年9月

松下茂人
26 5.有棘細胞癌 6.基底細胞癌
皮膚疾患診療実践ガイド第3版: 674-680, 2022年5月

松下茂人
37 悪性腫瘍 A.基底細胞癌 有棘細胞癌
皮膚科診療 秘伝の書: 200-206, 2022年6月

松下茂人
悪性黒色腫の最前線 手術療法の実際と意義
皮膚科; 2(1): 26-34, 2022年7月

松下茂人
転移性乳房外パジェット病に対するS-1/ドセタキセル(DOC)併用療法の有効性:他施設後ろ向き研究
皮膚科ポータルサイト Dermatology Today; 2022年4月8日

田中秀樹

急性期肺塞栓症に対する当院の治療選択の現状と将来の展望 田中 秀樹・23
鹿児島市医報、62(3): 23-30, 2023 年 3 月

高城沙也香、鳥山陽子、江崎 瞳、松尾圭祐、永石浩貴、谷口 潤、尾之江剛樹

末期心不全患者に対するモルヒネの使用状況調査
日本病院薬剤師会雑誌; 58(10): 1157-1163, 2022 年 10 月

樋渡まこ、梅橋功征、山口 俊、西方菜穂子、伊藤葉子、藤野達也

新型コロナウイルス感染早期における迅速抗原検査の有用性
国臨協九州支部会雑誌; 23(1)(168 号): 1~8, 2023 年 1 月

宮島隆一

Hippocampal Avoidance During Whole-Brain Radiotherapy Plus Memantine for Patients with Brain Metastases:
Phase III Trial NRG Oncology CC001 (脳転移への全脳照射では海馬回避により認知障害を減らせる)
公益社団法人日本放射線技術学会放射線防護部会誌; 22(2): 34-37, 2022 年 10 月

南 大雅、宮島隆一、堀田竜也、森 康哲、増井飛沙人

整形外科領域の透視手技における術者手指被ばくの評価について
九州国立病院機構診療放射線技師会誌; 134:32-36, 2022 年 9 月

宮島隆一、井手口大地、日高智子、渡辺武美、立石哲士、森 政裕

医療被ばく線量の実態調査と Japan DRLs2020 との比較
九州国立病院機構診療放射線技師会誌; 135(2), 2023 年 1 月

野口久美子

3STEP で学ぶ! 疾患 Basic Study 急性白血病
Clinical Study; 43(14): 18-34, 2022 年 11 月

山田 巧

看護基礎教育における呼吸器系のフィジカルアセスメント教育へのプロジェクションマッピングの有効性
日本医療マネジメント学会雑誌; 23(1): 20-24, 2022 年 6 月

③ 学会発表

筆頭演者が鹿児島医療センターの職員

<国際学会>

Yoshinaga M

Genetic testing from the view of a pediatric cardiologist in the era of school-based screening programs.
IN, "Symposium 7 The Role of Genetic Testing for Inherited Arrhythmia Syndromes in the Era of Next
Generation Sequence
第 68 回日本不整脈心電学会、横浜、2022/6/9

Yoshinaga M

Outcome of Childhood Long QT Syndrome (LQTS) in the Era of Screening Programs and Alternative
Approaches to Predict Their Outcome.
第 87 回日本循環器学会学術集会, Virtual, 2023/3/11

Shigeto Matsushita

From resection to reconstruction: Surgical procedures for skin cancers in Japan
The 12th Asian Dermatological Congress. Web, 2022/8/4

<国内学会>

川畑深恰、高崎州亜、新地秀也、稲津真穂人、福崎 篤、福元大地、福永研吾、片岡哲郎、金城玉洋、中島 均
術中病理所見から高安動脈炎に伴う大動脈基部拡大による重症大動脈弁閉鎖不全症と診断した1例
第337回日本内科学会九州地方会、Web開催、2022年5月28日

福崎 篤、高崎州亜、川畑深恰、稲津真穂人、新地秀也、福元大地、福永研吾、片岡哲郎、中島 均、大石 充
人工血管置換術後の病理診断でIgG4関連大動脈周囲炎の診断がついた右総腸骨動脈瘤の1例
第132回日本循環器学会九州地方会、Web開催、2021年6月25日

稲津真穂人、片岡哲郎、川畑深恰、福崎 篤、新地秀也、福元大地、福永研吾、高崎州亜、永富脩二、金城玉洋、城ヶ崎倫久、中島 均、大石 充
卵円孔に管状静脈血栓が嵌頓した交通外傷後の1例
第70回日本心臓病学会学術集会、京都、2022年9月23日

片岡哲郎

複数の要因のためSTEMI再開通に遅れた教育的な症例
第8回Pan-Pacific Primary Angioplasty Conference 2022、Web開催、2022年11月12日

小牟禮大地、稲津真穂人、川畑深恰、福崎篤、沖野秀人、野元裕太郎、福永研吾、高崎州亜、片岡哲郎、宇佐美環、末吉和宜、城ヶ崎倫久、中島 均、大石 充
アテゾルズマブによる薬剤性の劇症型心筋炎をきたした一例
第133回日本循環器学会九州地方会、久留米、2022年12月3日

濱田祐樹、山下悠亮、池田め衣、高口 剛、松岡秀樹

放射線誘発性の左総頸動脈狭窄症の1例
第36回日本脳神経血管内治療学会九州地方会、福岡、2022年7月30日

濱田祐樹、山下悠亮、池田め衣、高口 剛、松岡秀樹

機械的血栓回収療法後に有効再開通を得た後、delayed white matter lesion が出現し、意識障害が遷延した79歳男性例
第237回日本神経学会九州地方会、佐賀、2022年9月17日

濱田祐樹、濱田祐樹、山下悠亮、池田め衣、高口 剛、松岡秀樹

中大脳動脈分枝(M2)閉塞に対する機械的血栓回収療法において、血管径は再開通率、臨床転帰に影響する
第38回日本脳血管内治療学会、大阪、2022年11月11日

松岡秀樹、岡村智教、桑原和代、杉山大典、竹川英宏、中山博文、峰松一夫

保健医療従事者による心房細動に関する市民啓発介入場所・方法と効果
第48回日本脳卒中学会学術集会、横浜、2023年3月16日

山下悠亮、濱田祐樹、池田め衣、高口 剛、松岡秀樹

機械的血栓回収療法後の症例における高蛋白・消化態流動食を用いた栄養療法の利益についての検討
第48回日本脳卒中学会学術集会、横浜、2023年3月16日

田平悠二、岩屋博道、原口昌明、井上和彦、森内昭博、櫻井一宏、高取寛之、塗木健介、菰方輝夫、野元三治

心窩部痛を契機に発見された胆管内乳頭状腫瘍(IPNB)の1例
第119回日本消化器病学会九州支部例会／第113回日本消化器内視鏡学会九州支部例会、佐賀、2022年6月25日

二宮由美子、田中裕治、吉永正夫

ホルター心電図はQT延長症候群の管理に有用か？
第58回日本小児循環器学会総会・学術集会、札幌、2022年7月21日

吉永正夫

学校心臓検診の心電図の重要性を見直す。シンポジウム11 心筋症における心電図の意義を見直す
第58回日本小児循環器学会総会・学術集会、札幌、2022年7月22日

田中裕治

BAS 後に右腸骨静脈閉塞となり骨盤内静脈瘤から無症候性肺梗塞を来した 18 歳男性の 1 例
第 58 回日本小児循環器学会総会・学術集会、札幌、2022 年 7 月 23 日

精松貴成、安留悠希、三宮由美子、田中裕治

バルプロ酸ナトリウム投与中に重度の血小板減少と凝固異常を来した女児
第 181 回日本小児科学会鹿児島地方会、鹿児島、2023 年 2 月 5 日

郡山暢之

糖尿病医療学 Update

第 65 回糖尿病学会年次学術集会、神戸、2022 年 5 月 14 日

牧野美和、郡山暢之、堂蘭直樹、児島奈弥、西尾善彦

食事依存性コルチゾール産生性片側副腎腺腫の一例
第 95 回日本内分泌学会学術総会、大分、2022 年 6 月 2 日

牧野美和、郡山暢之、堂蘭直樹、児島奈弥、西尾善彦

無痛性甲状腺炎によると推察された甲状腺クリーゼの一例
第 22 回日本内分泌学会九州支部学術集会、熊本、2022 年 9 月 3 日

牧野美和、郡山暢之、堂蘭直樹、児島奈弥、西尾善彦

SGLT 阻害薬により高血糖浸透圧症候群が修飾されケトアシドーシスを呈した一例
第 60 回日本糖尿病学会九州地方会、福岡、2022 年 10 月 7 日

児島奈弥、郡山暢之、當房卓也、牧野美和、西尾善彦

2 型糖尿病の経過中に劇症 1 型糖尿病を発症した 1 例
第 60 回日本糖尿病学会九州地方会、福岡、2022 年 10 月 7 日

當房卓也、郡山暢之、牧野美和、児島奈弥、西尾善彦

2 型糖尿病を合併した IgG4 関連自己免疫性膵炎に対してステロイド治療を行った 1 例
第 60 回日本糖尿病学会九州地方会、福岡、2022 年 10 月 7 日

甲斐美帆

CA125 が異常高値を呈した低異型度漿液性癌の一例
第 148 回鹿児島産科婦人科学会、鹿児島、2023 年 2 月 4 日

今林 徹、二木貴弘、下野謙慎、井手上淳一、垣花泰之

ED チューブの留置時にポータブル X 線撮影装置を自ら操作することで透視法に近い方法となり得た症例の経験
日本集中治療医学会第 6 回九州支部学術集会、鹿児島、2022 年 7 月 23 日

長野えりな、井手上淳一、桑水流絵梨奈、榮鶴ゆかり、吉浦 敬、西本謙吾、野元三治

副鼻腔原発の CUC-rearranged sarcoma の 1 例
第 196 回日本放射線学会九州地方会、久留米、2023 年 2 月 11 日

後藤正道、鈴木定彦

ハンセン病研究と日米医学協力計画
第 95 回日本ハンセン病学会、東京、2022 年 6 月 10 日

後藤正道

ハンセン病の神経病理(基礎委員会セッション「ハンセン病の基礎」)
第 26 回日本神経感染症学会総会・学術大会、鹿児島、2022 年 10 月 15 日

中村康典

鹿児島医療センターにおける周術期口腔機能管理の現状と課題
第 76 回国立総合病院医学会、熊本、2022 年 10 月 9 日

青木恵美、山村健太郎、坂本翔一、藁川葉子、日高太陽、平野 唯、松下茂人
2021年 鹿児島医療センター皮膚腫瘍科・皮膚科 死亡患者集計
第190回日本皮膚科学会鹿児島地方会、鹿児島、2022年4月10日

西原克彦、八束和樹、土居千晃、戸澤麻美、武藤 潤、佐山浩二
前腕、手背に多中心性に生じた類上皮肉腫の1例
第121回日本皮膚科学会総会、京都、2022年6月2-5日

青木恵美、平野 唯、西原克彦、佐々木奈津子、松下茂人
皮膚腫瘍・皮膚外科を学ぶ若手医師育成のための取り組み(その1.頭頸部の診かた)
第191回日本皮膚科学会鹿児島地方会、鹿児島、2022年7月10日

青木恵美
全身状態が不良な進行期メラノーマの1例ー最適な治療を提供するために私たちができることー
Virtual M-Top、Web、2022年7月29日

青木恵美、藁川葉子、山村健太郎、日高太陽、西原克彦、平野 唯、松下茂人
遊離眼板結膜移植の術後合併症の検討
第37回日本皮膚外科学会 総会・学術集会、川崎(Web)、2022年9月4日

平野 唯、井上明葉、青木恵美、西原克彦、日高太陽、松下茂人
臀部に生じた Cutaneous ciliated cyst の2例ー皮下腫瘤の臨床診断における超音波検査の有用性ー
第37回日本皮膚外科学会 総会・学術集会、川崎(Web)、2022年9月4日

佐々木奈津子、日高太陽、山村健太郎、平野 唯、青木恵美、松下茂人
BRAF N581s 変異を有する悪性黒色腫への BRAF/MEK 阻害薬の有効性
日本皮膚科学会第402回福岡地方会、北九州、2022年9月11日

西原克彦
脂漏性角化症から生じた有棘細胞癌の検討
愛媛地方会第75回学術大会、愛媛、2022年10月9日

青木恵美、山村健太郎、西原克彦、平野 唯、松下 茂人
基底細胞癌が多発する頻度と傾向についての検討
第74回日本皮膚科学会西部支部学術大会、久留米、2022年10月22日

平野 唯、青木恵美、井上明葉、杉野仁美、坂本翔一、小森崇矢、山村健太郎、松下茂人
先天性巨大色素細胞母斑に対しハイブリッド移植(自家培養表皮+自家網状植皮)を行った症例
第74回日本皮膚科学会西部支部学術大会、久留米、2022年10月22日

松下茂人
シンポジウム5「皮膚悪性腫瘍(に対する外科的手術の活用と意義)」メルケル細胞癌の治療戦略
第74回日本皮膚科学会西部支部学術大会、久留米(Web)、2022年10月23日

木村菜美子
鹿児島医療センターにおける頭頸部癌患者の放射線治療中の周術期口腔機能管理について
日本医療マネジメント学会第20回九州・山口連合大会、鹿児島、2022年11月5日

古庄正英
Incremental PD における個別の初期メニュー作成シミュレーションについて
第28回日本腹膜透析医学会学術集会・総会、岡山、2022年11月26日
4回日本近視学会総会、大阪、2022年5月14日

塗木徳人
発作性上室頻拍の体表面心電図と鑑別
心電学関連春季大会 2022、横浜(Web)、2022年4月9日

中藺省太

頻繁に繰り返す発作性上室性頻拍症により頻脈誘発性心筋症をきたした1例
第338回日本内科学会九州地方会、Web、2022年8月27日

西村尚芳、谷口 潤、尾之江剛樹、山形真一

薬剤師業務を薬剤助手へタスクシフトするための訓練の効果
第24回日本医療マネジメント学会学術総会、神戸、2022年7月8日

鳥山陽子、大原義正、谷口 潤、山形真一

免疫チェックポイント阻害剤による甲状腺機能障害に関する解析
第32回日本医療薬学会年会、高崎、2022年9月24日

濱崎翔平、谷本憲哉、谷口 潤、尾上剛樹、山形真一

入院前支援としての写真付き手術・検査前休薬説明シートの導入
第32回日本医療薬学会年会、高崎、2022年9月24日

馬場華菜、谷口 潤、尾上剛樹、山形真一

TC療法により発現したCIPNに対するミロガバリンとデュロキセチンの有効性及び安全性に関する直接比較
第76回国立総合病院医学会、熊本、2022年10月7日

佐多菜穂子、杉尾由希子、大窪典子、山形真一

入院中薬学ケアにより副作用を軽減した症例について病院-薬局間の薬剤師が連携することで患者満足度向上につながった一例
九州地区国立病院薬剤師会宮崎・鹿児島地区薬学研究会、始良、2022年10月22日

上西菜月、野崎佳代子、城戸隆宏、宮下恵美、岡村優樹、日野出勇次、渡辺秀明、西方菜穂子

消化器領域に転移をきたした悪性黒色腫の一症例
第71回日本医学検査学会、大阪(Web)、2022年5月21日

原田美里、宮崎明信、中釜美乃里、大迫亮子、時吉恵美、高山瑞希、渡辺秀明、西方菜穂子

経胸壁心エコー図検査にてとらえた中隔枝単独梗塞の1例
第71回日本医学検査学会、大阪(Web)、2022年5月21日

宮崎明信、大迫亮子、岡村優樹、山本理絵、日野出勇次、城戸隆宏、高山瑞樹、渡辺秀明、高崎州亜、西方菜穂子

経過観察中に徐々に増悪した僧帽弁形成術後再逆流の一症例
第47回日本超音波検査学会学術集会、東京、2022年5月28日

原田美里、宮崎明信、中釜美乃里、大迫亮子、時吉恵美、高山瑞樹、渡辺秀明、西方菜穂子

アルカプトン尿症に伴う重度大動脈弁狭窄症をきたした一症例
第47回日本超音波検査学会学術集会大会、東京、2022年5月29日

中釜美乃里、宮崎明信、岡村優樹、原田美里、城戸隆宏、高山瑞希、渡辺秀明、馬場善政、西方菜穂子

Coronary-LV fistula
第47回日本超音波検査学会学術集会大会、東京、2022年5月29日

江藤裕哉、赤峯未紀、吉野 歩、宮良聖佳、城ヶ崎泰代、後藤正道、野元三治

尿中に腫瘍細胞が出現した原発不明神経内分泌腫の一症例
第28回国立病医院臨床検査技師協会九州支部学会、Web開催、2022年7月9日

吉野 歩、橋本剛志、松元亜由美、本郷 剛、一瀬康浩、吉原正保

臨床検査システム内物品管理ソフト導入効果と有用性に関する報告
第76回国立総合病院医学会、熊本、2022年10月7日

宮崎明信

経胸壁心エコー図による冠動脈血流評価が有用であったたこぼ症候群に典型的な壁運動異常を来した一症例
第76回国立総合病院医学会、熊本、2022年10月8日

波野真伍

シンポジウム臨床血液 異形成の程度判定(MDS)についてどこまで表記できますか
第 56 回日臨技九州支部医学検査学会、久留米、2022 年 11 月 5 日

中釜美乃里、宮崎明信、原田美里、岡村優樹、久保裕子、日野出勇次、梅橋功征、西方菜穂子
経胸壁心エコー図検査が診断の一助となった左室心筋内転移性悪性リンパ腫の一症例
第 56 回日臨技九州支部医学検査学会、久留米、2022 年 11 月 5 日

吉野 歩、橋本剛志、松元亜由美、本郷剛、一瀬康浩、吉原正保、
臨床検査システム内物品管理ソフトの導入効果と有用性に関する報告
第 56 回日臨技九州支部医学検査学会、久留米、2022 年 11 月 6 日

日野出勇次、原田美里、高山瑞稀、中釜美乃里、岡村優樹、久保祐子、梅橋功征、西方菜穂子
経胸壁心エコー図検査時にリニアプローブが診断に役立つ 6 症例
第 18 回鹿児島県医学検査学会、鹿児島、2023 年 2 月 11 日

草原 智、岡村優樹、大迫亮子、久保祐子、日野出勇次、梅橋功征、西方菜穂子
胸痛消失後に特徴的な心電図波形を呈する Wellens 症候群の一症例
第 18 回鹿児島県医学検査学会、鹿児島、2023 年 2 月 11 日

山口 俊、樋渡まこ、吉野 歩、宮良聖佳、梅橋功征、西方菜穂子
COVID-19 における PCR 検査で長期間陽性が持続した一例
第 18 回鹿児島県医学検査学会、鹿児島、2023 年 2 月 11 日

山口 俊、樋渡まこ、吉野 歩、宮良聖佳、日野出勇次、久保祐子、梅橋功征、西方菜穂子
当院での感染性心内膜炎における疣腫形成部位別でみた検出菌とその背景についての検討
第 18 回鹿児島県医学検査学会、鹿児島、2023 年 2 月 11 日

樋渡まこ、山口 俊、吉野 歩、宮良聖佳、梅橋功征、西方菜穂子
新型コロナウイルス感染早期における迅速抗原検査の有用性
第 18 回鹿児島県医学検査学会、鹿児島、2023 年 2 月 11 日

下新原杏成、久木野豊、阿南恵吾、宮島隆一
心臓カテーテル検査における線量最適化の取り組み
九州国立病院機構診療放射線技師会総会並びに学術大会、福岡、2022 年 10 月 29 日

安武 翼、岩元優樹、阿南恵吾、宮島隆一
冠動脈撮影プロトコルの被写体配置による線量変化についての基礎的検討
九州国立病院機構診療放射線技師会総会並びに学術大会、福岡、2022 年 10 月 29 日

上野 凌、宮島隆一、阿南恵吾
TI 心筋血流シンチグラフィ検査における心外集積低減法の検討
九州国立病院機構診療放射線技師会総会並びに学術大会、福岡、2022 年 10 月 29 日

岩元優樹、安武 翼、阿南恵吾、宮島隆一
冠動脈 CT 撮影における寝台配置位置による断面内線量変化について
第 17 回九州放射線医療技術学術大会、福岡、2022 年 11 月 19 日

久木野豊、宮島隆一、下新原杏成、阿南恵吾
経皮的カテーテル心筋焼灼術における被ばく線量の推移
第 17 回九州放射線医療技術学術大会、福岡、2022 年 11 月 19 日

日高 優、淵脇陽一、宮久保和久、中村充良、倉見谷耕太、植園航太、戸田拓弥、鮫島航己、
溝口将平、宮之下誠
経カテーテル的大動脈弁置換術(TAVI)400症例で V-AECMO(PCPS)を導入した症例の検討
第 34 回日本心血管インターベンション治療学会九州・沖縄地方会、宮崎、2022 年 8 月 19 日

倉見谷耕太

洗浄方式の異なる自己血回収装置 2 機種による回収式自己輸血データの比較検討
第 47 回日本体外循環技術医学会大会、福岡、2022 年 11 月 19 日

井上世雅、上村真由美、矢元千恵、菊樂祐太、園田真理子、花田道代、中之蘭妙子、崎向幸江
残食調査から見えてきた課題

第 76 回国立総合病院医学会、熊本、2022 年 10 月 8 日

園田真理子、井上世雅、花田道代、中之蘭妙子、崎向幸江、濱田祐樹

脳梗塞後、在宅医療にむけて栄養介入を行った一例

第 18 回九州国立病院管理栄養士協議会栄養管理学会、Web 開催、2022 年 11 月 26 日

田中美香

閉鎖切開陰圧療法を使用した創傷管理の検討

第 31 回日本創傷オストミー失禁管理学会学術集会、Web 開催、2022 年 5 月 20-21 日

木下天翔、八代利香

COVID-19 禍に関する手術室看護師が抱える倫理的問題

第 15 回日本看護倫理学会、沼津、2022 年 5 月 29 日

田中 康、山口翔吾、岩正佳子、中城真佐美、藤崎佑貴子、後藤隆彦、池田智子

吸湿性繊維保護具を使用した場合のドレープ内の湿度温度および蒸れ感の変化

第 34 回日本心血管インターベーション治療学会九州沖縄地方会、宮崎、2022 年 8 月 20 日

井手口和絵、末吉 瞳、井上真菜美、櫻井綾香、西辻美佳子、深野久美

改良型腹水濾過濃縮再静注法(KM-CART)を繰り返す患者の在宅生活における苦痛

第 76 回国立病院総合医学会、熊本、2022 年 10 月 7 日

厚地美穂、永住圭裕、山下佑優

経カテーテル的大動脈弁置換術(TAVI)を受ける患者の術前、術後、退院 1 か月後のフレイル評価

第 76 回国立病院総合医学会、熊本、2022 年 10 月 7 日

溝口 隼、宮永千夏、奥野夏美、池山七海、藁部町子、福迫夏美、石原史絵

循環器疾患患者のアドバンス・ケア・プランニングの実施に関する病棟看護師の認識

第 76 回国立病院総合医学会、熊本市、2022 年 10 月 7 日

田代祐子、前田麻美、大迫朋子、栗脇千春、野中美里、山元ちひろ

看護補助者クリニカルラダー作成の取り組み

第 76 回国立病院総合医学会、熊本、2022 年 10 月 7 日

栗脇千春、山下健一郎、大塚真紀

院内 COVID19 現局発生事例と集団発生事例における感染拡大要因

第 76 回国立病院総合医学会、熊本、2022 年 10 月 7 日

松比良恵美、下畠彩花、橋口未由紀、藤崎夏子、原田恵子、清水優一、北原こゆき、今吉弥生、口石智秀

看護師のリハビリテーションに対する認識とその影響因子

第 76 回国立病院総合医学会、熊本市、2022 年 10 月 8 日

野口久美子、福迫直美、西岡恵子、池田智子、中本 恵、西辻美佳子、奥野夏美、松本尚子、中嶋洋子、村田淳子

看護師長会で取り組む「ウィズコロナの病床管理」

第 76 回国立病院総合医学会、熊本市、2022 年 10 月 8 日

砂坂志織、西 美咲、石原 薫、平 誠也、久保田詳子、加藤崇志

外回り看護師が手術中に個人防護具着用を徹底できていない要因

第 36 回日本手術看護学会年次大会、Web、2022 年 11 月 4 日

大迫朋子、松崎 勉、緒方義史

結果確認漏れ防止に向けたレポート開封通知システムの導入と評価

日本医療マネジメント学会第 20 回九州・山口連合大会、鹿児島、2022 年 11 月 4 日

大迫朋子、松崎 勉、緒方義史

入退院支援システム導入と評価

日本医療マネジメント学会第 20 回九州・山口連合大会、鹿児島、2022 年 11 月 4 日

神宮寺由佳、勝山英里、水元玲子、中本恵

入院前支援における業務内容の見直し～看護記録の効率化～

日本医療マネジメント学会第 20 回九州・山口連合大会、鹿児島、2022 年 11 月 4 日

新坂享子、伊藤由加、東 健作

当院の PICC チーム4年間の活動報告

日本医療マネジメント学会第 20 回九州・山口連合大会、鹿児島、2022 年 11 月 5 日

花田栄理、野口美幸、山元ちひろ、田中真美、奥野夏美

COVID-19 クリティカルパス導入を行って

日本医療マネジメント学会第 20 回九州・山口連合大会、鹿児島、2022 年 11 月 5 日

伊藤由加

看護師特定行為がチーム医療へ与える影響と効果

日本医療マネジメント学会第 20 回九州・山口連合大会、鹿児島、2022 年 11 月 5 日

永江明香里、折田紋奈、山下彩納、横手三喜子、福元京子

A急性期病院に勤務する看護師の職務満足度への実態調査－看護職の傾向と組織的介入の一考察－

第 53 回日本看護学会学術集会、幕張、2022 年 11 月 9 日

井手之上涼子、内藺真矢、井手之内涼子、尾辻真由美、徳永志保、福元京子

循環器外来における未受診患者の実態と要因の分析に関する研究

第 53 回日本看護学会学術集会、幕張、2022 年 11 月 9 日

新坂享子、出口喬一、吉留しずか、田中秀樹

救急科所属の診療看護師(NP)がショック状態の患者を受け持ち意思決定に関与した症例

第 8 回日本 NP 学会学術集会、愛知、2022 年 11 月 12 日

榊 詩織、塗木さや香、有馬光代、野口久美子、石川志保

骨髄異形成症候群の患者へエンド・オブ・ライフ・ディスカッションを行う看護師の構えに関する要因の検討

第 37 回日本がん看護学会、横浜・Web、2023 年 2 月 25 日

大野美穂、黄 在南

病棟看護師長の医療安全管理の実態に関する一考察

第 26 回日本看護管理学会学術集会、清瀬、2022 年 8 月 20 日

山田 巧、深野久美、大野美穂、他

九州内の国立病院機構病院 28 施設に勤務する卒後 1～5 年目看護職の看護実践能力～病床数の違いによる看護実践能力の比較～

第 76 回国立総合病院医学会、熊本、2022 年 10 月 8 日

深野久美、山田 巧、大野美穂、渡邊真弓、本松美和子、山中真弓、荒川直子、村上由紀、石原史絵、

山本真由美

コロナ禍における臨地実習経験と卒業時の看護実践能力の自信度の関係

第 76 回国立総合病院医学会、熊本、2022 年 10 月 7 日

星野睦美、山田 巧

看護学生の認知症高齢者に抱くイメージの老年看護学実習前後の比較

第 76 回国立総合病院医学会、熊本、2022 年 10 月 7 日

山田 巧

ICTを活用した看護学校と実習施設の連携

第76回国立総合病院医学会、熊本、2022年10月8日

山田 巧

看護学生の呼吸音聴診技術の評価

日本医療マネジメント学会第20回九州・山口連合大会、鹿児島、2022年11月5日

緒方創、徳永志保、久保裕佳子、迫田真唯、村田淳子

オンライン面会の取り組み

第76回国立総合病院医学会、熊本、2022年10月7日

筆頭演者が鹿児島医療センターの職員以外

<国内学会>

堤 育代、米野琢哉、上野博則、齊藤明生、澤村守夫、関口直宏、平林幸生、吉尾伸之、井上 仁、牧田雅典、吉田 功、日下輝俊、高月 浩、末 陽子、岩崎浩己、吉田真一郎、日高道弘、長倉祥一、大塚真紀、伊藤 琢生、黒田芳明、今中雄一、齋藤明子、飯田浩充、永井宏和

A real-world multicenter prospective cohort study in localized diffuse large B-cell lymphoma)

第84回日本血液学会学術集会、福岡(Web開催)、2022年10月14日

中村大輔、山本 花、島 晃大、田淵智久、林田真衣子、鎌田勇平、吉満 誠、石塚賢治

ATL-PI at the start of second line treatment can successfully predict the survival.

第84回日本血液学会学術集会、福岡(Web開催)、2022年10月14日

内田友一朗、吉満 誠、鎌田勇平、八幡美保、石 賢治

Inhibition of ATL cell proliferation by targeting the c-MYC/mTOR pathway

第84回日本血液学会学術集会、福岡(Web開催)、2022年10月15日

上野卓也、吉満 誠、山本 花、島 晃大、田淵智久、林田真衣子、鎌田勇平、中村大輔、石塚賢治

Late mortality after allogeneic transplantation for adult T-cell leukemia/lymphoma.

第84回日本血液学会学術集会、福岡(Web開催)、2022年10月15日

豊留亜衣、馬渡誠一、森内昭博、室町香織、玉井 努、今村也寸志、谷山央樹、伊集院翔、坂江 遥、楠 一晃、小田耕平、熊谷公太郎、井戸章雄

ペマフィブラートが肝機能に与える影響に関する検討

第26回日本肝臓学会大会、福岡、2022年10月27日

熊谷公太郎、森内昭博、井戸章雄

自己免疫性肝疾患の病態解明と治療戦略 自己免疫性肝炎における早期 PT-INR を用いた予後予測および治療介入時期の検討

第26回日本肝臓学会大会、福岡、2022年10月27日

熊谷公太郎、森内昭博、井戸章雄

急性・慢性肝不全のマネジメントー予防・診断・治療 急性肝障害における治療介入指標としての早期 PT-INR の意義

第58回日本肝臓学会総会、横浜、2022年6月3日

鈴木寛人、津曲恭一、阿部香澄、鶴賀叶女、渡嘉敷崇、山形真一

神経筋難病患者に対する薬学ケアの必要性に関するパイロットスタディ

第63回日本神経学会学術集会、東京、2022年5月18日

鈴木寛人、山形真一、阿部香澄、鶴賀叶女、渡嘉敷崇、津曲恭一

神経筋難病患者に対する薬学ケアの必要性に関する後方視的検証

第76回国立病院総合医学会、熊本、2022年10月7日

大山量平、坂田潤一、岩元優樹、長岡里江子、有迫哲朗
CAP 組成中のポータブル撮影における FPD 保護具の導入
国立病院機構医学会、熊本、2022 年 10 月 7 日

花田 悠、長野智大、中垣明浩、岩元優樹、長岡里江子、有迫哲朗
CT 透視における被ばく低減ツールの特性と最適設定の検討
国立病院機構医学会、熊本、2022 年 10 月 7 日

石原史絵、山田 巧
学内で実施した精神看護学実習のシミュレーションにおける看護学生の学び
第 76 回国立総合病院医学会、熊本、2022 年 10 月 7 日

丸山こずえ、阿南裕介、有元友範、吉住秀之
医療業務委託の業者光台寺の対策と課題
第 76 回国立総合病院医学会、熊本、2022 年 10 月 7 日

④ 研究会

山下悠亮

網膜中心動脈閉塞症を機に独歩で来院した前床突起部内頸動脈閉塞の 1 例
第 7 回 TOYOKO stroke center WEB CONFERENCE、Web 開催、2022 年 10 月 13 日

高取寛之、塗木健介、小田原晃、菰方輝夫

脳塞栓症・心房内血栓症・直腸癌に対する集学的治療を行った 1 例
令和 4 年度鹿児島市外科医会春季例会、鹿児島、2022 年 4 月 7 日

甲斐美帆、牧瀬裕恵、神尾正樹

再発を繰り返す子宮内膜ポリープの 1 例
第 1 回鹿児島県産婦人科手術懇話会、鹿児島、2022 年 9 月 1 日

伊東小都子

頸部皮膚に転移性易出血性腫瘍を生じた HPV 陽性中咽頭癌症例、
令和 4 年度鹿児島県地方部会総会、鹿児島、2022 年 6 月 25 日

城戸隆宏、野崎加代子

回盲部癌を起因に発症した腸重積の一例
第 319 回鹿児島県超音波医学研究会(腹部)、鹿児島、2022 年 7 月 26 日

原田美里

Impella
第 320 回鹿児島県超音波医学研究会、鹿児島、2022 年 8 月 31 日

岡村優樹

超音波検査が診断・治療に有用だった 2 症例
第 320 回鹿児島県超音波医学研究会、鹿児島、2022 年 8 月 31 日

岡村優樹

effusive CP の一症例
第 322 回鹿児島県超音波医学研究会秋季大会、鹿児島(Web)、2022 年 11 月 30 日

吉野 歩

細胞診 症例提示(乳腺領域)
鹿児島県臨床細胞学会第 102 回定例会、鹿児島(Web)、2022 年 12 月 15 日

久保祐子

TAVI 後の心エコー図評価

第 326 回鹿児島超音波医学研究会、鹿児島、2023 年 2 月 28 日

上野 凌、宮島隆一、阿南恵吾

心筋シンチ検査の画像解析の評価

九州国立病院機構診療放射線技師会第 4 回核医学セミナー、Web 開催、2022 年 5 月 25 日

野口久美子

クラスターを経験して学んだがん看護の課題と看護管理者、がん看護専門看護師としての取り組み

鹿児島がん看護研究会第 15 回年次大会総会、鹿児島、2022 年 10 月 2 日

⑤ 学術講演会

片岡哲郎

当院における経カテーテル的大動脈弁形成術に対するハートチームの役割

第 51 回鹿児島 CT 研究会、Web 開催、2022 年 5 月 19 日

金城玉洋

respect rather than RESECTION

Road to Expert、Web 開催、2022 年 6 月 4 日

松岡秀樹

脳卒中診療 Up to date～再発予防から後遺症管理まで～

日置市医師会学術講演会、Web 開催、2022 年 6 月 21 日

松岡秀樹

鹿児島におけるこれからの脳卒中診療

脳卒中トータルケア Web セミナー、Web 開催、2022 年 10 月 17 日

松岡秀樹

脳卒中の最新治療と予防対策～循環器病対策基本計画をふまえて～

令和 4 年度県循環器病対策研修会、鹿児島、2022 年 10 月 26 日

松岡秀樹

心原性脳塞栓症の最新治療～出血リスクを考慮した抗凝固療法も含めて～

脳卒中トータルケア Web セミナー、Web 開催、2022 年 11 月 15 日

松岡秀樹

脳卒中診療 Up to date～再発予防から後遺症管理まで～

Stroke Care Seminar、Web 開催、2022 年 10 月 26 日

高口 剛

脳卒中後神経障害性疼痛の話題

脳神経内科疾患治療 Web セミナー、Web 開催、2022 年 9 月 5 日

池田め衣

当院における取り組みとペマフィブラートの使用経験

KOWA Web Conference、Web 開催、2022 年 10 月 18 日

濱田祐樹

超高齢化社会における Total Stroke Care

脳卒中トータルケア Web セミナー、Web 開催、2022 年 10 月 28 日

濱田祐樹

当院における Embotrap の使用経験
CERENOVIOUS Webinar、Web 開催、2022 年 12 月 13 日

濱田祐樹

急性期脳梗塞治療の最前線
第一三共 Web セミナー、Web 開催、2022 年 9 月 13 日

濱田祐樹

最新の脳卒中診療とてんかん
脳卒中トータルケア Web セミナー、Web 開催、2023 年 2 月 9 日

久保文克

脳血管内治療の最近の話題
脳卒中連携 Web セミナー、鹿児島 (Web)、2023 年 2 月 22 日

森内昭博

当院における肝硬変診療の実状
第 5 回 鹿児島県リフキシマ講演会、Web 開催、2023 年 2 月 10 日

田中裕治

フォンタン手術後の循環動態とクスリ
鹿児島フォンタンの会、鹿児島、2022 年 5 月 13 日

田中裕治

小児科が伝えたい先天性心疾患
成人先天性心疾患に伴う肺高血圧セミナー in 鹿児島、鹿児島、2022 年 6 月 17 日

吉永正夫

(先天性)QT 延長症候群
第 58 回日本小児循環器学会 (第 19 回教育講演)、札幌、2022 年 7 月 23 日

吉永正夫

若年者の心肺蘇生事例と突然死予防～九州地区の院外心停止事例からわかること～
第 66 回九州ブロック学校保健・学校医大会、長崎、2022 年 7 月 30 日

吉永正夫

小児科からみた QT 延長症候群と学校心臓検診
岡山大学学術研究院医歯薬学域 循環器内科学 不整脈アカデミー2022～Plenary～、Web 開催、2022 年

郡山暢之

糖尿病医療学 UPDATE
糖尿病療養支援における患者中心ケアを考える、佐賀 (Web)、2022 年 6 月 24 日

郡山暢之

『SDM カスタマイズド鹿児島』～早期治療の重要性と治療標準化～
DiaMond Seminar in 鹿児島、鹿児島 (Web)、2022 年 7 月 13 日

郡山暢之

この患者さんはインスリン？それとも GLP1RA？
第 25 回糖尿病医療連携体制講習会 レクチャー③、鹿児島 (ハイブリッド)、2022 年 7 月 19 日

郡山暢之

糖尿病診療 Update ～医学と医療学の視点から～
鹿児島県栄養士会第 3 回リレー研修会、鹿児島 (Web)、2022 年 10 月 15 日

郡山暢之

糖尿病患者の足病変 ～病態生理から治療まで～
糖尿病重症化予防(フットケア)研修、鹿児島、2022年11月16日

郡山暢之

糖尿病医療学 ～糖尿病患者を支えるために～
糖尿病と不眠症セミナー、佐賀(ハイブリッド)、2022年12月12日

郡山暢之

新規経口血糖降下薬とその位置づけを考える
DUAL Seminar in 始良霧島 WEB 講演会、鹿児島(Web)、2023年1月27日

郡山暢之

新規経口血糖降下薬イメグリミンとその位置づけ
第6回臨床に「薬だつ」研修会、鹿児島(Web)、2023年2月22日

郡山暢之

SDM カスタマイズド鹿児島 New Version
第27回糖尿病医療連携体制講習会 レクチャー③、鹿児島、2023年3月14日

郡山暢之

SDM カスタマイズド鹿児島 New Version
Oral GLP-1 Seminar in KAGOSHIMA、鹿児島、2023年3月17日

田中裕治

大人になっていく心臓病の子どもたち～移行期から成人期への諸問題
全国心臓病の子どもを守る会鹿児島県支部講演会、鹿児島、2022年12月18日

松下茂人

ランチョンセミナー6 メラノーマ診療のアジアコラボレーション:これまでとこれから
第38回日本皮膚悪性腫瘍学会学術大会、弘前(Web)、2022年6月25日

松下茂人

地域で取り組む irAE マネジメント:地域がん診療連携拠点病院の立場で
TEAM2022、Web 開催、2022年7月23日

松下茂人

Knowledge? Experience?
Dermatology Expert Session vol.3、Web 開催、2022年9月17日

松下茂人

日本人に適した BRAF 遺伝子変異陽性メラノーマの治療を考える
日本皮膚科学会愛媛地方会 佐山浩二教授退職記念・藤澤康弘教授就任記念 第75回学術大会、松山、
2021年4月22日

松下茂人

シンポジウム5「皮膚悪性腫瘍(に対する外科的手術の活用と意義)」メルケル細胞癌の治療戦略
第74回日本皮膚科学会西部支部学術大会、久留米(Web)、2022年10月23日

松下茂人

皮膚がん診療のリアル～患者さん一人ひとりに最適な治療を考える～
Meet the Real、長崎、2022年12月8日

松下茂人

日本人に適したメラノーマの治療を考える
ここまで進んだ、メラノーマ診療(尾三会)、Web 開催、2022年12月13日

松下茂人

皮膚がん診療 Up-to Date: メラノーマ、基底細胞がん、有棘細胞がん、などなど
第 26 回 九州昭和大学・形成外科同門会学術集会、鹿児島、2023 年 2 月 4 日

梅橋功征

続新型コロナウイルスにおける各種測定法の位置付け
第 5 回イムノケミストリーオンラインセミナー、Web 開催、2022 年 12 月 2 日

日野出勇次

心血管エコー時に役立つ？神経筋エコーの基礎
第 49 回 TheEchoWEB Biweekly Conference、Web 開催、2022 年 4 月 13 日

日野出勇次

心エコー図検査時にリニアプローブが役立つ 6 症例
第 322 回鹿児島超音波医学研究会、Web 開催、2022 年 10 月 26 日

日野出勇次

始業時点検表を作ろう～前半～
第 1 回 都城地区生涯教育研修会、Web 開催、2022 年 11 月 2 日

日野出勇次

心エコー図検査時にリニアプローブが役立つ 6 症例
第 10 回九州 Echocardiography Conference、Web 開催、2022 年 11 月 3 日

日野出勇次

やっぱり難しい器質性僧帽弁逆流
第 56 回日臨技九州医学検査学会、Web 開催、2022 年 11 月 6 日

日野出勇次

始業時点検表を作ろう～後半+α～
第 2 回 都城地区生涯教育研修会、Web 開催、2023 年 1 月 19 日

日野出勇次

明日から始める神経筋超音波の基礎～症例も少々
日臨技九州支部卒後教育研修会(第 21 回臨床生理部門研修会)、Web 開催、2023 年 2 月 5 日

梅橋功征

国立研究開発法人日本医療研究開発機構(AMED)での活動、経験について
第 23 回 国臨協九州支部会新春学術講演会、Web 開催、2023 年 1 月 28 日

波野真伍

押さえておきたい血算データの見方・考え方
鹿児島県臨床検査技師会令和 4 年度第 1 回臨床血液部門研修会、Web 開催、2022 年 7 月 6 日

波野真伍

異形成の程度判定(MDS)についてどこまで表記できますか？
2022 年度日臨技九州支部医学検査学会(第 56 回)、久留米、2022 年 11 月 5 日

波野真伍

症例カンファレンス 症例 1
第 6 回日本検査血液学会九州支部学術集会、Web 開催、2022 年 11 月 19 日

宮島隆一

放射線部門における感染対策
令和 4 年度新規採用者研修 診療放射線技師分科会、Web 開催、2022 年 4 月 21 日

宮島隆一

負荷心筋シンチにおけるテクニカルサポート～False を無くすために！～
第 3 回大分核医学技術セミナー、大分、2023 年 2 月 18 日

4. 論文

当院所属で筆頭者として発表された論文を掲載します。

[CASE REPORT]

Enhancement of the Ivy Sign during an Ischemic Event in Moyamoya Disease

Yuki Hamada¹, Ayano Shigehisa¹, Yoshiki Kanda¹, Mei Ikeda¹, Go Takaguchi¹,
Hideki Matsuoka¹ and Hiroshi Takashima²

Abstract:

We herein report a case of increased and expanded ipsilateral ivy sign paralleling the expansion of cerebral infarction in a patient with moyamoya disease. A 67-year-old woman visited our hospital with symptoms of left hemiplegia, left homonymous hemianopia, and left unilateral spatial neglect. Magnetic resonance imaging of the head showed cerebral infarction in the right parietal lobe. In addition, ivy signs were evident on fluid-attenuated inversion recovery imaging. These findings were enhanced by the expansion of cerebral infarction and disappeared once the ischemia resolved, implying hemodynamic changes. As a result of continuing medical treatment without antithrombotic therapy, the patient obtained a good outcome. Treatment for moyamoya disease in the acute phase is considered to require complex knowledge of multiple factors, such as the anatomical background of the individual patient and the progression grade of ischemia.

Key words: moyamoya disease, ivy sign, ischemic event

(Intern Med 62: 617-621, 2023)

(DOI: 10.2169/internalmedicine.9326-22)

Introduction

Moyamoya disease is a progressive cerebrovascular disease that causes stenosis at the ends of the bilateral internal carotid arteries and formation of an abnormal vascular network (moyamoya blood vessels) at the bottom of the brain as collateral circulation (1-3). Occlusion of the main artery may cause ischemic events, while cerebral and intraventricular hemorrhaging may occur due to the development or disruption of the fragile collateral circulation. Characteristic linear hyperintensities along the sulcus on fluid-attenuated inversion recovery (FLAIR) imaging are called the leptomeningeal ivy sign and are considered to represent a slow retrograde flow in the engorged pial vasculature via leptomeningeal anastomosis (4).

We herein report a case of ipsilateral ivy sign that enhanced and expanded with expansion of the cerebral infarction in a patient with moyamoya disease.

Case Report

A 67-year-old woman presented to our hospital with the sudden onset of left hemiparesis (manual muscle testing: 4/5), left homonymous hemianopia, and left unilateral spatial neglect. She had a medical history of hypertension and type 2 diabetes mellitus. The patient was being treated by her family physician with amlodipine (5 mg/day) and metformin (1,000 mg/day), and home blood pressure was in the 120/80 mmHg range. Vital signs on admission were as follows: blood pressure, 155/82 mmHg; heart rate, 78 beats/min; temperature, 36.3°C; respiratory rate, 16 breaths/min; and Glasgow Coma Scale score, 14 (E4V5M5). Laboratory findings showed hyperglycemia (fasting blood glucose level, 165 mg/mL; hemoglobin A1c, 7.8%). Other laboratory findings were unremarkable, including coagulation activity and autoimmune system disease. She had no retinopathy or nephropathy. Echocardiography showed no regional left ventricular motion abnormalities.

Emergent magnetic resonance imaging (MRI) demon-

¹Department of Stroke, Stroke Center, National Hospital Organization Kagoshima Medical Center, Japan and ²Department of Neurology and Geriatrics, Kagoshima University Graduate School of Medical and Dental Sciences, Japan

Received: January 5, 2022; Accepted: May 5, 2022; Advance Publication by J-STAGE: July 29, 2022

Correspondence to Dr. Yuki Hamada, sunamushi.elmonkichi@gmail.com

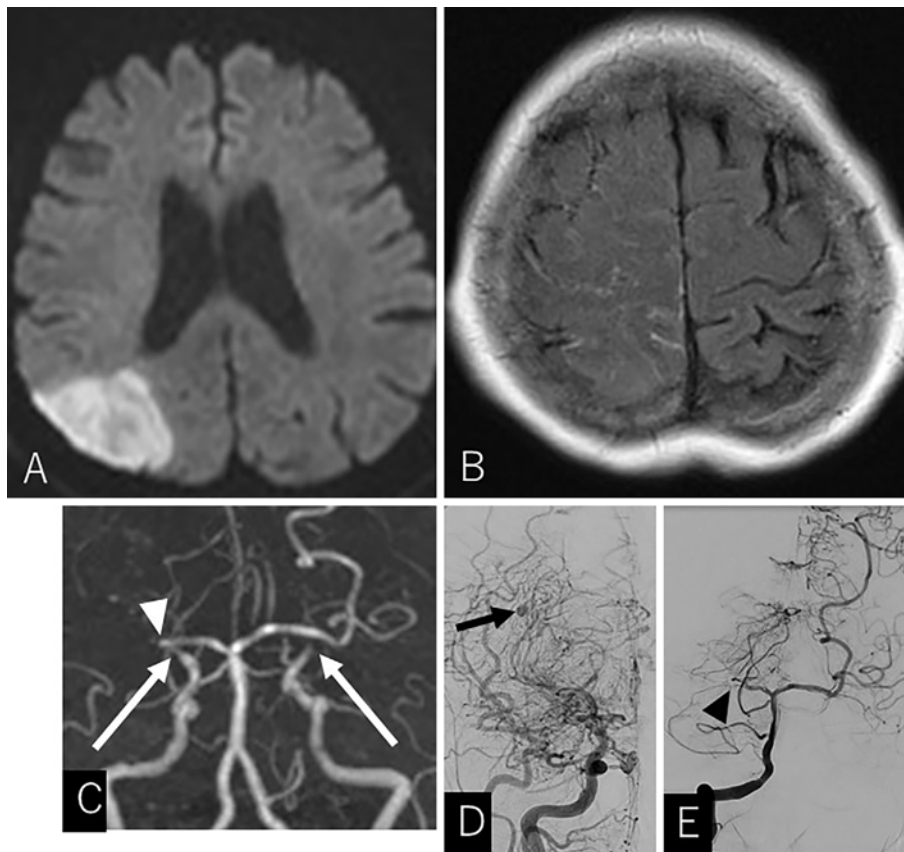


Figure 1. A) DWI of the head shows cerebral infarction from the right parietal lobe to the right occipital lobe. B) On FLAIR imaging, linear hyperintensities of the sulci are evident in the right cerebral hemisphere. C) MRA shows occlusion of the terminal portions of the bilateral internal carotid arteries (white arrows) and right PCA (white arrowhead). D) Angiography of the right internal carotid artery shows steno-occlusive changes at the terminal portion of the internal carotid artery and moyamoya blood vessels at the base of the brain. Micro-aneurysm is observed at the periphery of the lenticulostriate artery (black arrow). E) Angiography of the right vertebral artery shows occlusion of the PCA (black arrowhead).

strated signal hyperintensity involving the right parietal lobe on diffusion-weighted imaging (DWI) (Fig. 1A). Magnetic resonance angiography (MRA) revealed occlusion of the terminal portions of the bilateral internal carotid arteries and the right posterior cerebral artery (Fig. 1C). FLAIR imaging showed multiple hyperintensities in the subarachnoid space (Fig. 1B). After admission, edaravone was administered by drip infusion, but we did not start antithrombotic drugs, considering the possibility of subarachnoid hemorrhaging. In addition, considering the possibility of hemodynamic ischemic stroke, amlodipine was discontinued, and the blood pressure was controlled to around 160/80 mmHg with continuous intravenous infusion of dopamine hydrochloride at 5-7 $\mu\text{g}/\text{kg}/\text{min}$.

However, the neurological deficits were exacerbated, and follow-up MRI one day after admission showed expansion of the infarction territory and prominent signal enhancement of hyperintensities in the subarachnoid space (Fig. 2). We therefore started concentrated glycerin and fructose (200 mL) 3 times a day to prevent the spread of cerebral edema. Five days after admission, angiography showed steno-

occlusive changes at the terminal portions of the internal carotid arteries and an abnormal vascular network at the base of the brain, in addition to posterior cerebral artery (PCA) occlusion (Fig. 1D, E). Based on these findings, we diagnosed the patient with moyamoya disease.

Contrast-enhanced MRI revealed enhancement in the subarachnoid space corresponding to the area of hyperintensity on FLAIR imaging (Fig. 3A, B), explaining the ivy sign. Brain single photon emission computed tomography (SPECT) with ^{123}I -N-isopropyl-p-iodoamphetamine showed decreased regional cerebral perfusion in the right parietal lobe on admission and an increase in the hypo-perfused area around the ischemic lesion five days after admission (Fig. 4A, B). Since a micro-aneurysm was observed on angiography (Fig. 1D), we decided not to perform antithrombotic therapy for secondary prevention, considering the risk of aneurysm rupture. No abnormalities were detected on electrocardiography or Holter electrography. The cause of cerebral infarction in the PCA territory was considered to be progression of moyamoya disease.

Following the exacerbation of neurological symptoms, the

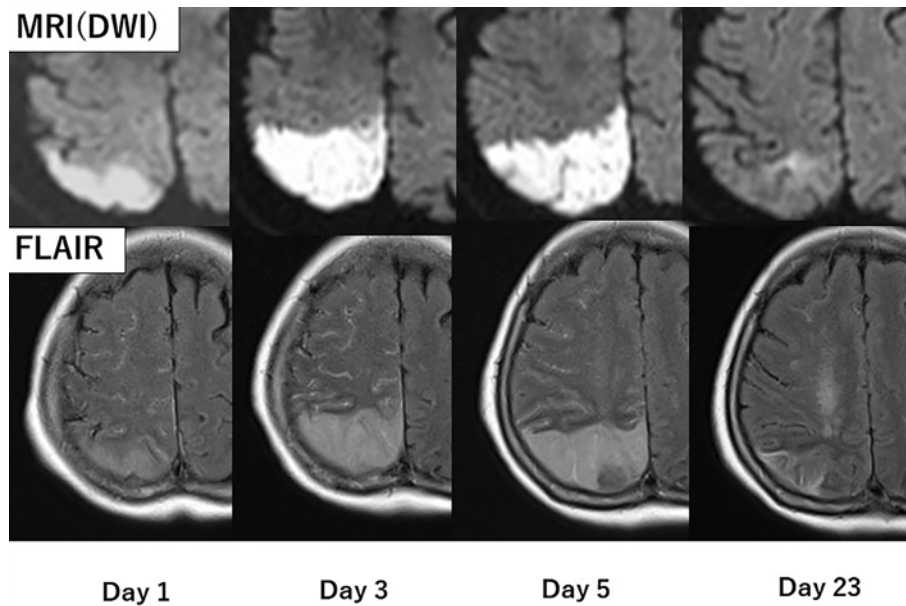


Figure 2. The comparison of FLAIR and DWI on admission and at 3, 5, and 23 days after admission. These comparisons show increased and expanded ipsilateral ivy sign paralleling expansion of the cerebral infarction. Five days after admission, progression of cerebral infarction had stopped on DWI, and the ivy sign was also diminished 23 days after admission. All immediate MRI studies were performed on a 1.5-T scanner (Siemens Healthcare, Erlangen, Germany) to examine patients with suspected stroke, including DWI, FLAIR, and MRA. DWI was performed with a standard protocol using the following parameters: field of view (FOV), 220 mm; spatial resolution, $1.7 \times 1.7 \times 5.5$ mm; and b-values of 0 and $1,000 \text{ s/mm}^2$. FLAIR was performed in the axial plane (FOV, 220 mm) with a common spatial resolution of $0.9 \times 0.9 \times 5.5$ mm.

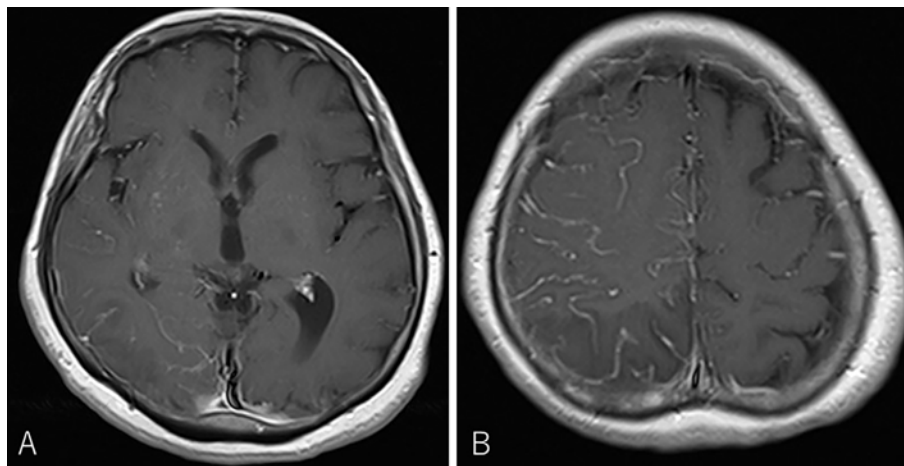


Figure 3. Gd-enhanced T1-weighted MRI (A, B) five days after admission reveals enhancement in the subarachnoid space corresponding to hyperintensity on FLAIR imaging.

blood pressure was controlled to around 180/90 mmHg with the continuous intravenous infusion of dopamine hydrochloride at $7\text{--}10 \mu\text{g/kg/min}$. Five days after admission, the progression of the neurological exacerbation stopped, and the progression of cerebral infarction appeared to have stopped as well based on DWI. Concentrated glycerin and fructose were administered for 14 days, and the dose of dopamine hydrochloride was gradually reduced and discontinued by 14 days after admission. The blood pressure was subsequently

controlled to around 150/80 mmHg, and no new neurological symptoms appeared. The ivy sign also diminished 23 days after admission (Fig. 2). Finally, the left homonymous hemianopia and left unilateral spatial neglect gradually improved, but the left hemiparesis remained moderate (manual muscle testing: 4/5).

The patient was transferred to a rehabilitation hospital with a modified Rankin Scale score of 3 at 24 days after admission.

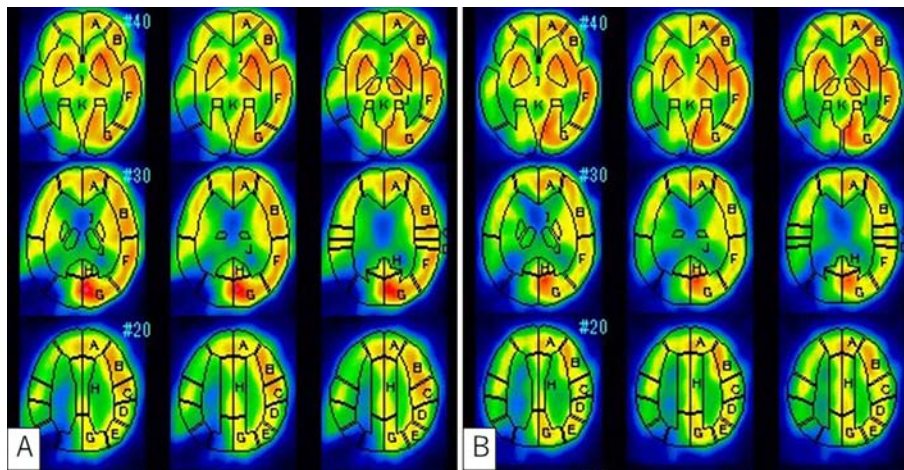


Figure 4. SPECT on admission (A) and five days after admission (B). Regional cerebral perfusion in the right parietal lobe is decreased. Five days after admission, there was an increased hypo-perfused area around the ischemic lesion.

Discussion

We described an interesting case of increased and expanded ipsilateral ivy sign paralleling the expansion of cerebral infarction in a patient with moyamoya disease. The ivy sign is reportedly found in 31-66% of cases of moyamoya disease and often appears in symptomatic cases (5). In terms of clinical significance, one report suggests that this sign reflects a state of decreased cerebral circulatory reserve (6). However, the ivy sign is also reportedly unrelated to the oxygen intake rate or collateral circulation (7). Other studies have speculated that only dilated leptomeningeal vessels, which act to supply blood during ischemia, are visualized (4, 7).

The relationship between the presence of an ivy sign and the expansion of cerebral infarction in the acute phase of cerebral infarction has not been clarified. Interestingly, the presence of the ivy sign has been reported to be a predictor of recurrent cerebral infarction in adults with moyamoya disease (8). This suggests that chronic hypoperfusion may be prone to progress to hemodynamic ischemic stroke. In addition, staging in moyamoya disease is associated with the appearance of ischemic disease. The appearance of infarction in the PCA territory reportedly reflects an increased risk of ischemic stroke as the stage progresses (9). Based on these findings, this case was considered to have involved ischemic stroke because of the presence of the PCA lesion and resulting disease progression. In addition, we speculated that the cerebral infarction expanded because the presence of the ivy sign showed chronic hypoperfusion, which failed to suppress the progression of hemodynamic cerebral infarction.

In this case, the ivy sign was enhanced by the expansion of cerebral infarction, and it disappeared once ischemia resolved. In particular, three days after admission, the cerebral infarction on DWI appeared to have expanded, paralleling

the expansion of the ivy sign, and five days after admission, SPECT findings showed an increased area of hypo-perfusion around the ischemic lesion in the right parietal temporal lobe compared to SPECT on admission. The reason for the enhancement of the ivy sign was presumed to involve reactive dilation of pial blood vessels due to increased flow demands resulting from expansion of the cerebral infarction (10). Furthermore, after the progression of cerebral infarction stopped, the ivy sign was considered to have diminished due to decreased flow demands in the ischemic territory. The patient had an expanded cerebral infarction due to an insufficient blood flow supply from the pial arteries. We considered that the ivy sign had weakened as a result of an increased blood flow from the pial arteries as a result of maintaining the blood pressure at a high level by means of the continuous intravenous infusion of dopamine hydrochloride.

No consensus has been reached regarding the medical treatment for moyamoya disease. In general, pediatric cases often develop with cerebral ischemic symptoms, whereas adult cases often develop with intracranial hemorrhaging in addition to cerebral ischemic symptoms. In the acute phase of ischemia and bleeding, medical treatment, such as blood pressure control and management for increased intracranial pressure, is performed. Although evidence is lacking, the use of edaravone, ozagrel sodium, argatroban, and aspirin is recommended for the treatment of acute ischemic moyamoya disease based on the treatment for acute-onset atherosclerotic cerebral infarction (3).

In the present case, the ischemic lesion expanded despite sufficient blood pressure control and intracranial pressure control with concentrated glycerin and fructose. The accumulation of ischemic cores may have been avoidable with the addition of antithrombotic therapy. However, in this case, due to concerns about subarachnoid hemorrhaging and the presence of micro aneurysm, we were hesitant to use antithrombotic therapy in combination. As a result of continu-

ing medical treatment without antithrombotic therapy, the spread of ischemia was minimized, and poor outcomes were avoided. If antithrombotic therapy had been used in combination, cerebral hemorrhaging might have developed, and the outcome might have been poor. Furthermore, if enhancement of the ivy sign is associated with progression of ischemia, small-molecular-weight dextran may have been useful for preventing progression of ischemia, in terms of increasing circulating plasma volume.

Based on the anatomical considerations, such as the localization of aneurysms at the periphery of the lenticulostriate artery making clipping difficult to perform directly and coil embolization being difficult because of the small vessel diameter, no surgery was performed. Treatment for moyamoya disease is thus considered to require complex knowledge of multiple factors, such as the anatomical background of each patient and the progression grade of ischemia.

Conclusion

The ivy sign in moyamoya disease with ischemic onset might enhance and diminish in response to hemodynamic changes, indicating flow demands in the ischemic territory. In particular, enhancement of the ivy sign may be associated with expansion of the ischemic area and warrants personalized medical treatment according to the patient background.

The authors state that they have no Conflict of Interest (COI).

References

1. Suzuki J, Takaku A. Cerebrovascular “moyamoya” disease. Disease showing abnormal net-like vessels in base of brain. *Arch Neurol* **20**: 288-299, 1969.
2. Nishimoto A, Takeuchi S. Abnormal cerebrovascular network related to the internal carotid arteries. *J Neurosurg* **29**: 255-260, 1968.
3. Research Committee on the Pathology and Treatment of Spontaneous Occlusion of the Circle of Willis. Health Labour Sciences Research Grant for Research on Measures for Intractable Diseases. Guidelines for diagnosis and treatment of moyamoya disease (spontaneous occlusion of the circle of Willis). *Neurol Med Chir (Tokyo)* **52**: 245-266, 2012.
4. Maeda M, Tsuchida C. “Ivy sign” on fluid-attenuated inversion-recovery images in childhood moyamoya disease. *AJNR Am J Neuroradiol* **20**: 1836-1838, 1999.
5. Kawashima M, Noguchi T, Takase Y, Nakahara Y, Matsushima T. Decrease in leptomeningeal ivy sign on fluid-attenuated inversion recovery images after cerebral revascularization in patients with Moyamoya disease. *AJNR Am J Neuroradiol* **31**: 1713-1718, 2010.
6. Vuignier S, Ito M, Kurisu K, et al. Ivy sign, misery perfusion, and asymptomatic moyamoya disease: FLAIR imaging and ¹⁵O-gas positron emission tomography. *Acta Neurochir (Wien)* **155**: 2097-2104, 2013.
7. Kaku Y, Iihara K, Nakajima N, et al. The leptomeningeal ivy sign on fluid-attenuated inversion recovery images in moyamoya disease: positron emission tomography study. *Cerebrovasc Dis* **36**: 19-25, 2013.
8. Nam KW, Cho WS, Kwon HM, et al. Ivy sign predicts ischemic stroke recurrence in adult moyamoya patients without revascularization surgery. *Cerebrovasc Dis* **47**: 223-230, 2019.
9. Kuroda S, Ishikawa T, Houkin K, Iwasaki Y. Clinical significance of posterior cerebral artery stenosis/occlusion in moyamoya disease. *No Shinkei Geka (Neurol Surg)* **30**: 1295-1300, 2002.
10. Mori A, Mugikura S, Higano S, et al. The leptomeningeal “ivy sign” on fluid-attenuated inversion recovery MR imaging in Moyamoya disease: a sign of decreased cerebral vascular reserve? *AJNR Am J Neuroradiol* **30**: 930-935, 2009.

The Internal Medicine is an Open Access journal distributed under the Creative Commons Attribution-NonCommercial-NoDerivatives 4.0 International License. To view the details of this license, please visit (<https://creativecommons.org/licenses/by-nc-nd/4.0/>).



Plaque Protrusion in a Patient with Left Common Carotid Artery Stenting after Radiation Therapy: A Case Report

Yuki Hamada, Mei Ikeda, Shinju Shimotakahara, Sayaka Tahara, Nao Onobuchi, Yoshiki Kanda, Go Takaguchi, and Hideki Matsuoka

Objective: We report a case of additional carotid artery stenting (CAS) for plaque protrusion occurring after initial CAS for radiation-induced common carotid artery (CCA) stenosis.

Case Presentation: A 69-year-old man with a history of radiotherapy for laryngeal cancer presented to our hospital with sudden-onset right hemiparesis. Since vulnerable plaque of the left CCA was considered the embolic source for ischemic stroke, CAS was performed for left CCA stenosis. No perioperative complications were observed and the patient was discharged with a modified Rankin Scale score of 0. However, 1 month after CAS, cerebral embolism recurred. As protruding plaque was found on CTA, additional endovascular treatment was performed with intravascular ultrasonography. He was discharged without complications and showed a good outcome at 3 months.

Conclusion: In CCA stenosis after radiotherapy, accelerated arteriosclerosis may cause drug-resistant cerebral embolism and plaque protrusion after CAS, making determination of the treatment strategy difficult. Appropriate treatment options need to be based on individual underlying diseases and plaque instability.

Keywords ▶ radiation induced, common carotid artery, plaque protrusion, carotid artery stenting

Introduction

Carotid artery stenting (CAS) is often required for radiation-induced carotid artery stenosis, but additional stenting for plaque protrusion occurring after CAS appears rare. Pathologically, the plaque is usually stable and the frequency of ischemic stroke is considered low because inflammatory changes at the lesion site are scarce and usually attributable to fibrosis.¹⁾ However, recent reports suggest that carotid artery stenosis after radiotherapy is a form of accelerated arteriosclerosis²⁾ and involves highly unstable plaque,³⁾ with fewer fibrous components

than have been considered in the past. Herein, we report an instructive case of plaque protrusion following CAS for left common carotid artery (CCA) stenosis after radiotherapy.

Case Presentation

A 69-year-old man presented to our hospital with sudden onset of right hemiparesis (manual muscle testing: 5-/5). The patient had a medical history of laryngeal microsurgery for laryngeal cancer 11 years earlier, and was subsequently treated with 60 Gy of radiotherapy for 1 month. Since then, no recurrence of cancer has been observed. In addition, the patient had a history of chronic occlusion of the right CCA, hypertension, and dyslipidemia.

Emergent MRI demonstrated multiple high-intensity signals on diffusion-weighted imaging in the territory of the middle cerebral artery (**Fig. 1A**). MRA of the head revealed no findings indicative of occlusion or stenosis of the right large vessels, except for the absence of the chronically occluded right internal carotid artery (**Fig. 1B**). No abnormalities were evident from laboratory findings. According to the European Carotid Surgery Trial criteria, ultrasonography detected 50%

Department of Strokology, Stroke Center, National Hospital Organization Kagoshima Medical Center, Kagoshima, Kagoshima, Japan

Received: April 10, 2022; Accepted: May 25, 2022

Corresponding author: Yuki Hamada. Department of Strokology, Stroke Center, National Hospital Organization Kagoshima Medical Center, 8-1, Shiroyama, Kagoshima, Kagoshima 892-0853, Japan
Email: sunamushi.elmonkichi@gmail.com



This work is licensed under a Creative Commons Attribution-NonCommercial-NoDerivatives International License.

©2022 The Japanese Society for Neuroendovascular Therapy

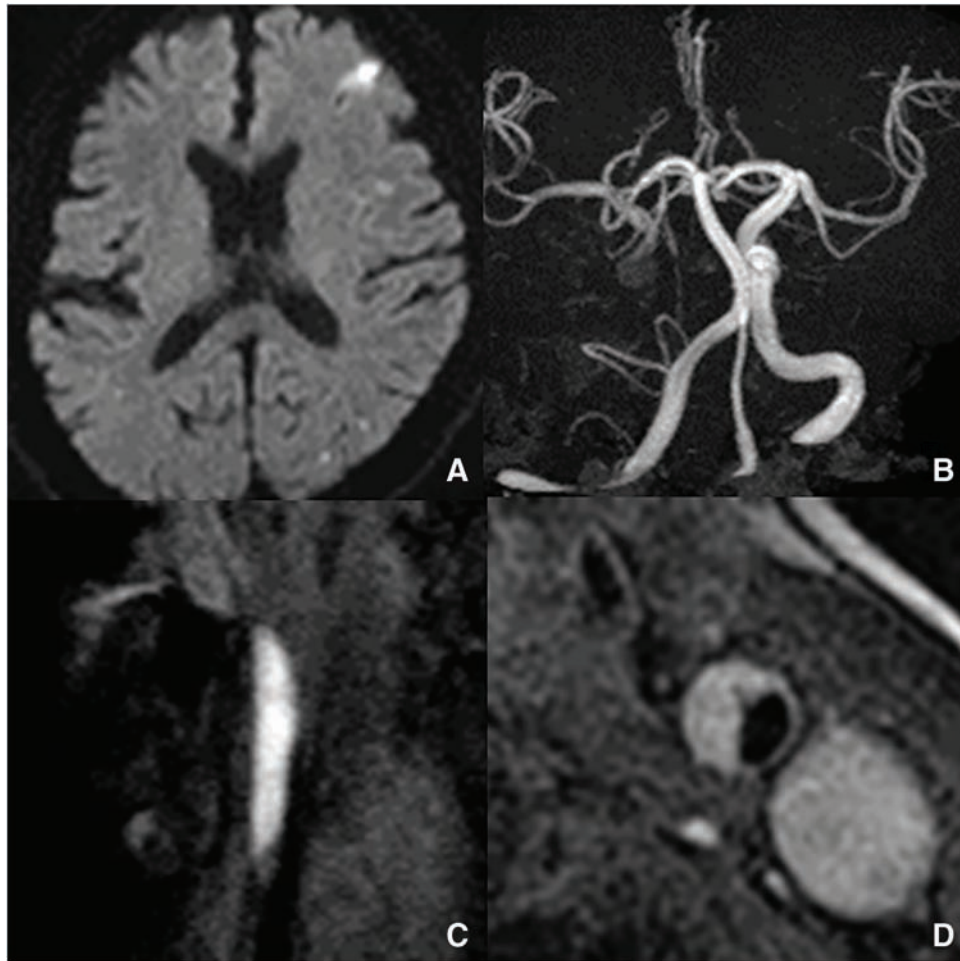


Fig. 1 (A) Diffusion-weighted imaging of the head shows cerebral infarction in the territory of the left middle cerebral artery. (B) MRA of the head reveals no findings suggestive of occlusion or stenosis of the right large vessels, except for the absence of the chronically occluded right internal carotid artery. (C) Magnetization-prepared rapid gradient-echo imaging shows a high-intensity signal of the CCA. (D) T1-weighted black-blood imaging demonstrates a high-intensity signal of the CCA, suggesting vulnerable plaque. CCA: common carotid artery

stenosis of the left CCA, which showed low-echoic lesions. MRI of neck plaque demonstrated high-intensity signals on magnetization-prepared rapid gradient echo sequences (**Fig. 1C**) and T1-weighted black-blood imaging (**Fig. 1D**). Based on these findings, we diagnosed vulnerable plaque of the left CCA as the embolic source of ischemic stroke.

On admission, 200 mg of aspirin and 300 mg of clopidogrel were administered. Angiography revealed a long, ulcerated plaque in the left CCA (**Fig. 2A**), which was located from the upper edge of the 3rd cervical vertebra to the lower edge of the 5th cervical vertebra. In addition, few leptomeningeal collateral pathways from the posterior circulation were present and the territory of the right middle cerebral artery was supplied by cross-circulation through the anterior communicating artery. Symptoms improved

markedly and the patient was discharged on hospital day 13 with a modified Rankin Scale score of 0. However, 1.5 months later, he was readmitted with recurrence of cerebral infarction. Since he appeared resistant to the best medical oral treatment, endovascular treatment was performed.

The procedure was performed with the patient awake and under minimal sedation. The right common femoral artery was punctured and an 8-Fr 30-cm sheath was placed. After systemic heparinization, a 4- to 6-Fr JB2 catheter (Medikit, Tokyo, Japan) was guided by a 0.035-inch guide-wire to the ascending aorta, and then an 8-Fr SEL-OSP insertion-support guiding catheter (Medikit) was placed at the origin of the left CCA. A PercuSurge GuardWire (Medtronic, Minneapolis, MN, USA) was carefully advanced across the stenotic lesion and blocked the blood stream in the distal internal carotid artery. The most

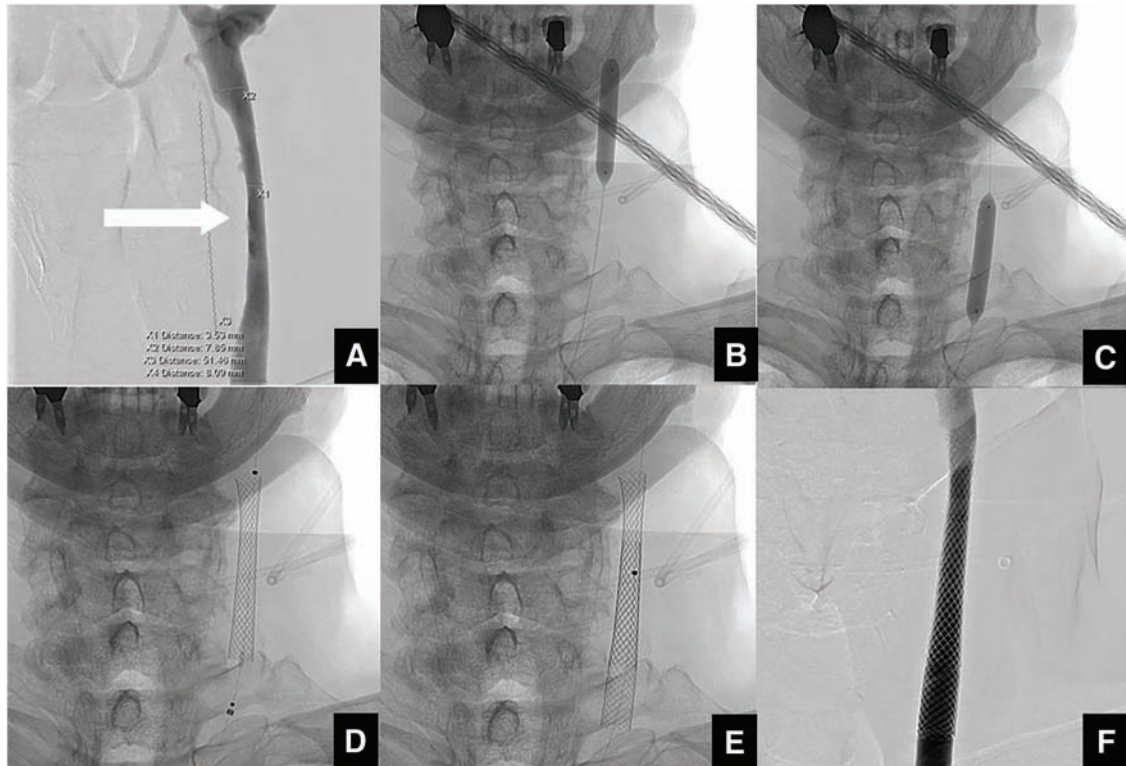


Fig. 2 (A) Left common carotid angiography before CAS (frontal view) shows long stenosis (white arrow). (B) and (C) Pre-dilation performed using a 7.0 mm × 40 mm balloon catheter at the site of stenosis at three locations: distal, middle, and proximal. (D) Fluoroscopic image of first stent placement. A 10 mm × 31 mm Carotid Wallstent is placed at the distal site of stenosis. (E) Subsequently, an additional 10 mm × 31 mm Carotid Wallstent is placed at the proximal site of stenosis. (F) Left common carotid artery injection shows no contrast-enhanced defect. CAS: carotid artery stenting

stenotic site of the lesion was 3.4 mm in diameter, the diameter of the distal CCA was 7.8 mm, the diameter of the proximal CCA was 8.2 mm, and the lesion length was 50 mm. Pre-dilation was performed using a 7.0 mm × 40 mm balloon catheter (Sterling; Boston Scientific, Natick, MA, USA) at the site of stenosis at three locations (distal, middle, and proximal) because of the long lesion (**Fig. 2B** and **2C**). Subsequently, two 10 mm × 31 mm carotid stents (Carotid Wallstent; Boston Scientific) were placed and partially overlapped to cover the plaque-rich area (**Fig. 2D** and **2E**). After floating debris was vacuumed out using an aspiration catheter, all procedures were completed. Left common carotid artery injection showed no contrast-enhanced defect (**Fig. 2F**). No perioperative complications were observed and ultrasonography at 1 and 5 days after CAS showed no plaque protrusion. The patient was discharged with a modified Rankin Scale score of 0 but was readmitted 1 month after CAS because of recurrent cerebral infarction.

Ultrasonography revealed low-echoic deposits distal to the stent, suggesting plaque protrusion. Moreover, a mobile thrombus was attached to the protruding plaque (**Fig. 3A**). CTA showed plaque protrusion at the distal end of the

Carotid Wallstent and at areas of overlap (**Fig. 3B**). Warfarin was added and 100 mg of aspirin was discontinued because of insufficient effect on platelet aggregation. Prothrombin time and international normalized ratio (PT-INR) were controlled to within the range of 2.0–3.0 s. Despite aggressive medical treatment, the patient experienced recurrent cerebral infarction and additional endovascular treatment was performed.

As in the first session, the procedure was performed with an 8-Fr SEL-OSP placed at the origin of the left CCA. Left internal carotid artery injection showed a contrast-enhanced defect on the distal right side of the Carotid Wallstent and on the distomedial side at areas of overlap (**Fig. 4A**). Before the operative procedure, intravascular ultrasonography (IVUS) (Volcano Visions PV 0.014P catheter with Chroma Flo; Volcano, Rancho Cordova, CA, USA) was navigated to the area of protruding plaque, which clearly indicated the position of the protruding area (**Fig. 4B** and **4C**). Based on these findings, a Filterwire EZ protection device (Boston Scientific) was carefully maneuvered across the stented region, and a 10 mm × 31 mm Carotid Wallstent was placed to cover the protruding

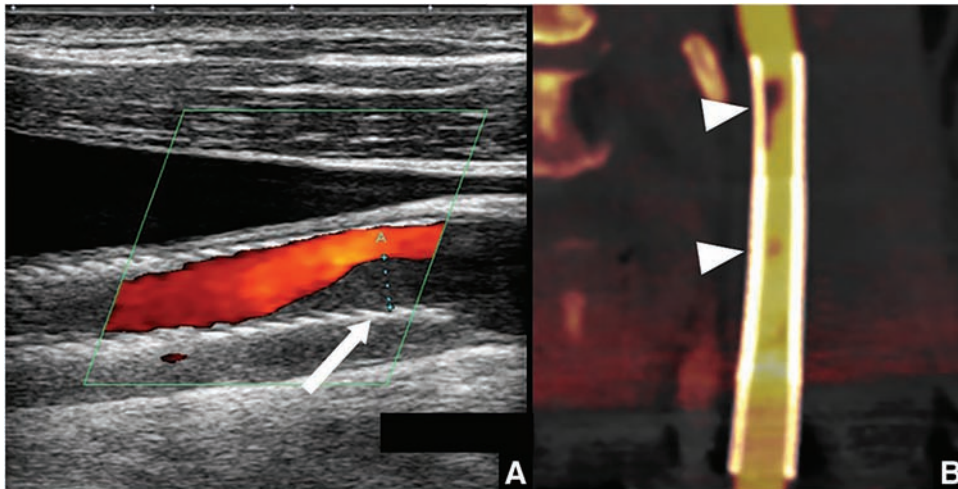


Fig. 3 (A) Ultrasonography reveals low-echoic deposits distal to the stent (white arrow), suggesting plaque protrusion. Mobile thrombus is attached to the protruding plaque. (B) CTA shows plaque protrusion at the distal end of the Carotid Wallstent and sites of areas of stent overlap (white arrowheads).

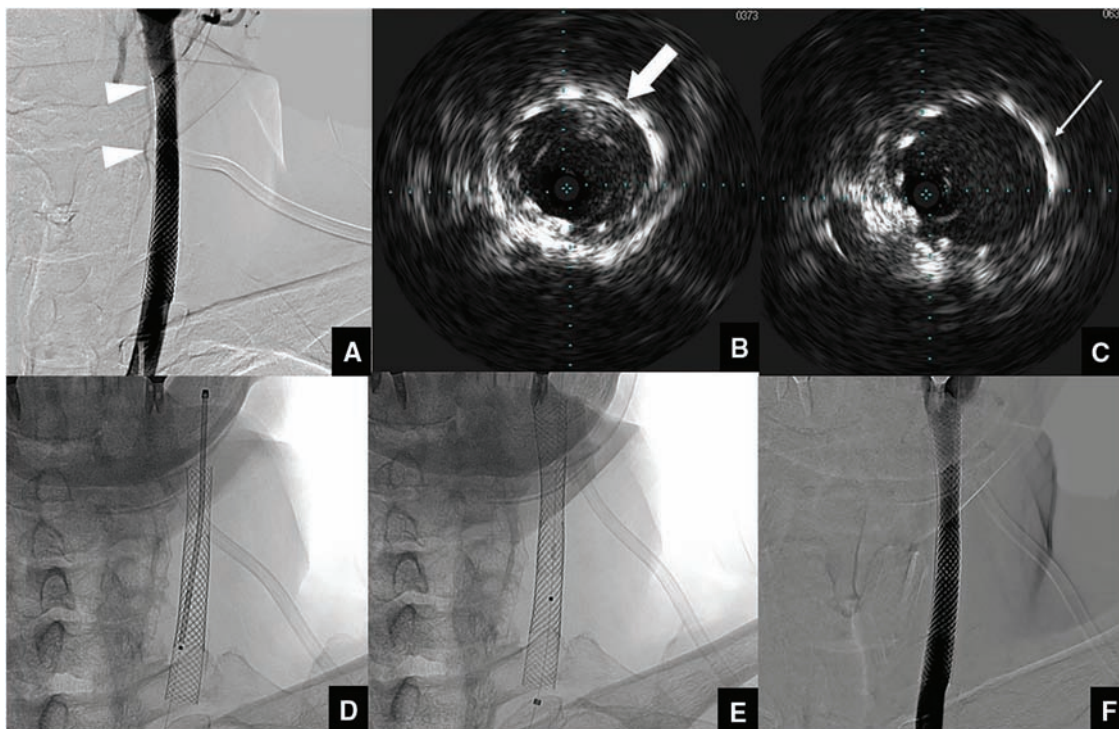


Fig. 4 (A) Left common carotid angiography before additional CAS (frontal view) showing plaque protrusion (white arrowheads). (B) IVUS before placement shows plaque protrusion at the distal end of the Carotid Wallstent in the direction of 1 o'clock (thick white arrow). (C) IVUS after stent placement shows plaque protrusion at the site of overlap in the direction of 2 o'clock (thin white arrow). (D) Fluoroscopic image before stent placement. (E) A 10 mm x 31 mm Carotid Wallstent was placed to cover the plaque protruded area. (F) Left common artery injection showed no contrast-enhanced defect. CAS: carotid artery stenting; IVUS: intravascular ultrasonography

plaque (**Fig. 4D** and **4E**). Neither pre- nor post-dilation was performed. After stent placement, IVUS confirmed the disappearance of plaque protrusion. IVUS was useful in determining the position for stent deployment. Left

internal carotid artery injection showed disappearance of the protruding plaque (**Fig. 4F**). During the perioperative period, the patient showed no neurological deficits and plaque protrusion disappeared on ultrasonography. Finally,

the patient was discharged with a modified Rankin Scale score of 1. On follow-up at 3 months after discharge, modified Rankin Scale score remained at 1. Ultrasonography 6 and 12 months after additional endovascular treatment did not show any protruding plaque or carotid artery restenosis. We therefore discontinued warfarin and only continued administration of clopidogrel at 12 months after additional CAS. Since then, the patient has been commuting to follow-up at our hospital without recurrence of cerebral infarction. The patient consented to the submission of this report for publication.

Discussion

To the best of our knowledge, this case represents the rare report of additional CAS for plaque protrusion occurring after initial stent-in-stenting for radiation-induced CCA stenosis due to resistance to pharmacotherapy. In the present case, a large amount of vulnerable plaque was suggested on preoperative examination, so two closed stents were placed in the lesion, but plaque protrusions still occurred. These protrusions were seen to progress during follow-up, and a thrombus was considered to have adhered to the protrusion, so anticoagulant therapy was added. However, since the cerebral infarction subsequently recurred, we decided to perform additional CAS. As no such cases have been reported previously, we report this as a didactic case.

Plaque protrusion is a phenomenon in which plaque protrudes from the mesh of the stent due to the radial force of the stent. Vulnerable plaque with large lipid cores, hemorrhage in the plaque, and the use of open-cell stents have been reported as predictors of plaque protrusion,⁴⁾ which has a frequency of 2.6%–7.8%.^{4,5)} The clinical course is characterized by the possibility of spontaneous regression, but growth over time leads to intra-stent occlusion and embolic stroke. Retreatment should be considered if narrowing of the stent lumen diameter, an increasing trend in areas of protruding plaque, and mobile plaque are observed. On the other hand, mild narrowing and slight protrusion require pharmacotherapy with frequent follow-up. Whether antiplatelet drugs or anticoagulants are more effective as drug treatments remains unclear.

In general, a history of radiotherapy to the neck represents a risk factor for carotid artery stenosis. In 1962, Lindsay et al. irradiated the abdominal aorta with X-rays in a canine model and discovered arteriosclerotic changes in the aortic wall.⁶⁾ Morphological characteristics of carotid

artery stenosis after radiotherapy have been reported to include presence in the CCA,³⁾ bilateral stenosis,⁷⁾ a high stenosis rate in the distal part of the lesion,⁷⁾ and a long distance between lesion sites,⁷⁾ all of which resemble the pathology in the present case.

We often encounter cases of symptomatic carotid artery stenosis several years after radiotherapy to the neck. A review of cerebrovascular incidents among patients with a history of cervical radiotherapy reported that 18%–38% of patients developed carotid artery stenosis.²⁾ This was explained as accelerated arteriosclerosis due to ischemic necrosis of the blood vessel wall involving vasa vasorum disorder and endothelial damage, and has also been called malignant stenosis. In addition, ischemic stroke was reportedly induced by the accumulation of plaque in the stenotic site after radiotherapy.⁸⁾ The patient in our case had hypertension and dyslipidemia as underlying diseases, exhibited accelerated arteriosclerosis due to the effects of radiotherapy, and was considered to have developed carotid artery stenosis after 11 years.

No consensus has been established regarding methods for preventing plaque protrusion. As a method to prevent plaque protrusion using standard carotid stents, CASPER micromesh stent (Terumo, Tokyo, Japan) may be effective for plaque protrusion, although plaque protrusion reportedly still developed in 44% of patients treated using CASPER stents.⁹⁾ On the other hand, the stent-in-stent technique with closed-cell stents has been reported to show no incidence of plaque protrusion or perioperative cerebral infarction.¹⁰⁾ However, different methods of evaluating plaque protrusion were used, with optical frequency domain imaging used in the former study and IVUS in the latter. In the future, further cases need to be accumulated regarding preventive measures against plaque protrusion.

The relationship between plaque protrusion and balloon post expansion is controversial. Clinically, excessive post-dilation of vulnerable plaque is recognized to increase the risk of plaque protrusions, but evidence remains lacking. Harada et al. performed pre- and post-dilation evaluations using optical coherence tomography and reported that post-dilation may reduce both the volume of protrusion and late-onset cerebral infarction.¹¹⁾ In this case, post-dilation was not performed in either of the two treatments, but further cases need to be accumulated to clarify this issue.

IVUS before and after stent placement is useful for observing morphological changes in plaque protrusions.^{12,13)} In this case, IVUS used before and after additional stent

placement was considered useful for visually confirming morphological changes in plaque protrusions. However, if IVUS had been performed before and after the initial treatment, we might have noticed the plaque protrusion earlier. Plaque protrusion was not detected by ultrasonography at 1 or 5 days after initial CAS in this case, but additional evaluation with CTA was more useful in detecting plaque protrusion.

Whether CAS or carotid endarterectomy (CEA) is more effective for treating carotid artery stenosis after cervical radiotherapy remains contentious. CAS for radiation-induced carotid artery stenosis has been reported to carry a high risk of ischemic stroke within 30 days due to formation of vulnerable plaque.¹⁴⁾ In this case, the stenotic lesion was located from the upper edge of the 3rd cervical vertebra to the lower edge of the 5th cervical vertebra, and so could be in a reachable position for CEA. However, this case involved CEA high-risk factors such as contralateral occlusion and a history of radiotherapy, and as the collateral circulation was also underdeveloped, CAS was selected. In general, CEA for carotid artery stenosis after cervical radiotherapy is generally known to be of high risk due to the problem of adhesion around the wound and blood vessels. Since 2004, when the history of cervical radiotherapy was considered a high-risk factor for CEA in the SAPHIRE trial, CAS has been considered the preferred treatment.^{15,16)} Regarding complications, CEA for carotid artery stenosis after cervical radiotherapy has been reported to be associated with neuropathy, while CAS shows a high frequency of restenosis.¹⁷⁾ On the other hand, a recent meta-analysis showed that treatment for carotid artery stenosis after cervical radiotherapy led to similar perioperative complications in both CAS and CEA, with no significant difference in long-term restenosis rates.¹⁸⁾ Such reports have been contradictory, so long-term restenosis rates may remain similar for both CAS and CEA. We await the accumulation of more knowledge on this issue in the future.

Relatively few reports have described outcomes for patients with carotid artery stenosis who have undergone CAS and have been treated with radiation. Choy et al.¹⁹⁾ followed cases after CAS for carotid artery stenosis with a history of radiotherapy or cervical surgery for 5 years, but no significant difference in adverse events was seen compared to cases with no history of CAS, and the outcomes were also reportedly good. In the present case, no recurrence of cerebral infarction was observed after additional

carotid stenting, and the outcome was favorable. However, the timing of surgery needed to be considered while observing responsiveness to antithrombotic therapy. This was one case in which the optimal treatment strategy was also difficult to determine.

Conclusion

CCA stenosis after radiotherapy-accelerated arteriosclerosis may cause drug-resistant cerebral embolism and plaque protrusion after CAS, making determination of the treatment strategy more difficult. Appropriate treatment options need to be considered based on individual underlying diseases and plaque instability.

Disclosure Statement

All authors have no conflicts of interest.

References

- 1) Fokkema M, den Hartog AG, van Lammeren GW, et al. Radiation-induced carotid stenotic lesions have a more stable phenotype than de novo atherosclerotic plaques. *Eur J Vasc Endovasc Surg* 2012; 43: 643–648.
- 2) Fernández-Alvarez V, López C, Suárez F, et al. Radiation-induced carotid artery lesions. *Strahlenther Onkol* 2018; 194: 699–710.
- 3) Ting ACW, Wu LLH, Cheng SWK. Ultrasonic analysis of plaque characteristics and intimal-medial thickness in radiation-induced atherosclerotic carotid arteries. *Eur J Vasc Endovasc Surg* 2002; 24: 499–504.
- 4) Kotsugi M, Takayama K, Myouchin K, et al. Carotid artery stenting: investigation of plaque protrusion incidence and prognosis. *JACC Cardiovasc Interv* 2017; 10: 824–831.
- 5) Shinozaki N, Ogata N, Ikari Y. Plaque protrusion detected by intravascular ultrasound during carotid artery stenting. *J Stroke Cerebrovasc Dis* 2014; 23: 2622–2625.
- 6) Lindsay S, Kohn HI, Dakin RL, et al. Aortic atherosclerosis in the dog after localized aortic x-irradiation. *Circ Res* 1962; 10: 51–60.
- 7) Shichita T, Ogata T, Yasaka M, et al. Angiographic characteristics of radiation-induced carotid arterial stenosis. *Angiology* 2009; 60: 276–282.
- 8) Gujral DM, Chahal N, Senior R, et al. Radiation-induced carotid artery atherosclerosis. *Radiother Oncol* 2014; 110: 31–38.
- 9) Yamada K, Yoshimura S, Miura M, et al. Potential of new-generation double-layer micromesh stent for carotid artery stenting in patients with unstable plaque: a

- preliminary result using OFDI analysis. *World Neurosurg* 2017; 105: 321–326.
- 10) Myouchin K, Takayama K, Wada T, et al. Carotid artery stenting using a closed-cell stent-in-stent technique for unstable plaque. *J Endovasc Ther* 2019; 26: 565–571.
 - 11) Harada K, Kajihara M, Sankoda Y, et al. Efficacy of post-dilatation during carotid artery stenting for unstable plaque using closed-cell design stent evaluated by optical coherence tomography. *J Neuroradiol* 2019; 46: 384–389.
 - 12) Kuroiwa T, Sakai N, Adachi H, et al. Stent-in-stenting for the plaque protrusion after stent deployments. *Surg Cereb Stroke* 2004; 32: 107–111. (in Japanese)
 - 13) Taguchi H, Takayama K, Kishida H, et al. A case of intraprocedural plaque protrusion during carotid artery stenting using the stent-in-stent technique for carotid artery stenosis with unstable plaque. *JNET J Neuroendovasc Ther* 2022; 16: 46–51.
 - 14) Sano N, Satow T, Maruyama D, et al. Relationship between histologic features and outcomes of carotid revascularization for radiation-induced stenosis. *J Vasc Surg* 2015; 62: 370–377.e1.
 - 15) Yadav JS, Wholey MH, Kuntz RE, et al. Protected carotid-artery stenting versus endarterectomy in high-risk patients. *N Engl J Med* 2004; 351: 1493–1501.
 - 16) Gurm HS, Yadav JS, Fayad P, et al. Long-term results of carotid stenting versus endarterectomy in high-risk patients. *N Engl J Med* 2008; 358: 1572–1579.
 - 17) Huang MP, Fang HY, Chen CY, et al. Long-term outcomes of carotid artery stenting for radiation-associated stenosis. *Biomed J* 2013; 36: 144–149.
 - 18) Giannopoulos S, Texakalidis P, Jonnalagadda AK, et al. Revascularization of radiation-induced carotid artery stenosis with carotid endarterectomy vs. carotid artery stenting: a systematic review and meta-analysis. *Cardiovasc Revasc Med* 2018; 19: 638–644.
 - 19) Choy HK, Kokkinidis DG, Cotter R, et al. Long-term outcomes after carotid artery stenting of patients with prior neck irradiation or surgery. *Cardiovasc Revasc Med* 2018; 19: 327–332.

[LETTERS TO THE EDITOR]

Development of Ivy Sign and Infarction in the Lateral Part of the Hemisphere or the Middle Cerebral Artery Territory in Association with Steno-occlusive Involvement of the Posterior Cerebral Artery in Moyamoya Disease

Key words: moyamoya disease, ivy sign, infarction, PCA involvement, deep collaterals, pial network

(Intern Med 62: 1703-1704, 2023)
(DOI: 10.2169/internalmedicine.0969-22)

The Authors Reply We would like to thank the editor and Mugikura et al. for the letter that included many constructive insights for our case report (1). As Mugikura et al. proposed, this case likely involves the compensatory development of so-called choroidal anastomosis, with progressive posterior cerebral artery (PCA) involvement (2). Occlusion at the bilateral internal carotid artery terminus was already present in this case, and the progressive PCA involvement was thought to have led to the onset of an ischemic event. The infarction started from the right parietal lobe at the border region of the right middle cerebral artery and right posterior cerebral artery, and it expanded into the superior parietal lobule, which corresponds to the vascular territory of the parieto-occipital artery, a terminal artery of the PCA.

On single-photon emission computed tomography, the area perfused by the right pericallosal artery was relatively well-maintained in the present case; this, as shown in a re-

port by Mugikura et al. (2), is thought to be due to the functioning of deep collateral circulation. Based on a report by Funaki et al. (3), there are a few potential routes, such as a route from the anterior or posterior choroidal artery via the subependymal artery or medullary artery, as well as a route from the thalamoperforating artery, thalamotuberal artery (a perforating branch of the posterior communicating artery), or the thalamogeniculate artery (a perforating branch of the P2 segment) via the medullary artery (Figure). Furthermore, in the present case, we were able to confirm anastomosis from the ophthalmic artery to the anterior cerebral artery via ethmoidal moyamoya on cerebral angiography, and we believe this also contributed to the CBF maintenance. To identify these blood vessels, a comparison with coronal images obtained via magnetic resonance angiography time-of-flight imaging was extremely useful.

While infarction of a portion of the PCA region (e.g., the calcarine artery region) was avoided in the present case, this, as explained by Mugikura et al., appears to be the effect of the pial network that formed before the PCA involvement progressed. The ivy sign was observed in the calcarine sulcus and parieto-occipital sulcus in the present case, suggesting the presence of hypervascularity at the superficial occipital lobe in the background. Recently, various methods of visualizing the collateral circulation path and the ischemic changes in moyamoya disease have become available, and we look forward to the further development of imaging studies.

We thank Mugikura et al. for their constructive sugges-

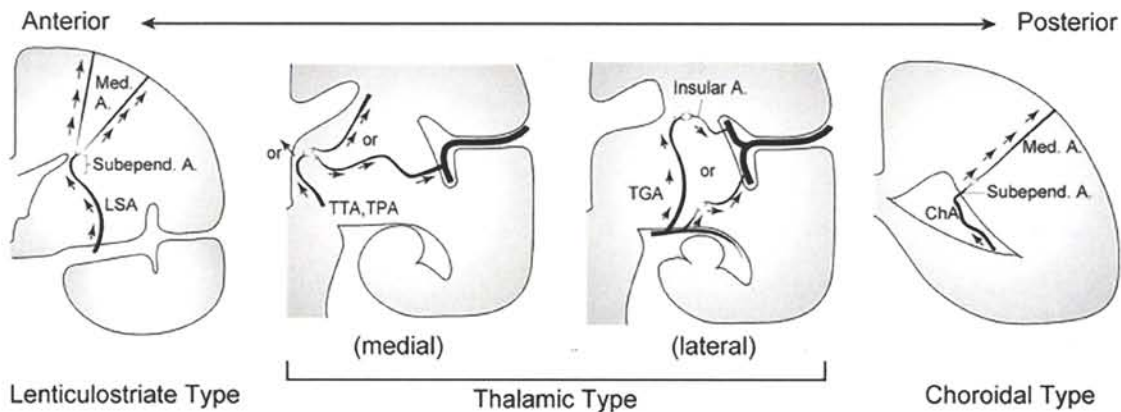


Figure. Schematic illustration showing the coronal plane of the left cerebral hemisphere and three subtypes of collateral anastomoses: lenticulostriate, thalamic, and choroidal anastomoses. A: artery, Med: medullary, Subepend: subependymal, TGA: thalamogeniculate artery, TPA: thalamoperforating artery, TTA: thalamotuberal artery. Reprinted with permission from Funaki et al. (3).

¹Department of Strokeology, Stroke Center, National Hospital Organization Kagoshima Medical Center, Japan and ²Department of Neurology and Geriatrics, Kagoshima University Graduate School of Medical and Dental Sciences, Japan
Received: September 5, 2022; Accepted: September 7, 2022; Advance Publication by J-STAGE: October 19, 2022
Correspondence to Dr. Yuki Hamada, sunamushi.elmonkichi@gmail.com

tions.

The authors state that they have no Conflict of Interest (COI).

Yuki Hamada¹, Hideki Matsuoka¹ and Hiroshi Takashima²

References

1. Mugikura S, Mori N. Development of ivy sign and infarction in the lateral part of the hemisphere or the middle cerebral artery territory in association with steno-occlusive involvement of the posterior cerebral artery in moyamoya disease. *Intern Med* **62**: 1701, 2023.
2. Mugikura S, Takahashi S, Higano S, et al. The relationship be-

tween cerebral infarction and angiographic characteristics in childhood moyamoya disease. *AJNR Am J Neuroradiol* **20**: 336-343, 1999.



3. Funaki T, Fushimi Y, Takahashi JC, et al. Visualization of periventricular collaterals in moyamoya disease with flow-sensitive black-blood magnetic resonance angiography: preliminary experience. *Neurol Med Chir (Tokyo)* **55**: 204-209, 2015.

The Internal Medicine is an Open Access journal distributed under the Creative Commons Attribution-NonCommercial-NoDerivatives 4.0 International License. To view the details of this license, please visit (<https://creativecommons.org/licenses/by-nc-nd/4.0/>).

© 2023 The Japanese Society of Internal Medicine
Intern Med 62: 1703-1704, 2023

ORIGINAL ARTICLE

Developmental trajectories at a high risk for childhood overweight/obesity

Masao Yoshinaga^{1,2}  | Hideto Takahashi³ | Yoshiya Ito⁴ | Machiko Aoki⁵ |
Ayumi Miyazaki⁶ | Toshihide Kubo⁷ | Masaki Shinomiya⁸ | Hitoshi Horigome⁹ |
Masakuni Tokuda¹⁰ | Lisheng Lin⁹  | Hiromitsu Ogata¹¹ | Masami Nagashima¹²

¹Department of Pediatrics, National Hospital Organization Kagoshima Medical Center, Kagoshima, Japan

²Orange Medical and Welfare Center for Severe Motor and Intellectual Disabilities, Kirishima, Japan

³National Institute of Public Health, Wako, Japan

⁴Clinical Medicine Area, Japanese Red Cross Hokkaido College of Nursing, Kitami, Japan

⁵Department of Pediatrics, Aoki Internal Medicine and Cardiovascular and Pediatrics Clinic, Fukuoka, Japan

⁶Department of Pediatrics, Japan Community Health Care Organization Takaoka Fushiki Hospital, Takaoka, Japan

⁷Department of Pediatrics, National Hospital Organization Okayama Medical Center, Okayama, Japan

⁸Department of Internal Medicine, Nishifuna Naika, Funabashi, Japan

⁹Department of Child Health, Graduate School of Comprehensive Human Sciences, University of Tsukuba, Tsukuba, Japan

¹⁰Tokuda Children's Clinic, Amagasaki, Japan

¹¹Epidemiology and Biostatistics, Kagawa Nutrition University, Sakado, Japan

¹²Aichi Saiseikai Rehabilitation Hospital, Nagoya, Japan

Correspondence

Masao Yoshinaga, Department of Pediatrics, National Hospital Organization Kagoshima Medical Center, 8-1 Shiroyama-cho, Kagoshima 892-0853, Japan.
Email: yoshinaga.masao.ks@mail.hosp.go.jp

Funding information

Health and Labour Sciences Research Grant from the Ministry of Health, Labour and Welfare of Japan, Grant/Award Number: H24-014

Abstract

Background: The associations between developmental patterns (trajectories) in children and maternal factors have been widely investigated, but paternal effects on these trajectories are unclear. This study aimed to determine child and parental factors involved in developmental trajectories at high risk for causing adverse cardiovascular (CV) profiles in children.

Methods: We analyzed longitudinal anthropometric data from birth to the present and CV profiles of 1,832 healthy volunteers (51% girls) aged 3–15 years who participated in a nationwide study between July 2012 and January 2014. Six trajectory latent class growth models were developed using body mass index z-scores. Predictors for being in developmental trajectories at high risk for causing adverse CV profiles were determined by multivariate regression analysis.

Results: The mean±standard deviation number of anthropometric data points was 12±3 for both boys and girls. Among the six trajectories, the infantile onset and continual increase groups had significantly worse levels of many CV profiles than those in the remaining groups. Paternal overweight/obesity was an independent predictor for boys being in the infantile onset group and for girls being in the continual increase group. Additionally, maternal pre-pregnancy overweight/obesity in boys and maternal excessive gestational weight gain in girls were independent predictors for being in the infantile onset group. Having no sibling in boys and an older maternal age were independent predictors for being in the continual increase group.

Conclusions: Interventions to prevent childhood obesity should include strategies that focus on fathers and mothers as well as those that focus on children with certain types of familial background.

KEYWORDS

cardiovascular profiles, childhood obesity, parental impact, sex difference, trajectory

INTRODUCTION

The prevalence of obesity in children and adolescents in Japan has remained stable for the last decade, with a peak in the year 2000.^{1,2} A new concern is that the prevalence of childhood/adult obesity is expected to rise as a result of the COVID-19 stay-at-home orders.^{3,4} Obesity from childhood to adulthood or childhood/adolescent obesity itself is associated with a risk of type 2 diabetes, coronary artery disease, and cardiovascular (CV) death.^{5–7}

Recent developments in statistical techniques that allow the analysis of longitudinal data generated from repeated measurements have enabled researchers to identify distinctive developmental patterns (trajectories) in an exploratory manner.⁸ Group-based trajectory models are designed to identify clusters of individuals who follow similar progressions of some behaviors or outcomes at a particular age or over time. The latent class growth model, one of the group-based trajectory models, assumes the presence of and identifies latent groups of individuals who share a particular developmental trajectory of a certain attribute, thus allowing a better understanding of the pattern of change in the variable.^{9,10} Among many studies that have reported childhood trajectory patterns,^{8,11–23} several showed the association between trajectories of developing obesity and adverse CV profiles. Regarding parental impact on these trajectories,^{8,11,14–24} several reports have focused on maternal body mass index (BMI) at various time points. However, few reports have discussed the impact of paternal factors,^{22,23} and no report has determined the impact of paternal BMIs on these trajectories using multivariate regression analysis. One longitudinal study showed that children with overweight or obese fathers were at a higher risk of becoming obese.²⁵

Therefore, this study aimed to determine the predictors for being in developmental trajectories with a high risk of adverse CV profiles in children by creating trajectories of longitudinal BMI z-scores from birth to the present. For this purpose, we analyzed separately the paternal and maternal impact on developmental trajectories by sex of the children.

RESEARCH DESIGN AND METHODS

Subjects

Participants consisted of 1,843 healthy child and adolescent volunteers (907 boys, 936 girls) aged 3–15 years who participated in a project between July 2012 and January 2014. This project was conducted in the following nine areas of Japan: Kagoshima, Fukuoka, Okayama, Hyogo, Aichi, Kanagawa, Chiba, Toyama, and Hokkaido. Participants were recruited via an announcement by

school officials, regional boards of education, or on the websites of the authors' affiliated hospitals. The project included medical examinations of participants at the time of the study and questionnaires that asked about current and past anthropometric data and lifestyle behavior of the participants and their parents. Written informed consent was obtained from the parents or guardians. The study was approved by the Ethics Committee of the National Hospital Organization of Kagoshima Medical Center.

Longitudinal anthropometric data for latent class models

Data on participants' height and weight at birth, during infancy, and after starting school were obtained using questionnaires. These exact data are available for all Japanese children and adolescents because the Ministry of Health, Labour and Welfare performs free medical examinations for infants. Additionally, the Ministry of Education, Culture, Sports, Science and Technology performs medical examinations for students in all school grades. These data are recorded in maternity health record books during the infant period and in report cards for school-age children; the records are kept by the parents. In this study, parents of the participants were asked to provide data on the height and weight of their children before medical examinations at the following data points: birth; 1, 3, 6, 9, 12 months; 1.5 and 3 years and at each grade after starting school. The inclusion criteria for the present study were the presence of three or more data points that should include the following anthropometric data taken at three points: less than 12 months, 1.5–6 years, and the current age. The mean±standard deviation (SD) number of anthropometric data points of the final subjects was 12±SD for both boys and girls.

Physical and blood biochemical parameters of participants at the time of the study

Height and weight were measured to the nearest 0.1 cm without shoes and to 0.1 kg with only underwear and without shoes, respectively. BMI was calculated as weight (kg) divided by the square of height (m²). The BMI z-score was calculated based on reference values for Japanese children.²⁶ Blood pressure was measured three times in the sitting position after 10 min of rest using an automated oscillatory system (TM-2571; A&D Co. Ltd.) and the mean value of the second and third measurements was used. Waist circumference was measured at the umbilical level to the nearest 0.1 cm without clothes.

Blood samples were collected in the morning after an overnight fast. High-density lipoprotein (HDL) cholesterol levels were determined using a direct quantitative assay. Levels of triglycerides, total cholesterol, alanine

TABLE 1 Values of Bayesian and Akaike information criterions for 2- to 6-trajectory models

	Boys		Girls	
	AIC ^a	BIC ^b	AIC ^a	BIC ^b
2-Trajectory model	-13,939	-13,977	-14,175	-14,213
3-Trajectory model	-13,466	-13,524	-13,729	-13,787
4-Trajectory model	-13,142	-13,219	-13,434	-13,512
5-Trajectory model	-12,942	-13,038	-13,229	-13,326
6-Trajectory model	-12,818 ^c	-12,933 ^c	-13,056 ^c	-13,172 ^c

^aAIC; Akaike Information Criterion^bBIC; Bayesian Information Criterion^cA smaller absolute value indicates a better fit for the model.

aminotransferase (ALT), and uric acid were determined with enzymatic assays using an automated analyzer (JCA-BM8060; JEOL Ltd.). Levels of fasting plasma glucose were determined using the hexokinase method (JCA-BM9000 series, JEOL Ltd.). Insulin levels were measured with a chemiluminescence immunological assay (Lumipulse® PrestoII; Fujirebio Inc.). Adiponectin, leptin, and high-sensitive C-reactive protein (CRP) levels were measured using a Human Adiponectin ELISA kit® (Otsuka Pharmaceutical Inc.), Human Leptin RIA kit® (Linco Research, Inc.), and N-Latex CRP II® kit (Dade Behring Inc.), respectively. All assays were performed by SRL Inc.

The homeostasis model assessment of insulin resistance (HOMA-IR)²⁷ was used as a surrogate marker for insulin resistance and was calculated as fasting insulin ($\mu\text{U/ml}$) \times fasting glucose (mmol/L)/22.5.

CV risk profile z-scores

Participants in each trajectory group had a wide range of ages, and each CV risk profile changed with age. Participants were divided into five age groups by sex: 3–5, 6–7, 8–9, 10–11, and 12–15 years, based on the age groups of the National Curriculum Standards by the Ministry of Education, Culture, Sports, Science and Technology.²⁸ z-scores of each CV risk profile in each group were obtained using the Lambda-Mu-Sigma method.²⁶

Predictors that might affect the trajectory

Predictors that might affect the trajectory (obtained through questionnaires) were birth order, number of siblings, breastfeeding duration, current parental age, parental height, parental weight, and parental smoking status. Parental overweight/obesity was defined as a BMI 25 kg/m^2 or more in the present study. We obtained maternal information for body weight immediately before pregnancy and immediately before delivery as well as information on the presence or absence of

gestational urinary glucose and gestational diabetes mellitus. These maternal data are recorded in maternity health record books. Gestational weight gain (GWG) was calculated by subtracting body weight immediately before pregnancy from body weight immediately before delivery. GWG was categorized in accordance with the recently updated recommendations of the Japan Society of Obstetrics and Gynecology for Japanese women as follows²⁹: underweight mothers (BMI $< 18.5 \text{ kg/m}^2$) who gained 12–15 kg; normal weight mothers (BMI ≥ 18.5 and $< 25 \text{ kg/m}^2$) who gained 10–13 kg; overweight mothers (BMI ≥ 25 and $< 30 \text{ kg/m}^2$) who gained 7–10 kg, and mothers with obesity (BMI $\geq 30.0 \text{ kg/m}^2$) who gained up to 5 kg. Mothers who gained weight below or above the relevant criteria were categorized as inadequate or excessive GWG, respectively. We determined the 10th and 90th percentiles of the participant's birthweight. Tenth percentile values were 2,529 and 2,468 g in boys and girls, respectively; 90th percentile values were 3,518 and 3,500 g in boys and girls, respectively.

Statistical analysis

Latent class growth models were applied using “proc traj”, which is a statistical analysis software macro used for identifying and describing the BMI z-score trajectory groups.^{8,11,13,14,18,20} The Bayesian Information Criterion (BIC) and Akaike Information Criterion (AIC) were used to determine the better trajectory group between the two and six trajectory models. The BIC and AIC values showed that the six-trajectory model was best in both boys and girls (Table 1); therefore, the six-trajectory model was applied in the present study. Seven or more trajectory models were not used because of their complexity.

Statistical significance for the difference in mean values of the variables among trajectory groups was determined using analysis of variance and Tukey's test. When the data were skewed in distribution, statistical analyses were performed using the Kruskal–Wallis and Bonferroni's tests. For analysis of the predictive factors of participants being in a certain trajectory, univariate and multiple logistic regression analyses were performed

using the middle-trajectory group (normal weight group) as the reference. In multiple regression analysis, variables that were significant in univariate regression analysis were used. Statistical analysis was performed using IBM SPSS® Statistics, version 23.0 (IBM Japan, Ltd.). A two-tailed probability value of less than 0.05 was considered statistically significant.

RESULTS

Of the 1,843 participants (907 boys, 936 girls), 11 (three boys and eight girls) were excluded because they did not fulfill the inclusion criteria. A final total of 1,832 participants (904 boys, 928 girls) were included in the study. Characteristics of the 1,832 participants by sex are shown in [Table 2](#).

BMI z-score trajectories

Six BMI z-score trajectories were denoted. Trajectory 1 to Trajectory 6 for boys and girls at 12 years old from the bottom to the top are shown in [Figure 1a,b](#), respectively.

Trajectory-6 boys were born with the highest mean BMI z-scores (0.42), which sharply increased during the early infantile period, and thereafter, the scores remained high. Participants in this pattern of trajectory were named the “infantile onset” group. Trajectory-5 boys were born with a relatively low mean z-score (−0.39), but not the lowest, and this score increased continually thereafter, until the elementary school period. Participants in this pattern of trajectory were named the “continual increase” group. Trajectory-4 boys were born with low mean-scores (−0.71), which increased slowly to nearly zero by 3 years old. The z-scores then remained the same during the preschool and school periods. Trajectory-3 boys showed slightly high z-scores during early infancy and then declined to near zero z-scores. Trajectory-2 boys were born with near zero z-scores and their scores decreased to the present. Trajectory-1 boys were born with the lowest mean z-scores (−0.97) and remained below zero from birth to the present. The six trajectory groups were re-categorized as “high-” (Trajectory-6 and -5), “middle-” (Trajectory-4 and -3), and “low-” (Trajectory-2 and -1).

Girls showed similar patterns to boys during infancy. The infantile onset group was born with the highest mean BMI z-scores (0.92) and the continual increase group was born with relatively low mean z-scores (−0.39), but they were not the lowest. The continual increase group finally reached the highest z-scores (Trajectory-6).

The number of anthropometric data points and the mean±SD of the BMI z-score at each point in each trajectory are shown in [Table S1](#).

Characteristics in CV risk profiles among the six groups by sex

In boys and girls, nearly all CV profiles showed statistically significant trends across the trajectory groups, except for fasting plasma glucose and HbA1c levels in boys, and total cholesterol, fasting plasma glucose, and HbA1c levels in girls ([Table 3](#)).

All CV profiles by z-score showed similar significant trends across the trajectory groups after z-score transformation ([Table 4](#)). There was a clear sex difference in changes across the six trajectories ([Figure 2](#) and [Figure S1](#)), which might reflect the sex difference of the trajectory patterns shown in [Figure 1](#). Boys showed a stepwise increase in CV profile z-scores as trajectories changed from low to middle and from middle to high trajectories, as shown by waist circumference, systolic blood pressure, and leptin. In contrast, girls showed a linear increase in CV profile z-scores from Trajectory-1 to Trajectory-6 as shown for BMI, waist circumference, HOMA-IR, and leptin. The z-scores of CV risk profiles by sex and by the three (high, middle, and low) trajectory groups showed that participants in the high-trajectory group had more adverse CV profiles than those in the middle-trajectory group ([Table S2](#)).

Predictive factors for being in the high-trajectory group

In the infantile onset group (Trajectory-6 in boys and Trajectory-5 in girls), univariate regression analysis showed that maternal present BMI of at least 25 kg/m², maternal pre-pregnancy BMI of at least 25 kg/m², and paternal present BMI of at least 25 kg/m² were significant predictors for being in this group in boys and girls. Additionally, birthweight less than the 10th percentile in boys, birthweight of the 95th percentile or more, and maternal excessive GWG in girls, were significant predictors ([Table 5](#)). Multiple regression analysis showed that maternal pre-pregnancy BMI of 25 kg/m² or more ($p = 0.009$) and paternal present BMI of 25 kg/m² or more ($p = 0.009$) in boys, and maternal excessive GWG ($p = 0.01$) were independent predictive factors for being in the high trajectory group.

In boys in the continual increase group (Trajectory-5), having no sibling was a significant predictor among all variables used in univariate regression analysis ([Table 6](#)). In girls (Trajectory 6), the following variables were significant risk factors by univariate analysis: low birthweight (<10th percentile), high maternal age, and paternal current BMI of 25 kg/m² or more. Multiple regression analysis showed that a high maternal age ($p = 0.01$) and paternal present BMI of 25 kg/m² or more ($p = 0.009$) were independent predictive factors for children being in the continual increase group.

TABLE 2 Characteristics of the participants

	Boys	Girls	<i>p</i> value
Number of participants	904	928	
Age (year)	10.1 ± 3.0	10.2 ± 2.9	0.77
Height (cm)	138.1 ± 18.9	137.0 ± 16.6	0.20
Weight (kg)	34.2 ± 13.3	33.3 ± 11.9	0.13
Body mass index (BMI, kg/m ²)	17.2 ± 2.9	17.1 ± 2.9	0.49
BMI z score	-0.26 ± 1.06	-0.31 ± 0.99	0.33
Weight status (Normal/Overweight/Obese)			
IOTF definition	779/95/30	840/69/19	0.004
CDC definition	764/93/47	844/57/27	<0.001
Waist (cm)	60.4 ± 9.7	59.8 ± 9.0	0.18
Systolic blood pressure (mmHg)	98 ± 11	97 ± 9	0.03
Diastolic blood pressure (mmHg)	54 ± 9	54 ± 8	0.62
Triglyceride (mmol/L)	0.58 [0.41, 0.80]	0.66 [0.46, 0.94]	<0.001
Total Cholesterol (mmol/L)	4.32 ± 0.68	4.42 ± 0.70	0.002
HDL-Cholesterol (mmol/L)	1.64 ± 0.33	1.61 ± 0.31	0.03
non-HDL Cholesterol (mmol/L)	2.68 ± 0.60	2.81 ± 0.64	<0.001
Fasting plasma glucose (mmol/L)	4.79 ± 0.37	4.68 ± 0.35	<0.001
Insulin (pmol/L)	30.9 [17.3, 48.7]	36.1 [21.5, 58.9]	<0.001
HbA1c (%)	5.28 ± 0.23	5.25 ± 0.24	0.005
HOMA-IR	0.93 [0.51, 1.49]	1.06 [0.62, 1.76]	<0.001
Alanine aminotransferase (U/L)	15 [12, 19]	13 [11, 16]	<0.001
Uric acid (μmol/L)	274 ± 71	254 ± 49	<0.001
Leptin (ng/ml)	3.0 [2.2, 4.9]	4.9 [3.3, 8.5]	<0.001
Adiponectin (μg/ml)	11.1 ± 4.5	10.8 ± 4.3	0.16
hs-C reactive protein (ng/ml)	95 [25, 259]	84 [25, 247]	0.23
Maternal characteristics			
Age (year)	39.8 ± 4.7	40.0 ± 5.0	0.38
BMI at present (kg/m ²)	21.5 ± 3.4	21.5 ± 3.2	0.92
BMI before pregnancy (kg/m ²)	20.5 ± 2.8	20.5 ± 2.6	0.73
Weight gain during pregnancy (kg) ^a	9.9 ± 4.1	10.0 ± 3.9	0.50
BMI retention (kg/m ²) ^b	3.0 ± 1.9	3.0 ± 2.0	0.94
Paternal characteristics			
Age (year)	41.6 ± 5.8		
BMI at present (kg/m ²)	41.9 ± 6.0	0.17	
BMI at present (kg/m ²)	23.8 ± 3.2	23.7 ± 3.1	0.64

Note: Normally distributed values are expressed as the mean and standard deviation. Data with a skewed distribution are expressed as the median and [25th/75th percentile] values. Statistical analysis was performed after natural logarithm transformation.

Abbreviations: CDC, Centers for Disease Control and Prevention; HbA1c, hemoglobin A1c; hs, high-sensitivity; HOMA-IR, homeostasis model assessment of insulin resistance; IOTF, International Obesity Task Force.

^aGestational weight gain was calculated by subtracting weight immediately before pregnancy from weight immediately before delivery.

^bBody mass index (BMI) retention was calculated by subtracting BMI immediately before pregnancy from current BMI in the present study.

Trajectories 5 and 6 in boys finally fused together (Figure 1), then predictive factors were determined after both groups were combined (Table S3). Multiple regression analysis showed that a maternal pre-pregnancy BMI of 25 or more and paternal present BMI of the same were independently predictive for boy's being in the high trajectory group.

DISCUSSION

The present study showed that children in the two high-trajectory groups (infantile onset and continual increase groups) had significantly worse levels of many CV profiles than those in the middle-trajectory groups. Paternal overweight/obesity was an independent predictor for

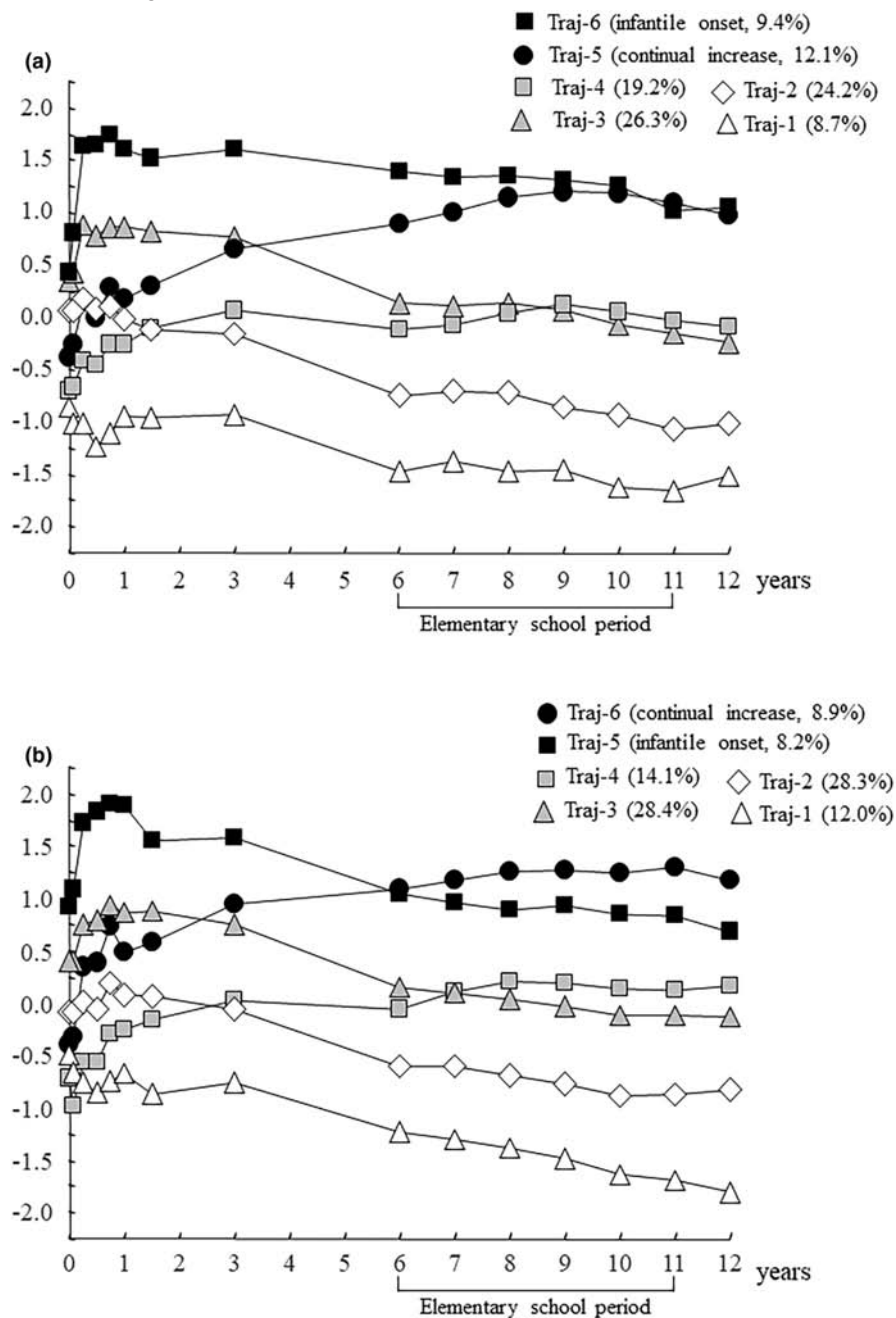


FIGURE 1 Trajectories of body mass index (BMI) z-scores in (a) boys and (b) girls using six trajectory latent class growth models. The six trajectories were denoted Trajectory-1 to Trajectory-6 in both sexes at 12 years old from the bottom to the top. Abbreviation: Traj-, Trajectory-.

boys being in the infantile onset group and for girls being in the continual increase group. Additionally, maternal pre-pregnancy overweight/obesity in boys and excessive GWG in girls were independent predictors for being in the infantile onset group. Having no sibling in boys and an older maternal age in girls were independent predictors for being in the continual increase group.

The association between trajectories of developing obesity and CV profiles has been previously reported.^{11,14,23} The present study showed that many CV profiles showed significant trends across the trajectory groups in both sexes, including waist circumference,

blood pressure, lipid profiles, insulin resistance, a marker of nonalcoholic steatohepatitis, and biomarkers (leptin, adiponectin, and high-sensitive CRP; Table 2). Interestingly, several CV risk variables across the trajectories were different by sex. Boys showed a stepwise increase in CV profile z-scores as they changed from the low- to high-trajectory groups, while girls showed a linear increase in CV profile z-scores from Trajectory-1 to Trajectory-6. The difference in CV profile z-scores across the six trajectories by sex (Figure 2) may have been associated with the difference in the trajectory patterns by sex (Figure 1). The present study revealed that

TABLE 3 Characteristics of participants by sex in each trajectory group

	Trajectory-1	Trajectory-2	Trajectory-3	Trajectory-4	Trajectory-5	Trajectory-6	Trend <i>p</i>
Males							
Number of subjects	79	219	238	174	109	85	
Age (year)	9.7 ± 3.2	9.8 ± 3.1	10.1 ± 2.9	10.3 ± 2.8	10.8 ± 2.7	10.0 ± 2.8	0.09
Height (cm)	133.7 ± 20.2	135.0 ± 19.1	137.9 ± 18.4	139.7 ± 19.1	144.0 ± 16.9	140.2 ± 18.3	<0.001
Weight (kg)	26.9 ± 10.6	28.9 ± 10.4	33.3 ± 11.3**	34.6 ± 12.1	44.9 ± 14.5***	42.7 ± 15.9	<0.001
Body mass index (kg/m ²)	14.4 ± 1.5*	15.2 ± 1.3***	16.9 ± 1.5	17.1 ± 1.9	21.0 ± 3.0***	20.9 ± 3.3	<0.001
Body mass index z-score	-1.79 ± 0.71***	-1.09 ± 0.59***	-0.15 ± 0.61	-0.17 ± 0.59	1.03 ± 0.60***	1.13 ± 0.61	<0.001
Weight status (Normal/Overweight/Obese)							
IOTF definition	79/0/0	219/0/0	234/4/0	166/8/0	45/51/13	36/32/17	<0.001
CDC definition	79/0/0	219/0/0	224/14/0	165/8/1	46/42/21	31/29/25	<0.001
Waist circumference (cm)	53.9 ± 6.0	55.2 ± 5.7	58.9 ± 6.3***	60.2 ± 7.7	71.6 ± 10.5***	69.7 ± 12.2	<0.001
Systolic blood pressure (mmHg)	95 ± 10	94 ± 8	98 ± 10**	98 ± 11	104 ± 11***	103 ± 11	<0.001
Diastolic blood pressure (mmHg)	53 ± 8	52 ± 7	54 ± 8	53 ± 8	57 ± 9*	58 ± 11	<0.001
Triglyceride (mmol/L)	45 [33, 59]	47 [34, 63]	53 [36, 66]	50 [36, 74]	60 [42, 82]	59 [42, 104]	<0.001
Total cholesterol (mmol/L)	4.23 ± 0.62	4.31 ± 0.64	4.18 ± 0.63	4.31 ± 0.71	4.54 ± 0.77*	4.51 ± 0.67	<0.001
HDL-cholesterol (mmol/L)	1.69 ± 0.33	1.68 ± 0.35	1.63 ± 0.30	1.64 ± 0.35	1.56 ± 0.32	1.6 ± 0.32	0.01
Non-HDL-cholesterol (mmol/L)	2.54 ± 0.53	2.62 ± 0.53	2.55 ± 0.55	2.67 ± 0.61	2.99 ± 0.73***	2.92 ± 0.60	<0.001
Fasting plasma glucose (mmol/L)	4.78 ± 0.45	4.76 ± 0.38	4.78 ± 0.34	4.80 ± 0.30	4.87 ± 0.42	4.78 ± 0.36	0.19
Insulin (pmol/L)	3.5 [2.0, 5.2]	3.2 [1.7, 5.5]	4.2 [2.7, 6.4]***	4.9 [3.0, 7.0]	7.2 [4.4, 11.1]***	5.7 [3.5, 9.3]	<0.001
Hemoglobin A1c (%)	5.3 ± 0.2	5.3 ± 0.2	5.3 ± 0.2	5.3 ± 0.2	5.3 ± 0.2	5.3 ± 0.2	0.08
HOMA-IR	0.71 [0.41, 1.15]	0.65 [0.33, 1.15]	0.86 [0.57, 1.38]***	1.05 [0.60, 1.43]	1.51 [0.89, 2.43]***	1.19 [0.74, 2.10]	<0.001
Alanine aminotransferase (U/L)	14 [12, 17]	14 [12, 18]	15 [12, 18]	15 [13, 18]	18 [14, 25]***	17 [14, 24]	<0.001
Uric acid (μmol/L)	259 ± 65	260 ± 59	270 ± 63	276 ± 66	309 ± 105	287 ± 72	<0.001
Leptin (ng/ml)	2.3 [1.8, 2.9]	2.5 [2.0, 3.0]	3.0 [2.2, 4.3]**	3.4 [2.3, 5.2]*	7.9 [3.9, 13.3]***	6.0 [3.8, 10.7]	<0.001
Adiponectin (μg/ml)	11.6 ± 3.7	11.6 ± 4.3	11.5 ± 5.0	10.7 ± 4.0	9.4 ± 4.6	10.8 ± 4.4	<0.001
High sensitive-CRP (ng/ml)	78 [25, 233]	62 [25, 198]	80 [25, 178]	90 [25, 279]	195 [87, 446]**	175 [89, 345]	0.04
Females							
Number of subjects	111	263	264	131	76	83	
Age (year)	9.7 ± 3.1	9.9 ± 3.0	10.2 ± 2.9	10.3 ± 2.8	10.5 ± 2.7	11.0 ± 2.4	0.02

(Continues)

TABLE 3 (Continued)

	Trajectory-1	Trajectory-2	Trajectory-3	Trajectory-4	Trajectory-5	Trajectory-6	Trend <i>p</i>
Height (cm)	133.1 ± 18.0	135.1 ± 17.1	137.2 ± 16.4	137.6 ± 16.5	140.5 ± 15.3	143.9 ± 13.0	<0.001
Weight (kg)	26.2 ± 8.9	29.6 ± 10.3*	33.3 ± 10.7**	34.5 ± 11.1	40.4 ± 11.6**	45.9 ± 12.6*	<0.001
Body mass index (kg/m ²)	14.3 ± 1.3	15.6 ± 1.8***	17.1 ± 1.8***	17.6 ± 2.1	20.0 ± 2.7***	21.7 ± 3.3***	<0.001
Body mass index z score	-1.71 ± 0.59	-0.87 ± 0.52***	-0.13 ± 0.55***	0.06 ± 0.58	0.79 ± 0.73***	1.18 ± 0.67***	<0.001
Weight status (Normal/Overweight/Obese)							
IOTF definition	111/0/0	263/0/0	257/7/0	125/5/1	48/21/7	36/36/11	<0.001
CDC definition	111/0/0	263/0/0	258/5/1	124/6/1	50/18/8	38/28/17	<0.001
Waist circumference (cm)	53.0 ± 5.6	56.3 ± 6.6**	59.3 ± 7.1***	61.3 ± 7.4	67.1 ± 8.6***	72.6 ± 9.8***	<0.001
Systolic blood pressure (mmHg)	93 ± 9	94 ± 9	98 ± 9**	97 ± 9	100 ± 9	104 ± 10	<0.001
Diastolic blood pressure (mmHg)	53 ± 7	53 ± 7	55 ± 7	53 ± 8	56 ± 8	56 ± 8	<0.001
Triglyceride (mmol/L)	54 [39,75]	52 [38,74]	57 [41,81]	59 [45,89]	67 [46,90]	72 [50,104]	<0.001
Total cholesterol (mmol/L)	4.49 ± 0.80	4.35 ± 0.67	4.41 ± 0.69	4.46 ± 0.75	4.51 ± 0.70	4.44 ± 0.61	0.41
HDL-cholesterol (mmol/L)	1.64 ± 0.29	1.61 ± 0.32	1.63 ± 0.29	1.62 ± 0.32	1.53 ± 0.29	1.51 ± 0.30	0.005
Non-HDL-cholesterol (mmol/L)	2.84 ± 0.72	2.74 ± 0.59	2.77 ± 0.61	2.84 ± 0.64	2.98 ± 0.73	2.93 ± 0.61	0.03
Fasting plasma glucose (mmol/L)	4.64 ± 0.34	4.67 ± 0.39	4.69 ± 0.33	4.68 ± 0.35	4.69 ± 0.32	4.75 ± 0.31	0.34
Insulin (pmol/L)	4.0 [2.7,6.2]	4.6 [2.6,7.6]	5.4 [3.2,8.1]	5.5 [4.2,8.2]	6.6 [4.0,10.8]	8.5 [6.1,11.5]	<0.001
Hemoglobin A1c (%)	5.3 ± 0.2	5.2 ± 0.2	5.2 ± 0.2	5.2 ± 0.3	5.3 ± 0.2	5.3 ± 0.2	0.37
HOMA-IR	0.79 [0.53, 1.29]	0.94 [0.52, 1.58]	1.07 [0.62, 1.66]	1.11 [0.79, 1.72]	1.37 [0.78, 2.28]	1.70 [1.28, 2.30]	<0.001
Alanine aminotransferase (U/L)	12 [11, 15]	13 [11, 15]	13 [11, 16]	13 [11, 16]	13 [11, 17]	15 [12, 22]**	<0.001
Uric acid (μmol/L)	242 ± 47	247 ± 45	249 ± 47	266 ± 49	259 ± 49	284 ± 56	<0.001
Leptin (ng/ml)	3.1 [2.5, 4.5]	3.8 [3.0, 5.9]**	4.7 [3.4, 7.5]**	6.6 [4.2, 9.6]***	8.7 [5.3, 14.4]**	15.0 [8.4, 20.0]**	<0.001
Adiponectin (μg/ml)	11.5 ± 3.9	11.4 ± 4.9	11.3 ± 4.1	9.5 ± 3.6***	10.4 ± 4.7	8.4 ± 3.1*	<0.001
High sensitive-CRP (ng/ml)	83 [25, 293]	64 [25, 181]	75 [25, 183]	104 [38, 239]	136 [32, 480]	228 [88, 539]	<0.001

Note: Normally distributed values are expressed as mean and ± standard deviation. Data with a skewed distribution are expressed as the median and [25th/75th percentile] values.

Statistical analyses for trend *P* were performed by analysis of variance. Differences in the mean values between groups were analyzed by Tukey's test. When the data were skewed in distribution, statistical analyses were performed by the Kruskal-Wallis and Bonferroni's tests. Statistical significance (****p* < 0.001, ***p* < 0.01, **p* < 0.05) is indicated when the group showed a significantly different mean value compared with the former group. Abbreviations: CDC, Centers for Disease Control and Prevention; CRP, C-reactive protein; HDL, high density lipoprotein; HOMA-IR, homeostasis assessment of insulin resistance; IOTF, International Obesity Task Force.

TABLE 4 z-scores of cardiovascular risk profiles of participants by sex in each trajectory group

	Trajectory-1	Trajectory-2	Trajectory-3	Trajectory-4	Trajectory-5	Trajectory-6	Trend P
Males							
Number of subjects	79	219	238	174	109	85	
Height	-0.37±0.85	-0.22±0.94	-0.02±1.02	0.07±0.97	0.32±1.00	0.41±1.04	<0.001
Weight	-0.91±0.50	-0.61±0.54*	-0.05±0.73***	-0.03±0.70	1.06±1.00***	1.21±1.09	<0.001
Body mass index	-1.79±0.71	-1.09±0.59***	-0.15±0.61***	-0.17±0.59	1.03±0.60***	1.13±0.61	<0.001
Waist circumference	-0.79±0.42	-0.61±0.48	-0.13±0.71***	-0.07±0.65	1.21±1.02***	1.24±1.16	<0.001
Systolic blood pressure	-0.27±1.00	-0.33±0.80	0.00±0.96**	-0.05±1.01	0.54±1.06***	0.50±1.05	<0.001
Diastolic blood pressure	-0.17±0.92	-0.18±0.88	0.03±0.99	-0.11±0.96	0.24±1.06*	0.46±1.21	<0.001
Triglyceride	-0.38 [-0.77 to 0.21]	-0.35 [-0.76 to 0.11]	-0.18 [-0.72 to 0.28]	-0.24 [-0.69 to 0.48]	0.06 [-0.53 to 0.78]	0.08 [-0.51 to 1.21]	<0.001
Total cholesterol	-0.12±0.93	0.00±0.97	-0.20±0.94	-0.02±1.04	0.30±1.06	0.30±1.01	<0.001
HDL cholesterol	0.17±0.98	0.15±1.07	-0.03±0.89	0.01±1.06	-0.27±0.96	-0.13±0.97	0.005
Non-HDL cholesterol	-0.25±0.90	-0.11±0.86	-0.23±0.92	-0.03±1.03	0.47±1.13***	0.39±1.05	<0.001
Fasting plasma glucose	0.01±1.26	-0.05±1.03	-0.02±0.94	0.01±0.84	0.19±1.10	-0.05±0.98	0.45
Insulin	-0.39 [-0.83 to 0.11]	-0.40 [-0.76 to -0.05]	-0.21 [-0.59 to 0.24]**	-0.08 [-0.51 to 0.28]	0.38 [-0.31 to 1.13]**	-0.02 [-0.29 to 0.94]	<0.001
Hemoglobin A1c	-0.01±1.01	-0.01±1.05	-0.12±0.98	0.03±0.94	0.17±0.97	0.08±1.03	0.20
HOMA-IR	-0.32 [-0.78 to 0.11]	-0.37 [-0.74 to -0.03]	-0.23 [-0.59 to 0.16]*	-0.14 [-0.54 to 0.31]	0.27 [-0.26 to 1.19]**	0.02 [-0.33 to 0.94]	<0.001
Alanine aminotransferase	-0.28 [-0.49 to -0.04]	-0.25 [-0.43 to -0.01]	-0.27 [-0.48 to 0.03]	-0.23 [-0.41 to -0.03]	0.01 [-0.28 to 0.56]***	-0.09 [-0.32 to 0.31]	<0.001
Uric acid	-0.19±0.96	-0.18±0.90	-0.06±0.86	0.01±0.93	0.38±1.36*	0.27±1.09	<0.001
Leptin	-0.51 [-0.70 to -0.35]	-0.51 [-0.64 to -0.35]	-0.38 [-0.59 to -0.05]***	-0.27 [-0.50 to 0.18]	0.67 [0.02 to 1.48]***	0.40 [-0.18 to 1.28]	<0.001
Adiponectin	0.08±0.79	0.08±0.98	0.10±1.08	-0.04±0.95	-0.31±1.05	-0.07±1.00	0.01
High sensitive-CRP	-0.24 [-0.31 to -0.17]	-0.25 [-0.31 to -0.17]	-0.24 [-0.30 to -0.17]	-0.22 [-0.29 to -0.13]	-0.15 [-0.23 to 0.18]***	-0.18 [-0.27 to -0.03]	<0.001
Females							
Number of subjects	111	263	264	131	76	83	
Height	-0.28±0.99	-0.05±1.00	0.06±1.00	-0.08±0.93	0.24±1.00	0.30±1.04	<0.001
Weight	-0.95±0.58	-0.42±0.62***	0.08±0.79***	0.08±0.66***	0.96±0.98***	1.41±1.17**	<0.001
Body mass index	-1.71±0.59	-0.87±0.52***	-0.13±0.55***	0.06±0.58*	0.79±0.73***	1.18±0.67***	<0.001
Waist circumference	-0.94±0.47	-0.41±0.58***	-0.03±0.74***	0.15±0.72	0.98±1.00***	1.54±1.20***	<0.001
Systolic blood pressure	-0.35±0.92	-0.25±0.95	0.07±0.94**	0.05±0.93	0.31±0.94	0.67±1.19	<0.001

(Continues)

TABLE 4 (Continued)

	Trajectory-1	Trajectory-2	Trajectory-3	Trajectory-4	Trajectory-5	Trajectory-6	Trend <i>P</i>
Diastolic blood pressure	-0.11 ± 0.95	-0.12 ± 0.96	0.09 ± 1.01	-0.09 ± 0.98	0.32 ± 1.06	0.14 ± 1.02	0.003
Triglyceride	-0.19 [-0.75 to 0.27]	-0.38 [-0.81 to 0.28]	-0.26 [-0.75 to 0.44]	-0.17 [-0.66 to 0.66]	0.05 [-0.48 to 0.73]	0.12 [-0.47 to 1.08]	<0.001
Total cholesterol	0.10 ± 1.16	-0.10 ± 0.95	-0.02 ± 0.99	0.05 ± 1.06	0.12 ± 0.98	0.03 ± 0.85	0.37
HDL-cholesterol	0.15 ± 0.95	0.03 ± 1.03	0.08 ± 0.97	0.02 ± 1.05	-0.26 ± 0.96	-0.35 ± 0.98	0.002
Non-HDL cholesterol	0.07 ± 1.12	-0.09 ± 0.93	-0.04 ± 0.93	0.06 ± 0.99	0.27 ± 1.10	0.20 ± 0.91	0.03
Fasting plasma glucose	-0.12 ± 0.98	-0.01 ± 1.05	0.02 ± 0.97	-0.01 ± 1.04	0.00 ± 1.04	0.14 ± 0.93	0.67
Insulin	-0.42 [-0.73 to 0.10]	-0.35 [-0.71 to 0.17]	-0.21 [-0.60 to 0.39]	-0.15 [-0.52 to 0.40]	0.01 [-0.50 to 0.72]	0.18 [-0.34 to 1.14]	<0.001
Hemoglobin A1c	0.07 ± 1.01	-0.03 ± 1.01	-0.04 ± 0.88	-0.04 ± 1.11	0.18 ± 1.09	0.06 ± 1.03	0.52
HOMA-IR	-0.43 [-0.67 to 0.06]	-0.35 [-0.67 to 0.20]	-0.22 [-0.60 to 0.27]	-0.11 [-0.49 to 0.42]	-0.03 [-0.47 to 0.71]	0.16 [-0.30 to 1.01]	<0.001
Alanine aminotransferase	-0.27 [-0.53 to 0.05]	-0.24 [-0.47 to 0.14]	-0.24 [-0.51 to 0.19]	-0.18 [-0.47 to 0.11]	-0.24 [-0.53 to 0.29]	0.00 [-0.38 to 0.82]	0.005
Uric acid	-0.22 ± 0.95	-0.11 ± 0.95	-0.10 ± 0.94	0.23 ± 1.00*	0.10 ± 1.03	0.54 ± 1.14	<0.001
Leptin	-0.62 [-0.81 to -0.45]	-0.47 [-0.67 to -0.21]**	-0.33 [-0.59 to 0.13]**	-0.04 [-0.46 to 0.41]*	0.38 [-0.30 to 1.32]	1.21 [0.07 to 2.16]	>0.001
Adiponectin	0.13 ± 0.92	0.12 ± 1.11	0.13 ± 0.94	-0.30 ± 0.82**	-0.05 ± 1.18	-0.50 ± 0.74*	<0.001
High sensitive-CRP	-0.17 [-0.25 to -0.09]	-0.20 [-0.28 to -0.13]	-0.18 [-0.26 to -0.11]	-0.13 [-0.23 to -0.08]	-0.13 [-0.21 to -0.02]	-0.03 [-0.13 to 0.19]	<0.001

Note: Normally distributed values are expressed as the mean and standard deviation. Data with a skewed distribution are expressed as the median [25th/75th percentile] values. Statistical analyses for trend *P* were performed by analysis of variance. Differences in the mean values between groups were analyzed by Tukey's test. When the data were skewed in distribution, statistical analyses were performed by the Kruskal-Wallis and Bonferroni's tests. Statistical significance (****p* < 0.001, ***p* < 0.01, **p* < 0.05) is indicated when the group showed a significantly different mean value compared with the former group.

Abbreviations: CDC, Centers for Disease Control and Prevention; CRP, C-reactive protein; HOMA-IR, homeostasis assessment of insulin resistance; IOTF, International Obesity Task Force.

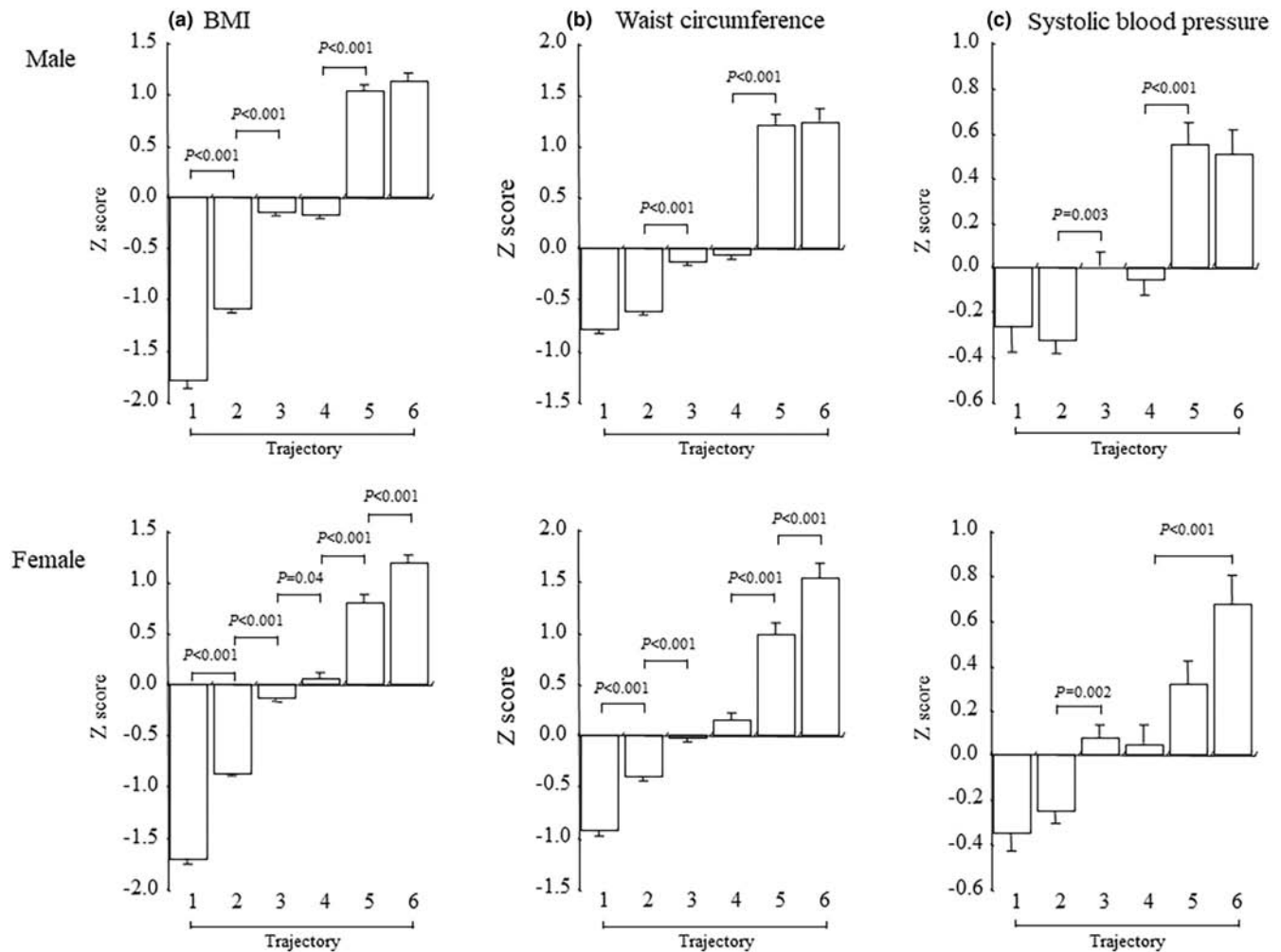


FIGURE 2 Representative data of the difference in z-scores across six trajectories for (a) body mass index (BMI) (b) waist circumference, and (c) systolic blood pressure by sex. The upper panels show data for boys and the lower panels show data for girls. Data are mean and standard error of the mean.

this difference in CV profiles by sex was present not only in the change in HOMA-IR,³⁰ but also in many other CV profiles including BMI, waist circumference, systolic blood pressure, and leptin (Figure 2). Our findings suggest that developing unfavorable profiles differ by sex.

This study showed that paternal overweight/obesity had a significant effect on children being in the high-risk trajectory groups. One potential reason was that a relatively large number of data points, particularly those in infancy, made it possible to differentiate the high-risk groups from others. Another reason might be that we analyzed paternal and maternal impacts on developmental trajectories by sex of children separately. The association between maternal BMIs at various time points and children's growth trajectories has been extensively investigated.^{13,14,18–22,24} However, a few reports have shown that paternal BMI is associated with children's growth trajectories.^{21,22} Koning et al.²¹ reported that the odds ratio (OR) for paternal overweight status was significantly higher (OR, 1.6; 95% confidence interval [CI] 1.1–2.4) for children in the increasing trajectory compared with those in the decreasing trajectory at

12 years old. Magee et al.²² described that paternal overweight was significantly associated with the “early-onset” trajectory group only (OR, 2.87; 95% CI 1.40–5.89) among three overweight/obesity trajectory groups at 10–11 years old. These studies analyzed the combined data of boys and girls and used univariate regression analysis. Systematic review articles have unequivocally demonstrated that fathers are underrepresented in observational research on childhood obesity.^{31,32} Davison et al. reported that in more than 600 studies, only 1% of studies included only fathers and only 10% of all eligible studies included independent results for fathers.³¹ Morgan et al.³² reported that in 133 randomized controlled trials in which participation was open to both parents, 92% did not report objective data on father involvement. They concluded that researchers should strive to report more comprehensive data to highlight the involvement and engagement of fathers in their studies. To the best of our knowledge, this is the first report to show that paternal overweight/obesity is an independent predictor for children being in the high-risk trajectory group in boys and girls using multivariate regression analysis.

TABLE 5 Predictive factors of being in the infantile onset group (trajectories 6 in boys and 5 in girls) using the middle trajectory group (trajectories 3 and 4) as a reference by univariate and multiple logistic regression analysis

Variable	Reference	Boys (<i>n</i> = 904)				Girls (<i>n</i> = 928)			
		Univariate		Multivariate (<i>n</i> = 365)		Univariate		Multivariate (<i>n</i> = 189)	
		Total	OR	95% CI	<i>p</i>	Total	OR	95% CI	<i>p</i>
Child									
Age	Per 1 year	497	0.96	0.87–1.06		471	1.09	0.98–1.21	
Birth weight <10th percentile	10≤ & <90th	425	0.20	0.05–0.86*	0.08	397	0.31	0.07–1.35	
Birth weight ≥90th percentile	10≤ & <90th	444	1.30	0.67–2.52		422	3.19	1.74–5.83***	1.76
Number of siblings	≥1 sibling	497	0.82	0.35–1.95		470	0.81	0.34–1.90	0.77–3.99
Mother									0.18
Age	Per 1 year	493	1.00	0.95–1.06		469	1.03	0.98–1.08	
BMI ≥25 at present	Normal weight	441	2.42	1.31–4.48**	0.62	418	2.18	1.15–4.12*	0.73
BMI ≥25 before pregnancy	Normal weight	413	3.38	1.52–7.54**	0.009	402	2.76	1.20–6.24*	1.22
Excess gestational weight gain ^a	Adequate	254	1.51	0.81–2.81		253	3.10	1.60–6.02***	2.75
BMI retention ^b	Per 1 BMI	489	1.07	0.94–1.22		462	0.94	0.81–1.09	1.26–5.99
Father									0.01
Age	Per 1 year	468	1.00	0.96–1.04		441	1.01	0.97–1.06	
BMI ≥25 at present	Normal weight	442	1.93	1.15–2.87*	0.009	429	2.20	1.28–3.78**	2.05

Note: Each analysis was adjusted for geographic areas.

Variables which were significant by multiple regression analysis were expressed in bold.

Abbreviations; BMI, body mass index; CI, confidence interval; OR, Odds's ratio. *p* value: ****p* < 0.001; ***p* < 0.01; **p* < 0.05.

^aGestational weight gain was calculated by subtracting weight immediately before pregnancy from weight immediately before delivery and was categorized as inadequate, adequate, and excess based on the recommendation of the Japan Society of Obstetrics and Gynecology (refer to the text).

^bBMI retention was calculated by subtracting BMI immediately before pregnancy from present BMI. Parental smoking status was not significant.

TABLE 6 Predictive factors of being in the continual increase group (trajectory 5 in boys and trajectory 6 in girls) using the middle trajectory group (trajectories 3 and 4) as a reference by univariate and multiple logistic regression analysis

Variable	Reference	Boys (<i>n</i> = 904)				Girls (<i>n</i> = 928)			
		Univariate		Multiple		Univariate		Multiple	
		Total	OR	95% CI	<i>p</i>	Total	OR	95% CI	<i>p</i>
Child									
Age	Per 1 year	521	1.09	0.99–1.20		478	1.11	0.99–1.23	
Birth weight < 10th percentile	10 ≤ & < 90th	454	1.37	0.72–2.64		422	2.06	1.07–3.98*	1.96
Birth weight ≥ 90th percentile	10 ≤ & < 90th	453	0.44	0.18–1.07		416	0.59	0.22–1.58	0.94–4.10
Number of siblings	≥ 1 sibling	520	1.88	1.04–3.43*		476	1.22	0.61–2.44	0.08
Mother									
Age	Per 1 year	516	1.04	0.99–1.09		474	1.07	1.01–1.12*	1.07
BMI ≥ 25 at present	Normal weight	457	1.27	0.65–2.49		424	1.33	0.68–2.57	1.02–1.14
BMI ≥ 25 before pregnancy	Normal weight	424	1.87	0.76–4.62		404	1.76	0.69–4.47	0.01
Excess gestational weight gain ^a	Adequate	252	1.39	0.69–2.51		250	1.39	0.70–2.78	
BMI retention ^b	Per 1 BMI	511	1.05	0.93–1.18		469	1.07	0.94–1.21	
Father									
Age	Per 1 year	485	1.02	0.98–1.06		446	1.03	0.99–1.08	
BMI ≥ 25 at present	Normal weight	460	1.52	0.94–2.44		435	2.06	1.22–3.41**	2.11
									1.20–3.69
									0.009

Note: Each analysis was adjusted for geographic areas.

Variables which were significant by multiple regression analysis were expressed in bold.

Abbreviations: BMI, body mass index; CI, confidence interval; OR, odds ratio. *p* value: ****p* < 0.001; ***p* < 0.01; **p* < 0.05.

^aGestational weight gain was calculated by subtracting weight immediately before pregnancy from weight immediately before delivery and was categorized as inadequate, adequate, and excess based on the recommendation of the Japan Society of Obstetrics and Gynecology (refer to the text).

^bBMI retention was calculated by subtracting BMI immediately before pregnancy from present BMI. Parental smoking status was not significant.

The following maternal factors are significantly associated with growth trajectories: pre- or early pregnancy overweight/obesity,^{13,14,18–20,24} excessive GWG,^{18,20} postpartum weight retention,²⁴ and current overweight/obesity.^{21,22} Many studies suggest that pre-pregnancy overweight is universally associated with early- or infantile-onset patterns.^{14,15,20–22}

Regarding maternal excessive GWG, previous studies showed that excessive GWG was associated with an increased likelihood of a child being in the high-risk trajectory.^{18,20} Excessive GWG was associated with girls being in the infantile onset group in our study. Excessive GWG should be avoided; however, it should not be over-emphasized in Japan. Among 1,799 mothers whose data were obtained in the present study, the percentages of inadequate, adequate, and excessive GWG were 66.9%, 24.5%, and 6.9%, respectively. The recommendation for adequate GWG was updated by the Japan Society of Obstetrics and Gynecology for Japanese women in 2021.²⁹ The need for adequate GWG should be emphasized in healthcare workers. The effect of excessive GWG should be further investigated.

Maternal age was an independent predictor for girls being in the continual increase group in the present study. Previous studies,^{17,19} including systematic reviews,^{33,34} showed no association of childhood obesity with maternal age. One exception was a study by Haga et al.⁸ in Japan, which showed that maternal age was associated with girls being in the “progressive overweight” group by univariate analysis, although it was not significant by multivariate analysis. An increase in the average age of getting married has become a concern in Japan.³⁵ Therefore, the association between maternal age and childhood obesity by sex should be analyzed more extensively.

This study showed that having no siblings was an independent significant predictor for boys being in the continual increase group. Being an only child was reported to be associated with obesity using the data of combined sexes.^{36–38} Ochiai et al.³⁶ reported that being an only or youngest child was associated with childhood overweight and having a larger number of younger siblings was negatively associated with overweight, using the data of 4,026 fourth-grade Japanese children. Mosli et al.³⁹ showed that children who did not experience the birth of any siblings by the time they were in the first grade had 2.94 greater odds of obesity in the first grade compared with children who experienced the birth of any siblings when they were aged between 36 and 54 months, using data of combined sexes. Liang⁴⁰ reported that boys, but not girls, as the only child were more likely to belong in the “rapid rising up to school age and then become-overweight” trajectory (OR, 2.04; 95% CI 1.45–2.86), which is similar to the present study. These data suggest that public health interventions to prevent childhood overweight need to focus on children from these familial backgrounds.³⁶

There are limitations to the present study. First, current parental weight was obtained using questionnaires and was not actually measured. However, maternal weight immediately before pregnancy and that immediately before delivery were written in a maternity book. Current data should be obtained using actual measurements. Second, we could not find the reason for the fact that the continual increase group in girls reached the highest z-scores (Trajectory 6). Some reports showed the gradually increase group reached the highest in children¹⁵ and adolescents¹¹ without describing sex difference. Further studies are needed to clarify the sex difference in the high-risk trajectory group. Third, we did not discuss the low BMI groups, namely the Trajectory-1 and -2 groups, in the present study. Leanness is an important issue and should be further discussed with appropriate viewpoints. Finally, the present study showed that predictive factors for children being in the infantile onset or continual increase group were different by sex. However, we had no data to explain the reasons for this sex difference. Further detailed studies about the relationship between children and parents regarding diet, physical activity, and sedentary style are required in the future.

In conclusion, among the six trajectory groups, two trajectory groups (infantile onset and continual increase groups) had significantly less favorable levels of many CV risk profiles than the remaining groups. Paternal overweight/obesity was an independent predictor for boys being in the infantile onset group and for girls being in the continual increase group. Additionally, maternal pre-pregnancy overweight/obesity in boys and excessive GWG in girls were independent predictors for being in the infantile onset group. Having no sibling in boys and an older maternal age were independent predictors for being in the continual increase group. Interventions to prevent childhood obesity should include strategies that focus on fathers and mothers and focus on children with certain types of familial background.

AUTHOR CONTRIBUTIONS

All authors were involved in conceiving the study design. Masao Yoshinaga, Yoshiya Ito, Machiko Aoki, Ayumi Miyazaki, Toshihide Kubo, Masaki Shinomiya, Hitoshi Horigome, Masakuni Tokuda, Lisheng Lin, and Masami Nagashima collected data. Masao Yoshinaga, Hideto Takahashi, Yoshiya Ito, and Hiromitsu Ogata carried out statistical analysis. Masao Yoshinaga wrote the first draft of the manuscript. All authors were involved in writing the manuscript and read and approved the final manuscript.

ACKNOWLEDGMENTS

This study was supported by a Health and Labour Sciences Research Grant from the Ministry of Health, Labour and Welfare of Japan (H24-014).

CONFLICT OF INTEREST

The authors declare no relevant conflicts of interest.

ORCID

Masao Yoshinaga  <https://orcid.org/0000-0002-5054-6074>

Lisheng Lin  <https://orcid.org/0000-0003-4886-4767>

REFERENCES

- Ministry of Education, Culture, Sports, Science and Technology. Annual Report of School Health Survey of 2018. The Printing Office, Ministry of Finance, Tokyo (in Japanese). [cited 2022 Feb 26]. Available from: https://warp.ndl.go.jp/info:ndljp/pid/11293659/www.mext.go.jp/b_menu/toukei/chousa05/hoken/kekka/k_detail/1411711.htm
- Yoshinaga M, Ichiki T, Tanaka Y, Hazeki D, Horigome H, Takahashi H, et al. Prevalence of childhood obesity from 1978 to 2007 in Japan. *Pediatr Int*. 2010;52:213–7.
- Dunton GF, Do B, Wang SD. Early effects of the COVID-19 pandemic on physical activity and sedentary behavior in children living in the U.S. *BMC Public Health*. 2020;20:1351.
- Flanagan EW, Beyl RA, Fearnbach SN, Altazan AD, Martin CK, Redman LM. The impact of COVID-19 stay-at-home orders on health behaviors in adults. *Obesity*. 2021;29:438–45.
- Bjerregaard LG, Wasenius N, Nedelec R, Gjørde LK, Ångquist L, Herzig KH, et al. Possible modifiers of the association between change in weight status from child through adult ages and later risk of type 2 diabetes. *Diabetes Care*. 2020;43:1000–7.
- Baker JL, Olsen LW, Sørensen TI. Childhood body-mass index and the risk of coronary heart disease in adulthood. *N Engl J Med*. 2007;357:2329–37.
- Twig G, Yaniv G, Levine H, Leiba A, Goldberger N, Derazne E, et al. Body-mass index in 2.3 million adolescents and cardiovascular death in adulthood. *N Engl J Med*. 2016;374:2430–340.
- Haga C, Kondo N, Suzuki K, Sato M, Ando D, Yokomichi H, et al. Developmental trajectories of body mass index among Japanese children and impact of maternal factors during pregnancy. *PLoS One*. 2012;7:e51896.
- Jones BL, Nagin DS, Roeder K. A SAS procedure based on mixture models for estimating developmental trajectories. *Sociol Method Res*. 2001;29:374–93.
- Jones BL, Nagin DS. Advances in group-based trajectory modeling and an SAS procedure for estimating them. *Sociol Method Res*. 2007;35:542–71.
- Araújo J, Barros H, Ramos E, Li L. Trajectories of total and central adiposity throughout adolescence and cardiometabolic factors in early adulthood. *Int J Obes (Lond)*. 2016;40:1899–905.
- Burrows R, Correa-Burrows P, Bunout D, Barrera G, Rogan J, Kim E, et al. Obesity and impairment of pancreatic beta-cell function in early adulthood, independent of obesity age of onset: the Santiago longitudinal study. *Diabetes Metab Res Rev*. 2021;37:e3371.
- Ziyab AH, Karmaus W, Kurukulaaratchy RJ, Zhang H, Arshad SH. Developmental trajectories of body mass index from infancy to 18 years of age: prenatal determinants and health consequences. *J Epidemiol Community Health*. 2014;68:934–41.
- Oluwagbemigun K, Buyken AE, Alexy U, Schmid M, Herder C, Nöthlings U. Developmental trajectories of body mass index from childhood into late adolescence and subsequent late adolescence-young adulthood cardiometabolic risk markers. *Cardiovasc Diabetol*. 2019;18:9.
- Berentzen NE, van Rossem L, Gehring U, Koppelman GH, Postma DS, de Jongste JC, et al. Overweight patterns throughout childhood and cardiometabolic markers in early adolescence. *Int J Obes (Lond)*. 2016;40:58–64.
- Stuart B, Panico L. Early-childhood BMI trajectories: evidence from a prospective, nationally representative British cohort study. *Nutr Diabetes*. 2016;6:e198.
- Liu JX, Liu JH, Frongillo EA, Boghossian NS, Cai B, Hazlett LJ. Body mass index trajectories during infancy and pediatric obesity at 6 years. *Ann Epidemiol*. 2017;27:708–15.
- Demment MM, Haas JD, Olson CM. Changes in family income status and the development of overweight and obesity from 2 to 15 years: a longitudinal study. *BMC Public Health*. 2014;14:417.
- Rzehak P, Oddy WH, Mearin ML, Grote V, Mori TA, Szajewska H, et al. Infant feeding and growth trajectory patterns in childhood and body composition in young adulthood. *Am J Clin Nutr*. 2017;106:568–80.
- Hu Z, Tylavsky FA, Han JC, Kocak M, Fowke JH, Davis RL, et al. Maternal metabolic factors during pregnancy predict early childhood growth trajectories and obesity risk: the CANDLE study. *Int J Obes (Lond)*. 2019;43:1914–22.
- Koning M, Hoekstra T, de Jong E, Visscher TL, Seidell JC, Renders CM. Identifying developmental trajectories of body mass index in childhood using latent class growth (mixture) modelling: associations with dietary, sedentary and physical activity behaviors: a longitudinal study. *BMC Public Health*. 2016;16:1128.
- Magee CA, Caputi P, Iverson DC. Identification of distinct body mass index trajectories in Australian children. *Pediatr Obes*. 2013;8:189–98.
- Plank LD, Obolonkin V, Smith M, Savila F, Jalili-Moghaddam S, Tautolo ES, et al. Pacific Islands families study: physical growth to age 14 and metabolic risk. *Pediatr Obes*. 2019;14:e12497.
- Leonard SA, Rasmussen KM, King JC, Abrams B. Trajectories of maternal weight from before pregnancy through postpartum and associations with childhood obesity. *Am J Clin Nutr*. 2017;106:1295–301.
- Freeman E, Fletcher R, Collins CE, Morgan PJ, Burrows T, Callister R. Preventing and treating childhood obesity: time to target fathers. *Int J Obes (Lond)*. 2012;36:12–5.
- Kato N, Takimoto H, Sudo N. The cubic function for spline smoothed L, S, M values for BMI reference data of Japanese children. *Lin Pediatr Endocrinol*. 2011;20:47–9.
- Matthews DR, Hosker JP, Rudenski AS, Naylor BA, Treacher DF, Turner RC. Homeostasis model assessment: insulin resistance and beta-cell function from fasting plasma glucose and insulin concentrations in man. *Diabetologia*. 1985;28:412–9.
- Ministry of Education, Culture, sports, science and technology. The National Curriculum Standards P142 in Japanese. [cited 2022 Aug 06]. Available from: https://www.mext.go.jp/content/1413522_001.pdf
- Kimura T, Ikeda T. A guide for weight gain during pregnancy. *Acta Obstet Gynaecol Jpn*. 2021;73:642 (in Japanese).
- Yoshinaga M, Sameshima K, Jougasaki M, Yoshikawa H, Tanaka Y, Hashiguchi J, et al. Emergence of cardiovascular risk factors from mild obesity in Japanese elementary school children. *Diabetes Care*. 2006;29:1408–10.
- Davison KK, Gicevic S, Aftosmes-Tobio A, Ganter C, Simon CL, Newlan S, et al. Fathers' representation in observational studies on parenting and childhood obesity: a systematic review and content analysis. *Am J Public Health*. 2016;106(11):e14–21.
- Morgan PJ, Young MD, Lloyd AB, Wang ML, Eather N, Miller A, et al. Involvement of fathers in pediatric obesity treatment and prevention trials: a systematic review. *Pediatrics*. 2017;139(2):e20162635.
- Weng SF, Redsell SA, Swift JA, Yang M, Glazebrook CP. Systematic review and meta-analyses of risk factors for childhood overweight identifiable during infancy. *Arch Dis Child*. 2012;97:1019–26.
- Robinson HA, Dam R, Hassan L, Jenkins D, Buchan I, Sperrin M. Post-2000 growth trajectories in children aged 4–11 years: a review and quantitative analysis. *Prev Med Rep*. 2019;14:100834.

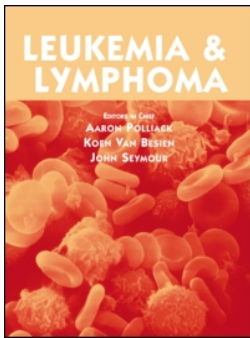
35. Iijima S, Yokoyama K. Socioeconomic factors and policies regarding declining birth rates in Japan. *Nihon Eiseigaku Zasshi*. 2018;73:305–12. (in Japanese, English abstract).
36. Ochiai H, Shirasawa T, Ohtsu T, Nishimura R, Morimoto A, Obuchi R, et al. Number of siblings, birth order, and childhood overweight: a population-based cross-sectional study in Japan. *BMC Public Health*. 2012;12:766.
37. Haugaard LK, Ajslev TA, Zimmermann E, Ångquist L, Sørensen TIA. Being an only or last-born child increases later risk of obesity. *PLoS One*. 2013;8:e56357.
38. Wang H, Sekine M, Chen X, Kanayama H, Yamagami T, Kagamimori S. Sib-size, birth order and risk of overweight in junior high school students in Japan: results of the Toyama birth cohort study. *Prev Med*. 2007;44:45–51.
39. Mosli RH, Kaciroti N, Corwyn RF, Bradley RH, Lumeng JC. Effect of sibling birth on BMI trajectory in the first 6 years of life. *Pediatrics*. 2016;137:e20152456.
40. Liang J, Zheng S, Li X, Xiao D, Wang P. Associations of community, family and early individual factors with body mass index

z-scores trajectories among Chinese children and adolescents. *Sci Rep*. 2021;11:14535.

SUPPORTING INFORMATION

Additional supporting information can be found online in the Supporting Information section at the end of this article.

How to cite this article: Yoshinaga M, Takahashi H, Ito Y, Aoki M, Miyazaki A, Kubo T, et al. Developmental trajectories at a high risk for childhood overweight/obesity. *Pediatr Int*. 2023;65:e15425. <https://doi.org/10.1111/ped.15425>



A decrease in newly diagnosed patients with adult T-cell leukemia/lymphoma in Kagoshima, a highly endemic area of HTLV-1 in southwestern Japan

Satsuki Owatari, Masahito Tokunaga, Daisuke Nakamura, Kimiharu Uozumi, Yasuko Sagara, Hitomi Nakamura, Koichi Haraguchi, Nobuaki Nakano, Makoto Yoshimitsu, Yoshikiyo Ito, Atae Utsunomiya, Maki Otsuka, Shuichi Hanada, Masako Iwanaga & Kenji Ishitsuka

To cite this article: Satsuki Owatari, Masahito Tokunaga, Daisuke Nakamura, Kimiharu Uozumi, Yasuko Sagara, Hitomi Nakamura, Koichi Haraguchi, Nobuaki Nakano, Makoto Yoshimitsu, Yoshikiyo Ito, Atae Utsunomiya, Maki Otsuka, Shuichi Hanada, Masako Iwanaga & Kenji Ishitsuka (2023): A decrease in newly diagnosed patients with adult T-cell leukemia/lymphoma in Kagoshima, a highly endemic area of HTLV-1 in southwestern Japan, *Leukemia & Lymphoma*, DOI: [10.1080/10428194.2023.2173524](https://doi.org/10.1080/10428194.2023.2173524)

To link to this article: <https://doi.org/10.1080/10428194.2023.2173524>



Published online: 10 Feb 2023.



Submit your article to this journal [↗](#)




View related articles [↗](#)



View Crossmark data [↗](#)

A decrease in newly diagnosed patients with adult T-cell leukemia/lymphoma in Kagoshima, a highly endemic area of HTLV-1 in southwestern Japan

Satsuki Owatari^a, Masahito Tokunaga^b, Daisuke Nakamura^c, Kimiharu Uozumi^d, Yasuko Sagara^e, Hitomi Nakamura^e, Koichi Haraguchi^a, Nobuaki Nakano^b, Makoto Yoshimitsu^c, Yoshikiyo Ito^b, Atae Utsunomiya^b, Maki Otsuka^a, Shuichi Hanada^a, Masako Iwanaga^f and Kenji Ishitsuka^c 

^aDepartment of Hematology, National Hospital Organization Kagoshima Medical Center, Kagoshima, Japan; ^bDepartment of Hematology, Imamura General Hospital, Kagoshima, Japan; ^cDepartment of Hematology and Rheumatology, Kagoshima University, Kagoshima, Japan; ^dDepartment of Medical Oncology, National Hospital Organization Kagoshima Medical Center, Kagoshima, Japan; ^eDepartment of Quality, Japanese Red Cross Kyushu Block Blood Center, Fukuoka, Japan; ^fDepartment of Medical Technology, The Japanese Red Cross Nagasaki Genbaku Hospital, Nagasaki, Japan

ABSTRACT

Adult T-cell leukemia/lymphoma (ATL) is a peripheral T-cell malignancy caused by human T-cell leukemia virus type-I (HTLV-1). This study investigated whether the number of newly diagnosed patients with ATL is decreasing in the background of a declining number of individuals infected by HTLV-1 in Kagoshima, Japan, one of the most endemic areas of HTLV-1 in the world. We retrospectively analyzed the number of newly diagnosed patients with ATL between January 2001 and December 2021 in three major hospitals. The number of newly diagnosed patients with B-cell non-Hodgkin lymphoma (B-NHL) in the same period was examined as an internal control. One thousand eighteen and 2,029 patients with ATL and B-NHL were registered, respectively. The age-adjusted incidence of ATL steadily increased between 2001 and 2012, whereas that between 2013 and 2021 decreased. Despite the limitation of its retrospective nature, this is the first report indicating a decrease in ATL patients in Japan.

ARTICLE HISTORY

Received 24 October 2022
Revised 18 January 2023
Accepted 21 January 2023

KEYWORDS

HTLV-1; seropositivity; ATL; incidence

Introduction

ATL is a peripheral T-cell malignancy caused by human T-cell leukemia virus type-I (HTLV-1), which is endemic in Japan, sub-Saharan Africa, South America, the Caribbean area, and foci in the Middle East and Australo-Melanesia [1–4]. ATL is classified into 4 clinical subtypes: smoldering, chronic, lymphoma, and acute [3,5]. There are currently between 5 and 20 million HTLV-1 carriers worldwide, and 3–5% of HTLV-1-infected individuals develop ATL in their lifetime [3,6]. Based on estimates of seropositivity in first-time blood donors, the number of HTLV-1 carriers in Japan is decreasing, i.e. 1.2 million in 1990, at least 1.08 million in 2006–2007, and between 0.72 and 0.82 million in 2014 [7–9]. The infection route of HTLV-1 includes breastfeeding and sexual transmission as well as unscreened blood transfusions [8,10–13]. Individuals infected by mother-to-child transmission *via* breastfeeding were previously reported to be at the higher

risk of developing ATL as compared to other transmission routes such as blood transfusion and sexual intercourse [14,15].

The age of newly diagnosed patients with ATL is increasing, which has been attributed to the decrease in HTLV-1 carriers in younger populations [3,16,17]. The findings of a nationwide study on 818 ATL patients diagnosed between 1983 and 1987 showed that mean ages at diagnosis for the acute, lymphoma, chronic, and smoldering subtypes were 56.0, 59.2, 57.7, and 59.3 years, respectively [5]. In a subsequent nationwide study on 1594 patients with ATL between 2000 and 2009, median ages at diagnosis for the acute, lymphoma, chronic, and smoldering subtypes were 63, 66, 61, and 67 years [18]. A recent study on 996 ATL patients diagnosed in 2010–2011 revealed that median ages at diagnosis for the acute, lymphoma, chronic, and smoldering subtypes were 68, 70, 65, and 68 years, respectively [19]. Therefore, age of the diagnosis of ATL has gradually increased.

This study investigated whether the number of newly diagnosed patients with ATL is declining in the context of the marked decrease in the number of HTLV-1 carriers in recent years.

Methods

Study design and data collection

Information on the number of HTLV-1-seropositive individuals by age among first-time volunteer blood donors in Kagoshima prefecture between 2008 and 2016 was provided by the Japanese Red Cross Blood Center.

Data analysis

Age-adjusted incidence is a weighted average of age-specific incidence in an observed population. The weight for each age category is the proportion of individuals in an age category in the standard population. The 1985 model population of Japan is used as the standard population. Age adjustments are used to adjust for differences in age distribution when comparing the incidence of each population. By convention, incidence is expressed per 100,000 per year. The formula used for this calculation is shown below [21].

$$\text{Age-adjusted incidence} = \sum_i \frac{[\text{Observed IR in } i\text{th age category}] \times [\text{Population of } i\text{th age category in SP}]}{[\text{Total Population in SP}]}$$

The annual number of and clinical information on newly diagnosed patients with ATL and the annual number of newly diagnosed patients with B-cell non-Hodgkin lymphoma (B-NHL) between January 2001 and December 2021 in three major hospitals in Kagoshima City, Imamura General Hospital, the Kagoshima Medical Center, and Kagoshima University Hospital, were collected. Diagnostic criteria for ATL in this study were histologically or cytologically proven peripheral T-cell malignancy with seropositivity for the anti-HTLV-1 antibody. B-NHL was also simultaneously analyzed as an internal control [20].

We also collected information on the annual number of newly diagnosed patients with ATL, diffuse large B-cell lymphoma (DLBCL), peripheral T-cell lymphoma (PTCL), and angioimmunoblastic T-cell lymphoma (AITL) in Japan from the registry of the Japanese Society of Hematology between 2012 and 2019, which is available to the public at http://www.jshem.or.jp/modules/member/index.php?content_id=7 (accessed 2021-09-12).

To evaluate the age-adjusted incidence of ATL and B-NHL per 100,000 population in Kagoshima, information on the general population of Kagoshima Prefecture were obtained from the e-Stat, Portal Site of Official Statistics of Japan (<https://www.e-stat.go.jp>) (accessed 2021-09-21).

This study was approved by the research Ethics Committees of Kagoshima University Hospital (#180078) and the other participating hospitals, and was conducted in accordance with the Declaration of Helsinki.

IR and SP denote incidence rate and the standard population, respectively.

Correlation analysis was performed by using scatterplot of age-adjusted incidence of ATL and year. After that, we created regression line for 2001–2012 and 2013–2021, respectively, and compared the slopes of the lines.

Results

HTLV-1 seropositivity

HTLV-1 seropositivity was lower in younger age groups at any time points tested during this period, and remarkably decreased between 2008 and 2016 in all age groups (Figure 1(A)). HTLV-1 seropositivity in individuals aged 50 years and older markedly decreased each year (Figure 1(B)). Since the population aged 50 years and older in Kagoshima Prefecture remained stable at approximately 818,000 to 838,000 between 2008 and 2016 (data not shown), it will be obvious that the decrease of actual number of HTLV-1 carriers aged 50 years and older.

Incidence of ATL

In the period between January 2001 and December 2021, a total of 1,033 patients with newly diagnosed ATL were registered in this study. Of those, fifteen patients were excluded from the analysis due to double registration. The date of birth and gender of

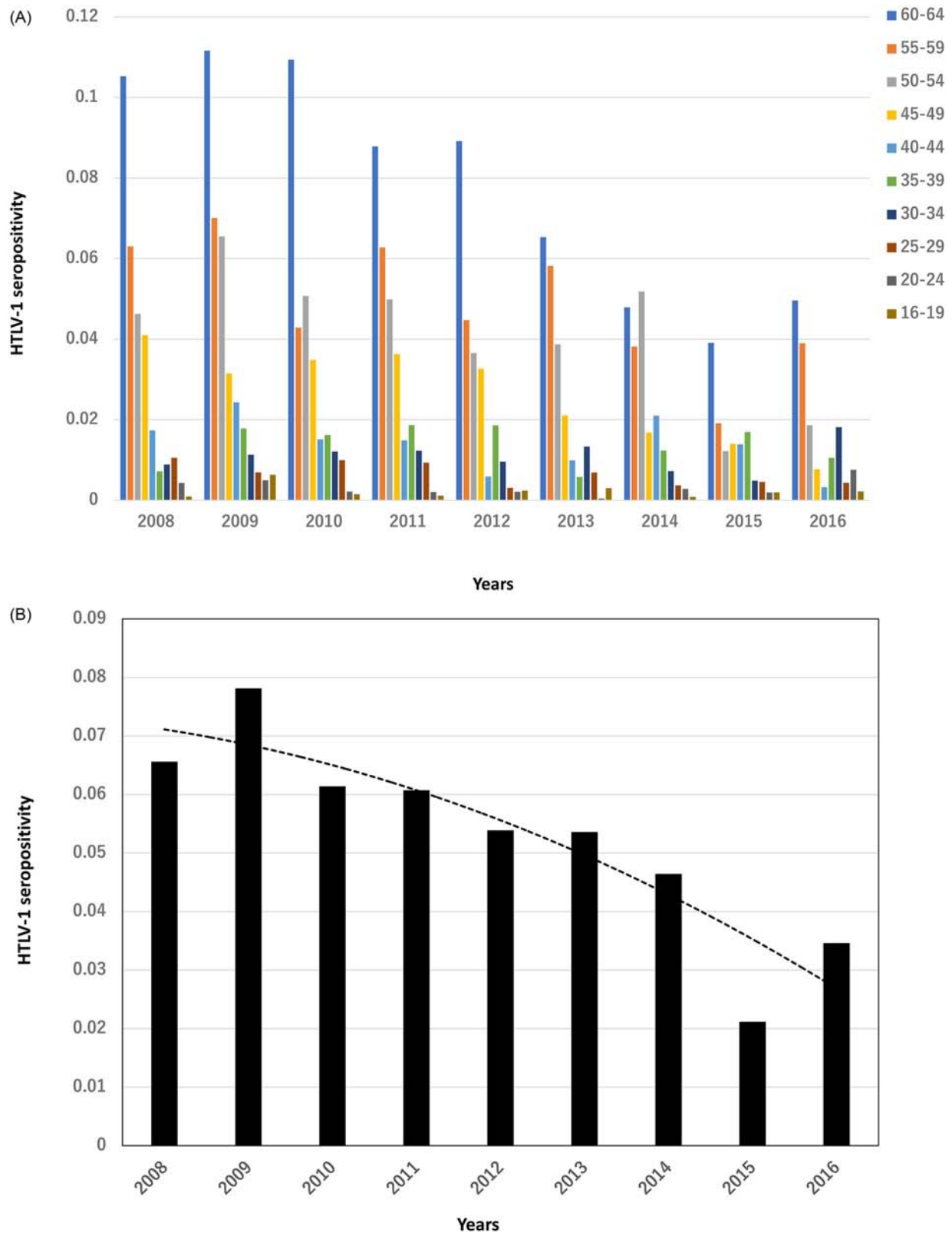


Figure 1. (A) The rate of HTLV-1 seropositivity among first-time blood donors by age at the time of donation in Kagoshima Prefecture between 2008 and 2016. (B) The ratio of HTLV-1 carriers aged 50 years and older among first-time blood donors in Kagoshima Prefecture between 2008 and 2016.

Table 1. Characteristics of ATL patients at diagnosis in the periods 2001–2012, 2013–2021 and 2001–2021.

	2001–2012	2013–2021	2001–2021
Characteristics			
Number of patients (n)	532	486	1018
Median age (n, range)	64.9 (21.2–88.6)	70.6 (39.4–95.2)	67.6 (21.2–95.2)
Sex			
Male (%)	277 (52.1)	271 (55.8)	548 (53.8)
Female (%)	255 (47.9)	215 (44.2)	470 (46.2)
Subtype of ATL			
Acute (%)	323 (60.7)	256 (52.7)	579 (56.9)
Lymphoma (%)	139 (26.1)	122 (25.1)	261 (25.6)
Chronic (%)	30 (5.7)	51 (10.5)	81 (8.0)
Smoldering (%)	40 (7.5)	57 (11.7)	97 (9.5)
ECOG performance status			
0–1 (%)	344 (64.7)	334 (68.7)	678 (66.6)
2 (%)	104 (19.6)	66 (13.6)	170 (16.7)
3 (%)	46 (8.6)	42 (8.7)	88 (8.7)
4 (%)	13 (2.4)	23 (4.7)	36 (3.5)
Unknown (%)	25 (4.7)	21 (4.3)	46 (4.5)
Stage of disease			
1 (%)	8 (1.5)	12 (2.5)	20 (2.0)
2 (%)	33 (6.2)	22 (4.5)	55 (5.4)
3 (%)	55 (10.3)	65 (13.4)	120 (11.8)
4 (%)	398 (74.8)	379 (78.0)	777 (76.3)
Unknown (%)	38 (7.2)	8 (1.6)	46 (4.5)

patients registered from the three sites were tallied, and patients with the same date of birth and gender were contacted at each facility to confirm if they were the same person. If they were the same person, the registration of one of the patients was excluded. Finally, 1,018 patients, including 579 (56.9%), 261 (25.6%), 81 (8.0%), and 97 (9.5%) with the acute, lymphoma, chronic, and smoldering subtypes, respectively, were analyzed. Median age was 67.6 years (21.2–95.2), and the numbers of males and females were 548 (53.8%) and 470 (46.2%) (Table 1). The number of newly diagnosed patients with B-NHL in the same period was 2,029 following the exclusion of 14 duplicates. Age-adjusted incidence and an approximate curve of the age-adjusted incidence of ATL and B-NHL per 100,000 population in Kagoshima between 2001 and 2021 are shown in Figure 2(A). In contrast to the steady increase in the age-adjusted incidence of B-NHL, a decrease was noted in ATL from 2013. This result suggests that the incidence of ATL in Kagoshima Prefecture was decreasing since 2013. The regression line of age-adjusted incidence of ATL for 2001–2012 was shown (Figure 2(B)). The slope of the quadratic function of the regression line was 11.009. The correlation coefficient was 0.962 that showed this regression line had a strong positive correlation. Similarly, a regression line of age-adjusted incidence of ATL was created for 2013–2021 (Figure 2(C)). The correlation coefficient was -0.776 , indicating a strong negative correlation. The slope of the regression line was negative at -9.4519 . These results indicate that age-adjusted incidence of ATL patients enrolled

increased during the period 2001–2012, while that age-adjusted incidence of ATL decreased during the period 2013–2021. In addition, the age of newly diagnosed patients with ATL shifted from elderly between the period of 2001 and 2021 (Figure 3). The median ages of patients newly diagnosed with ATL were 63.7(21.2–86.4), 67.0 (26.7–92.0), and 71.1 (39.4–95.2) years for 2001–2007, 2008–2014, and 2015–2021, respectively.

In order to confirm the decreasing trend in the incidence of ATL even throughout Japan, we additionally analyzed the ratio of the number of patients with ATL divided by those with DLBCL or PTCL-NOS and AITL by using data from the nationwide registry by the Japanese Society of Hematology (Figure 4(A,B)). The results showed that the ratio of the number of patients with ATL divided by those with DLBCL or PTCL-NOS and AITL was also decreasing.

Discussion

Kagoshima Prefecture located in southwestern Japan, is one of the most highly endemic areas of HTLV-1 in the world. This study is the first longitudinal epidemiological study on HTLV-1 carriers and patients with ATL in Kagoshima.

We initially indicated the number of HTLV-1 carriers older than 50 years, an age at which ATL is most likely to occur, as demonstrated not only herein, but also in previous studies [18,22], and found a marked decrease between 2008 and 2016 based on information obtained from the database of first-time blood donors

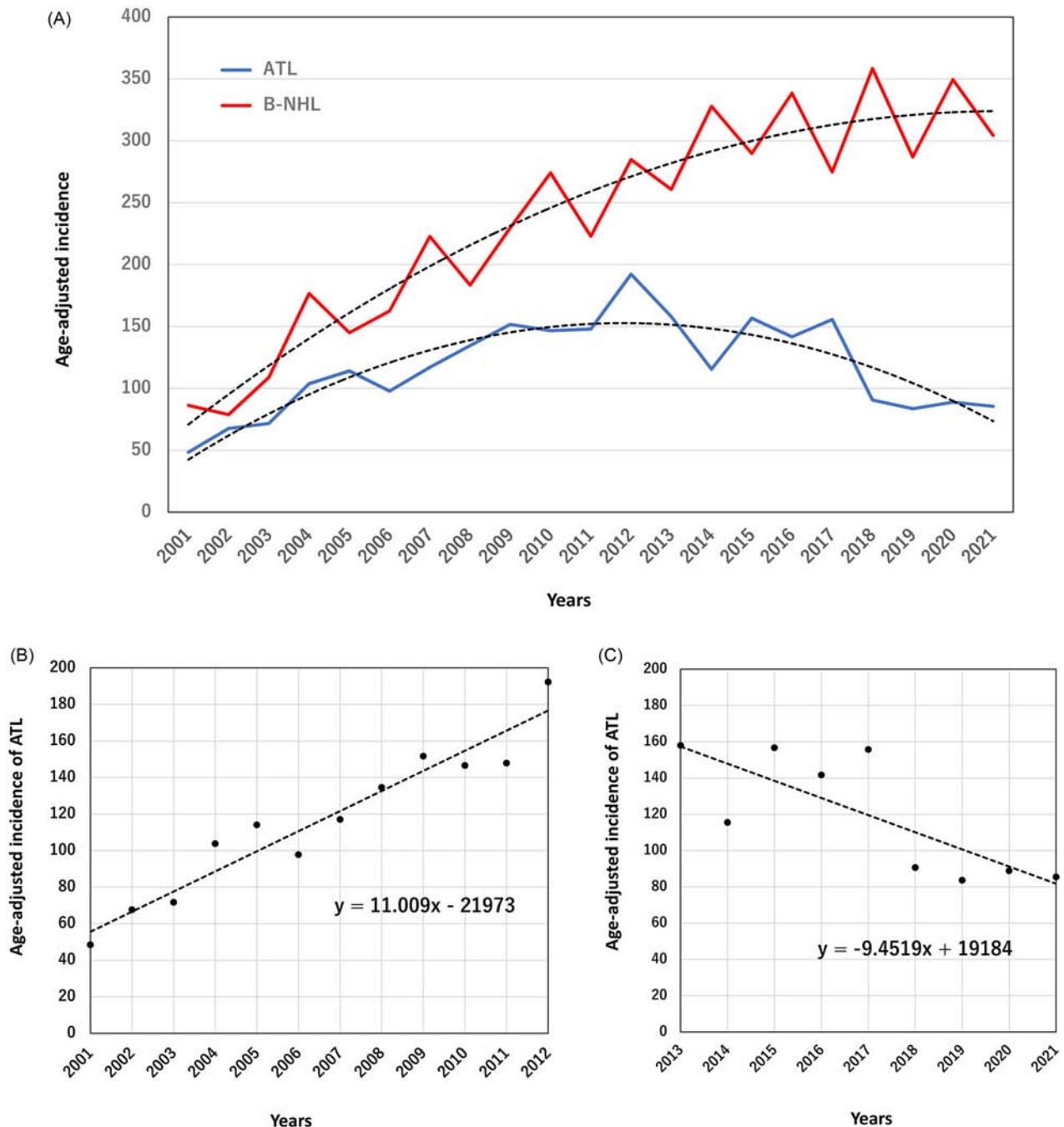


Figure 2. (A) The age-adjusted incidence of ATL and B-NHL per 100,000 population in Kagoshima Prefecture between 2001 and 2021. Blue and red lines indicate the incidence of ATL and B-NHL, respectively. (B) Scatter plots of age-adjusted incidence of ATL and year from 2001 to 2012 were created and regression line was generated. (C) Scatter plots of age-adjusted incidence of ATL and year from 2013 to 2021 were created and regression line was generated.

in Kagoshima Prefecture. A decline was observed in newly diagnosed ATL patients in Kagoshima Prefecture after 2013. In contrast to the decrease in the number of patients with ATL from 2013 to 2021, the number of those with B-NHL was constantly increasing. There are two possible reasons for this increment in the number of patients with B-NHL. The number of registered patients has become more

accurate in recent years due to the nature of a retrospective survey, in other words, the number of overlooked and unregistered cases will be higher in former years. This is applicable not only to the annual number of patients with B-NHL but also those with ATL. The second reason is that the actual increase of patients with B-NHL which has been reported in Japan [23]. To establish whether the decrease in the

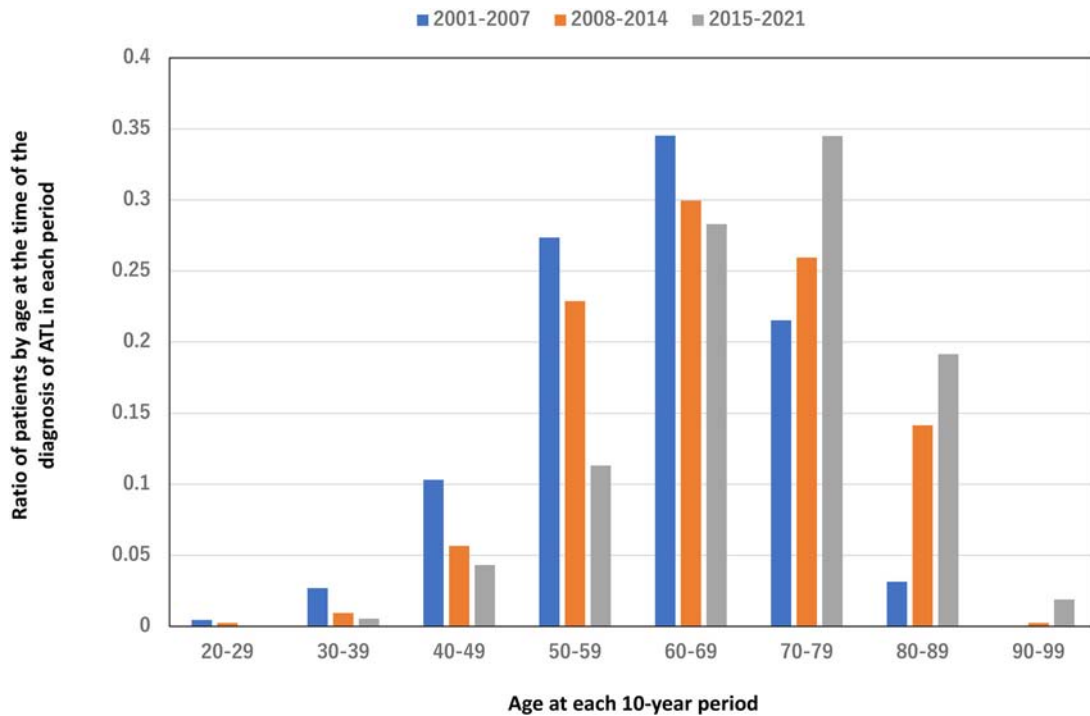


Figure 3. The ratio of ATL patients by age in 2001–2007, 2008–2014, and 2015–2021.

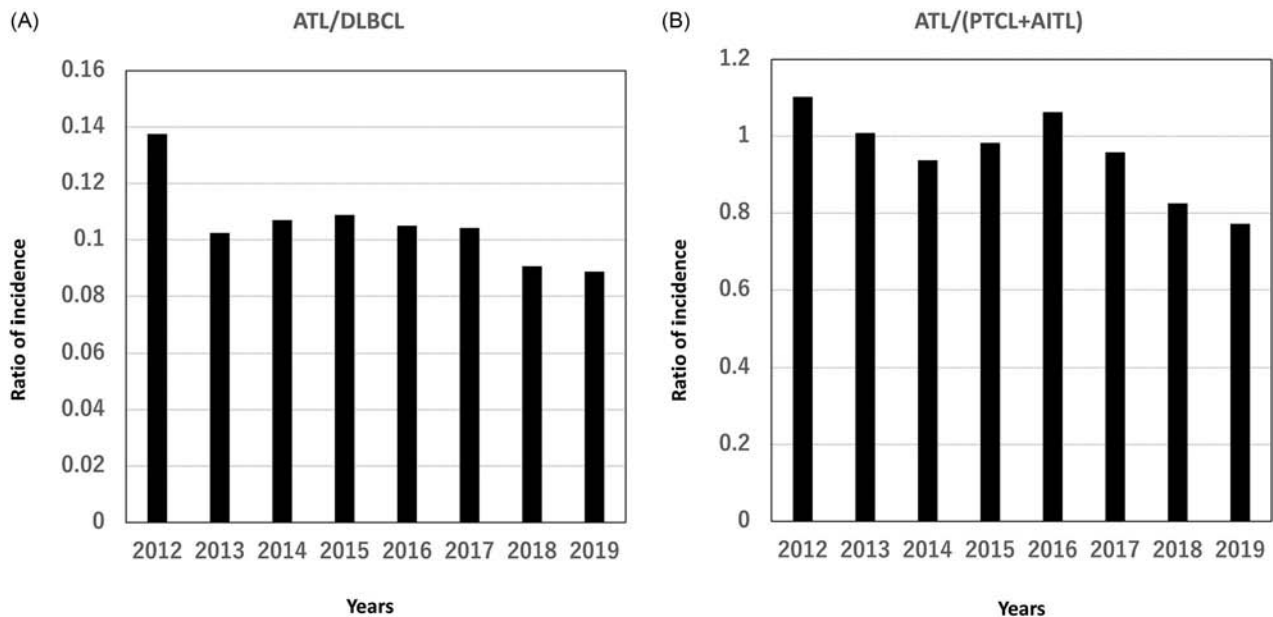


Figure 4. (A) The ratio of the number of patients with ATL to those with DLBCL between 2012 and 2019 in Japan in the nationwide registry of the Japanese Society of Hematology. (B) The ratio of ATL/(PTCL + AITL) according to the number of ATL patients and that of PTCL and AITL patients between 2012 and 2019 in Japan in the nationwide registry of the Japanese Society of Hematology.

number of newly diagnosed ATL patients in Kagoshima was occurring nationwide, we examined changes in the number of ATL patients enrolled to the registry of the Japanese Society of Hematology (JSH). In contrast to our retrospective study, the JSH one is registered from hospitals caring hematological

diseases throughout Japan by gathering data annually. The results showed a recent decline in the ratio of ATL/DLBCL. Similarly, the ratio of ATL/(PTCL + AITL) was also decreasing. Therefore, the number of patients with ATL can be in decline not only in Kagoshima, but also nationwide.

The rates of HTLV-1 seropositivity among pregnant women in Kagoshima Prefecture were 5.3% (702/13,296) and 1.3% (112/8,717) in 1992 and 2012, respectively [24,25], indicating a marked decrease within these two decades. In Kagoshima Prefecture, the Kagoshima ATL Control Committee has recommended testing for anti-HTLV-1 antibodies in pregnant women and abstaining from breastfeeding or breast-feeding for a shorter duration by those with a positive test result since 1997 [26]. However, the decrease in the prevalence of HTLV-1 carriers among pregnant women in Kagoshima in 2012 is not directly related to the interventions preventing mother-to-child transmission because the majority of women had been born before the initiation of these interventions. Similarly, even before the commencement of local interventions to prevent the mother-to-child transmission of HTLV-1, a decline in the number of HTLV-1 carriers in the younger population had been reported [12,27]. The most likely reason for these phenomena is a shorter duration of breastfeeding along with lifestyle changes, including the introduction of bottle-feeding. In Japan, majority of HTLV-1 carriers are considered to be infected by mother-to-child transmission of HTLV-1 through breast milk, and prevention of mother-to-child transmission of HTLV-1 is thought to be the most effective means of reducing the number of HTLV-1 carriers. Prevention of mother-to-child transmission of HTLV-1 is expected to reduce the number of future ATL patients. Moreover, a nationwide prevention program for the mother-to-child transmission of HTLV-1 initiated in 2011 will further decrease the number of HTLV-1 carriers in the future. However, there is a concern that avoidance of breastfeeding to prevent mother-to-child transmission may cause loss of passive immunity from the mother, which may be detrimental to the infant. Particularly in developing nations, where impaired access to clean drinking water, socio-economic and healthcare resources are limited [28].

The epidemiology of HTLV-1 has been vigorously investigated in most developed and some developing nations in the mid-1980s. However, no expanded survey for HTLV-1 has been conducted in other developing nations [29]. Accurate estimates of some developing nations with large populations suggest that the current number of HTLV-1 carriers might be much higher [4]. In developing nations, HTLV-1 transmission can be caused by blood transfusion. Therefore, in order to prevent HTLV-1 infection, improving HTLV-1 detection techniques and proper screening of donated blood in developing countries are very important [30,31].

It is reported that age-standardized incidence rate of ATL showed an increasing trend in the HTLV-1 non-endemic areas but was stable in the HTLV-1-endemic areas. It has been speculated that the increasing trend in the areas could be a result of the diffusion of HTLV-1 carriers that has moved to non-endemic areas from endemic areas [32,33]. This study was conducted at only three facilities in endemic area, not data from throughout Japan. It is uncertain that the similar degree of reduction in the incidence of ATL is seen in other areas in Japan.

This is the first study to elucidate the decline in the number of newly diagnosed patients with ATL in Kagoshima along with the decrease in the number of HTLV-1 carriers. The present study includes the limitation of a retrospective analysis, and it cannot be denied that the recent decline in the number of newly diagnosed patients with ATL is overestimated due to the social reason, e.g. very elderly patients might be cared in local hospitals in the background of changing distribution by age as shown in Figure 3. We have therefore established a prospective and exhaustive registry of newly diagnosed patients with ATL in Kagoshima since 2021. The Japanese government has implemented nationwide measures to prevent mother-to-child transmission through breast milk since 2011. If Japanese measures to prevent the mother-to-child transmission of HTLV-1 succeed, it will be followed by a decrease in the number of ATL patients, and, ultimately, we hope the chance to eradicate this disease in the future.

Acknowledgments

The authors are deeply grateful to the hematologists at the following institutions for their patient referrals and other contributions: Nobuhito Ohno at the Department of Hematology, Ikeda Hospital, Yoshifusa Takatsuka at the Department of Hematology, Idzuro-Imamura hospital, Kyoko Mizukami at the Department of Internal Medicine, the Kirishima Medical Center, Kosuke Obama at the Department of Hematology, Imakiire General Hospital, and Shigemi Shimotakahara at the Department of Internal Medicine, Maruta Hospital, Kagoshima, Japan.

Author contributions

SO, MI and KI contributed to the study concept, design and data interpretation. SO, MT, DN, KU, KH, NN, MY, YI, AU, MO and SH collected and analyzed data at their respective facilities. YS and HN provided data for blood donors of Kagoshima in the Japanese Red Cross Blood Center. SO and KI wrote the manuscript. All authors critically reviewed the approved the manuscript.

Disclosure statement

No potential conflict of interest was reported by the author(s).

Funding

This work was supported by the President's Discretionary Expenses of Kagoshima University, and Research Program [21fk0108124h0802] on Emerging and Reemerging Infectious Diseases from the Japan Agency for Medical Research and Development, AMED.

ORCID

Kenji Ishitsuka  <http://orcid.org/0000-0002-7030-497X>

References

- [1] Uchiyama T, Yodoi J, Sagawa K, et al. Adult T-cell leukemia: clinical and hematologic features of 16 cases. *Blood*. 1977;50(3):481–492.
- [2] Poiesz BJ, Ruscetti FW, Gazdar AF, et al. Detection and isolation of type C retrovirus particles from fresh and cultured lymphocytes of a patient with cutaneous T-cell lymphoma. *Proc Natl Acad Sci U S A*. 1980; 77(12):7415–7419.
- [3] Ishitsuka K, Tamura K. Human T-cell leukaemia virus type I and adult T-cell leukaemia-lymphoma. *Lancet Oncol*. 2014;15(11):e517–526–e526.
- [4] Gessain A, Cassar O. Epidemiological Aspects and world distribution of HTLV-1 infection. *Front Microbiol*. 2012;3:388.
- [5] Shimoyama M, members of The Lymphoma Study Group (1984–87)*Diagnostic criteria and classification of clinical subtypes of adult T-cell leukaemia-lymphoma. A report from the lymphoma study group (1984–87). *Br J Haematol*. 1991;79(3):428–437.
- [6] Hermine O, Ramos JC, Tobinai K. A Review of new findings in adult T-cell Leukemia-Lymphoma: a focus on current and emerging treatment strategies. *Adv Ther*. 2018;35(2):135–152.
- [7] Tajima K. The 4th nation-wide study of adult T-cell leukemia/lymphoma (ATL) in Japan: estimates of risk of ATL and its geographical and clinical features. The T- and B-cell malignancy study group. *Int J Cancer*. 1990;45(2):237–243.
- [8] Satake M, Yamaguchi K, Tadokoro K. Current prevalence of HTLV-1 in Japan as determined by screening of blood donors. *J Med Virol*. 2012;84(2):327–335.
- [9] Hamaguchi I. Current status of HTLV-1 infection. *Neuroinfection*. 2020;25(1):92–94. [Japanese]
- [10] Kinoshita K, Hino S, Amagaski T, et al. Demonstration of adult T-cell leukemia virus antigen in milk from three sero-positive mothers. *Gan*. 1984;75(2):103–105.
- [11] Proietti FA, Carneiro-Proietti AB, Catalan-Soares BC, et al. Global epidemiology of HTLV-I infection and associated diseases. *Oncogene*. 2005;24(39):6058–6068.
- [12] Hino S. Establishment of the milk-borne transmission as a key factor for the peculiar endemicity of human T-lymphotropic virus type 1 (HTLV-1): the ATL prevention program Nagasaki. *Proc Jpn Acad Ser B Phys Biol Sci*. 2011;87(4):152–166.
- [13] Percher F, Jeannin P, Martin-Latil S, et al. Mother-to-Child transmission of HTLV-1 epidemiological aspects, mechanisms and determinants of mother-to-Child transmission. *Viruses*. 2016;8(2):40.
- [14] Take H, Umemoto M, Kusuvara K, et al. Transmission routes of HTLV-I: an analysis of 66 families. *Jpn J Cancer Res*. 1993;84(12):1265–1267.
- [15] Miyazawa T, Hasebe Y, Murase M, et al. The Effect of early postnatal nutrition on human T cell leukemia virus type 1 mother-to-Child transmission: a systematic review and Meta-Analysis. *Viruses*. 2021;13(5):819.
- [16] Iwanaga M, Watanabe T, Yamaguchi K. Adult T-cell leukemia: a review of epidemiological evidence. *Front Microbiol*. 2012;3:322.
- [17] Nosaka K, Iwanaga M, Imaizumi Y, et al. Epidemiological and clinical features of adult T-cell leukemia-lymphoma in Japan, 2010–2011: a nationwide survey. *Cancer Sci*. 2017;108(12):2478–2486.
- [18] Katsuya H, Ishitsuka K, Utsunomiya A, ATL-Prognostic Index Project, et al. Treatment and survival among 1594 patients with ATL. *Blood*. 2015;126(24):2570–2577.
- [19] Imaizumi Y, Iwanaga M, Nosaka K, for collaborative Investigators, et al. Prognosis of patients with adult T-cell leukemia/lymphoma in Japan: a nationwide hospital-based study. *Cancer Sci*. 2020;111(12):4567–4580.
- [20] Yamada Y, Atogami S, Hasegawa H, et al. [Nationwide survey of adult T-cell leukemia/lymphoma (ATL) in Japan]. *Rinsho Ketsueki*. 2011;52(11):1765–1771. [Japanese]
- [21] Ministry of Health, Labour and Welfare. Special Vital Statistics Report for Fiscal Year 2017. Summary of Age-Adjusted Mortality Rates by Prefecture in 2015. 2022. <https://www.mhlw.go.jp/toukei/saikin/hw/jin-kou/other/15sibou/index.html>
- [22] Ito S, Iwanaga M, Nosaka K, Collaborative Investigators, et al. Epidemiology of adult T-cell leukemia-lymphoma in Japan: an updated analysis, 2012–2013. *Cancer Sci*. 2021;112(10):4346–4354.
- [23] Chihara D, Ito H, Matsuda T, et al. Differences in incidence and trends of haematological malignancies in Japan and the United States. *Br J Haematol*. 2014; 164(4):536–545.
- [24] Nerome Y, Kojyo K, Ninomiya Y, et al. Current human T-cell lymphotropic virus type 1 mother-to-child transmission prevention status in Kagoshima. *Pediatr Int*. 2014;56(4):640–643.
- [25] Oki T, Yoshinaga M, Otsuka H, et al. A sero-epidemiological study on mother-to-child transmission of HTLV-I in Southern kyushu, Japan. *Asia Oceania J Obstet Gynaecol*. 1992;18(4):371–377.
- [26] Satake M, Iwanaga M, Sagara Y, et al. Incidence of human T-lymphotropic virus 1 infection in adolescent and adult blood donors in Japan: a nationwide retrospective cohort analysis. *Lancet Infect Dis*. 2016; 16(11):1246–1254.

- [27] Tashiro Y, Matsuura E, Sagara Y, et al. High Prevalence of HTLV-1 carriers among the elderly population in Kagoshima, a highly endemic area in Japan. *AIDS Res Hum Retroviruses*. 2022;38(5): 363–369.
- [28] Millen S, Thoma-Kress AK. Milk Transmission of HTLV-1 and the need for innovative prevention strategies. *Front Med (Lausanne)*. 2022;9:867147.
- [29] Du J, Chen C, Gao J, et al. History and update of HTLV infection in China. *Virus Res*. 2014;191:134–137.
- [30] Chang YB, Kaidarova Z, Hindes D, et al. Seroprevalence and demographic determinants of human T-lymphotropic virus type 1 and 2 infections among first-time blood donors—United States, 2000–2009. *J Infect Dis*. 2014;209(4):523–531.
- [31] Manns A, Wilks RJ, Murphy EL, et al. A prospective study of transmission by transfusion of HTLV-I and risk factors associated with seroconversion. *Int J Cancer*. 1992;51(6):886–891.
- [32] Chihara D, Ito H, Katanoda K, et al. Increase in incidence of adult T-cell leukemia/lymphoma in non-endemic areas of Japan and the United States. *Cancer Sci*. 2012;103(10):1857–1860.
- [33] Iwanaga M. Epidemiology of HTLV-1 infection and ATL in Japan: an update. *Front Microbiol*. 2020;11: 1124.

ORIGINAL ARTICLE

Respiratory epithelial adenomatoid hamartomas of the sinonasal tract: A histopathological analysis of 50 patients

Masamichi Goto¹  | Kengo Nishimoto² | Yasuyo Jougasaki¹ |
Tsutomu Matsuzaki² | Mitsuharu Nomoto¹

¹Department of Pathology, National Hospital Organization Kagoshima Medical Center, Kagoshima, Japan

²Department of Otorhinolaryngology, National Hospital Organization Kagoshima Medical Center, Kagoshima, Japan

Correspondence

Masamichi Goto, MD, PhD, Department of Pathology, National Hospital Organization Kagoshima Medical Center, 8-1 Shiroyama-cho, Kagoshima 892-0853, Japan.
Email: masagoto@po4.synapse.ne.jp

Abstract

Respiratory epithelial adenomatoid hamartoma (REAH) is a benign lesion of the nasal cavity and paranasal sinuses. Here, we report the clinicopathological characteristics of REAH identified in 2065 cases with nasal/paranasal polypoid lesions treated with endoscopic sinus surgery (ESS) at our hospital from 2008 to 2021. Cases including the olfactory area were reviewed and 50 patients of REAH were identified pathologically (50/2065, 2.4%). The average age was 58.9 years old and the male/female ratio was 45/5. Grossly, REAH showed a whitish surface and elastic firm consistency. The histopathological characteristics included proliferation of small to medium-sized glands composed of ciliated respiratory epithelium containing goblet cells; thickening of the basement membrane compared to that for inverted papilloma (9.6 ± 2.4 vs. $1.3 \pm 1.6 \mu\text{m}$, $p < 0.001$); and no intra-epithelial neutrophilic infiltration. Among the REAH cases, 81% were associated with sinonasal inflammatory polyps. Many olfactory cleft polyps were REAH (38/98, 39%). The rate of REAH found in ESS in the last 7 years was higher than that in the first 7 years (3.17% vs. 1.62%, $p = 0.032$). Our results in Japanese patients are similar to those found in other countries, including male predominance. REAH is relatively common and that 39% of polyps taken from olfactory clefts are REAH.

KEYWORDS

basement membrane, differential diagnosis, epidemiology, hamartoma, nasal cavity, paranasal sinus, pathology, sinonasal polyps

INTRODUCTION

Hamartoma of the nasal/paranasal cavities is rare. Baillie and Batsakis first described glandular (seromucinous) hamartoma of the nasopharynx in 1974.¹ Respiratory epithelial adenomatoid hamartoma (REAH) is another benign hamartomatous lesion of the nasal/paranasal cavities that was first reported by Wenig in 1995.² In the World Health Organization (WHO) Classification of Head and Neck Tumours, REAH has

been described since 2005,^{3,4} but it is still not well recognized in surgical pathology practice. In Japan, except for 10 cases of REAH in eosinophilic chronic rhinosinusitis reported by Akiyama et al.,⁵ only a few case reports have been published.^{6,7}

In this study, we examined the significant pathological findings for REAH by comparing basement membrane thickness and intra-epithelial neutrophilic infiltration among REAH, inverted Schneiderian papilloma and inflammatory polyp. REAH is known to occur in the olfactory cleft, but

Abbreviations: ESS, endoscopic sinus surgery; REAH, respiratory epithelial adenomatoid hamartoma; REAHi, isolated respiratory epithelial adenomatoid hamartoma; REAHnp, respiratory epithelial adenomatoid hamartoma associated with sinonasal inflammatory polyps; WHO, World Health Organization.

other locations are also known.² At our hospital, we have encountered many cases of REAH, and in this study we examined the true incidence and location by reviewing all pathological specimens suggestive of hamartoma or those taken from the olfactory area (olfactory cleft, ethmoid sinus, sphenoid sinus, sphenoidal recess, and nasal septum).

MATERIALS AND METHODS

All cases that underwent endoscopic sinus surgery (ESS) for nasal/paranasal polyps and polypoid lesions of chronic sinusitis in the Department of Otorhinolaryngology, National Hospital Organization Kagoshima Medical Center, Kagoshima, Japan from 2008 to 2021 were reviewed. Pathological examination was performed based on the exact location of the polyps, for example left olfactory cleft, right middle meatus or right sphenoidal recess. The following criteria were applied for pathological diagnosis of definite REAH: (i) polypoid lesions with a smooth surface; (ii) proliferation of small to medium-sized glands in direct continuity with the surface epithelium; (iii) glands composed of ciliated respiratory epithelium containing goblet cells; and (iv) thickening of the basement membrane. Lesions that resembled REAH, but did not meet some of these criteria, were classified as a focal hamartomatous lesion or doubtful case.

Using the text-based surgical pathology database of the Department of Pathology of the hospital, cases that matched more than one of the following criteria were selected: (i) a pathological diagnosis of REAH already made; (ii) cases including the word “hamartoma;” and (iii) cases including the terms “olfactory cleft,” “ethmoid sinus,” “sphenoid sinus,” “sphenoidal recess,” or “nasal septum.” Hematoxylin–eosin (H&E)-stained sections of the matched cases were reviewed by two pathologists (MG, MN) independently using the following criteria: 0, no hamartomatous lesion; 1, focal hamartomatous lesion or doubtful case; 2, definite REAH; 3, hamartoma other than REAH; 4, Schneiderian papilloma. When the evaluation differed between the pathologists, a final decision was made by consensus.

Respiratory epithelial hamartoma was divided into isolated cases and cases associated with sinonasal inflammatory polyps, which were subdivided into polyps with and without eosinophilic infiltration, based on eosinophil counts of ≥ 70 and < 70 /high power field, respectively.⁸ Clinical records of the patients with REAH were surveyed for clinical diagnosis of eosinophilic sinusitis and chronic sinusitis.

To identify the histopathological characteristics of REAH, inverted Schneiderian papillomas, and sinonasal inflammatory polyps, microscopic pictures of all definite REAH cases ($n = 52$) and cases of inverted

Schneiderian papilloma ($n = 25$) and inflammatory polyps ($n = 25$) were taken. Twenty-five cases of Schneiderian papillomas were semi-consecutively sampled from 2008 to 2018, and 25 cases of inflammatory polyps were randomly sampled from 2011 to 2021. The thickness of the basement membrane around the glands was measured using ImageJ software. Three representative basement membranes were measured and the average thickness was calculated. Infiltration of neutrophils and eosinophils in the lesional epithelium was also evaluated.

Statistics

Data were analyzed using the “R” computing environment (EZR).⁹ A nonparametric test of group difference was performed by Mann–Whitney U test. A p -value < 0.05 was considered to be statistically significant.

Ethical considerations

This study was approved by the Ethical Committee of National Hospital Organization Kagoshima Medical Center (Accession Number 2021-17).

RESULTS

Olfactory cleft REAH on nasal endoscopy appeared as a whitish polypoid lesion with a smooth surface and an elastic firm consistency. After formalin fixation, the lesions retained their whitish and firm characteristics (Figure 1). There was often an association between definite REAH (Figure 2a–d) and a focal hamartomatous lesion or doubtful case (Figure 2e,f), but 19 cases had only the latter classification. These cases were excluded from further analysis.

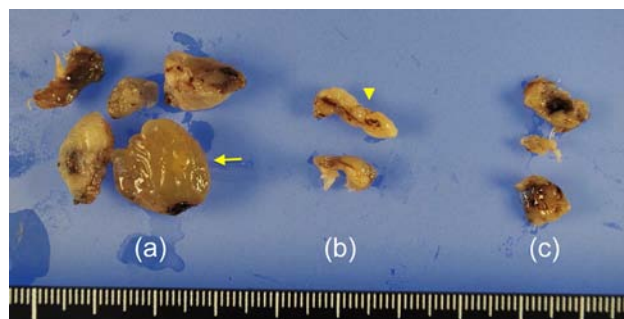


FIGURE 1 Macroscopic characteristics of respiratory epithelial hamartoma (REAH) and inflammatory polyp after formalin fixation. (a) Inflammatory polyp of the nasal cavity showing a semitranslucent soft appearance (arrow). (b, c) REAH of bilateral olfactory clefts. Entire specimens b and c showed REAH histology with a typical whitish opaque rubbery appearance (arrowhead).

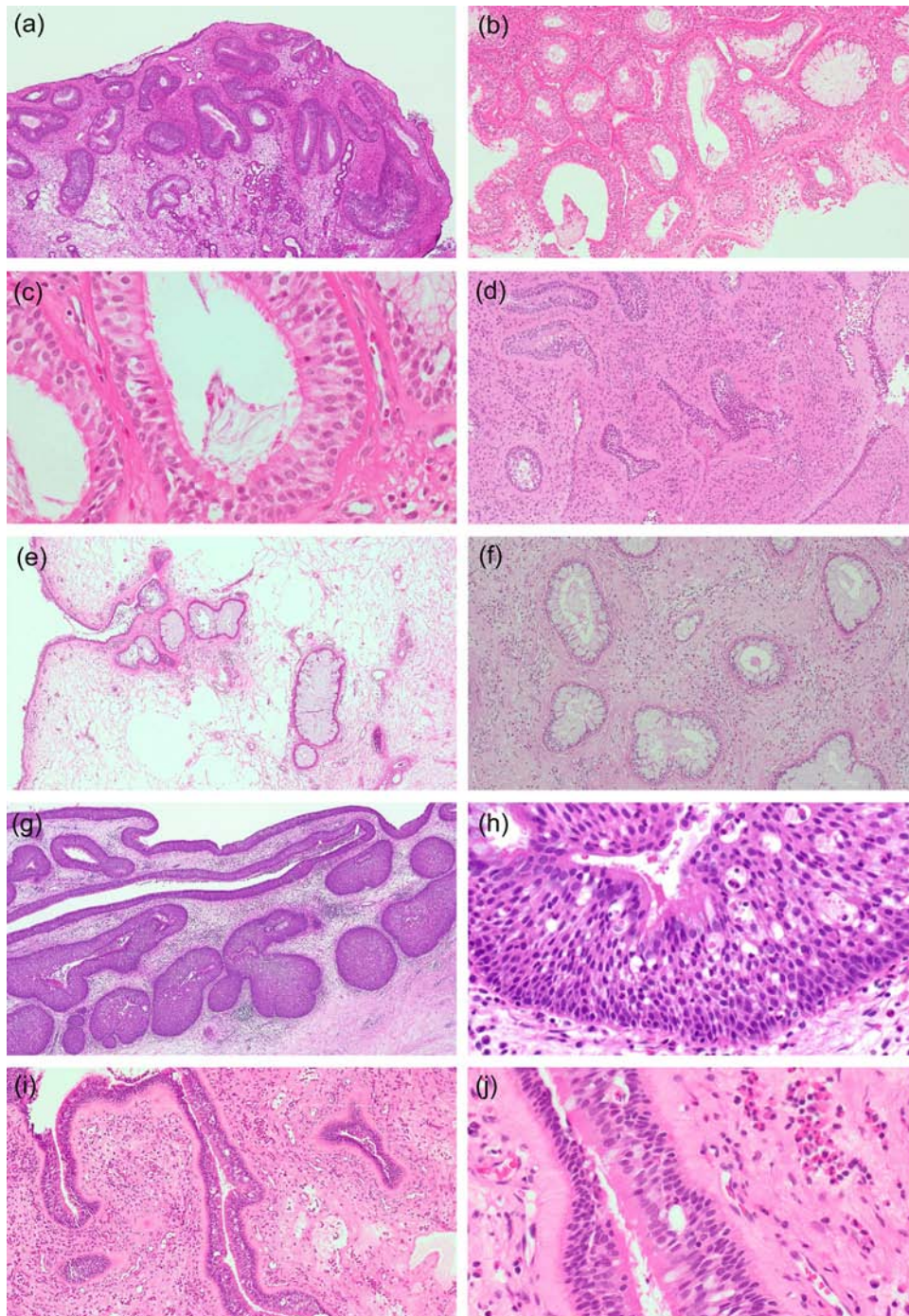


FIGURE 2 Histopathology of respiratory epithelial hamartoma (REAH) and related lesions. (a–d) Definite REAH showing proliferation of glands in direct continuity with the surface epithelium. The glands are ciliated respiratory epithelium containing goblet cells, and the basement membrane is thickened (a, b). Cilia are long and evenly distributed (c). The glands are often atrophic and surrounded by thick basement membrane and dense fibrous tissue (d). (e, f) Focal hamartomatous lesion or doubtful cases resemble definite REAH, but lack some characteristics of REAH. (g, h) Inverted Schneiderian papilloma lacks a thick basement membrane and shows intra-epithelial neutrophilic infiltration. (i, j) Inflammatory polyp has a thick basement membrane. (a–j) Hematoxylin and eosin staining.

A total of 2065 nasal/paranasal polyps were treated with ESS between April 2008 and September 2021 (Table 1). Pathological examination was performed based on the exact location of the polyps. The average age in these cases was 57.4 years (SD 17.1, median 60.0, range 5–93) and the male/female ratio was 1272/793 (1.60). A

total of 225 cases (225/2065, 10.9%) in the database with criteria of (i) pathological diagnosis of REAH, (ii) cases including the word “hamartoma,” and (iii) cases including the terms “olfactory cleft,” “ethmoid sinus,” “sphenoid sinus,” “sphenoidal recess,” or “nasal septum” were identified (Table 1). The average age in these cases was

TABLE 1 Demographic data of REAH

Item	ESS of nasal/paranasal polypoid lesions	Histologically reviewed cases ^a	REAH cases	REAH patients
Number of cases	2065 ^b	225 ^b	52 ^b	50
Gender				
Male	1272	170	47	45
Female	793	55	5	5
Male/Female	1.60	3.09	9.40	9.00
Age				
Range	5–93	13–89	32–84	32–84
Average	57.4	57.7	58.5	58.9
Standard deviation	17.1	15.0	13.3	13.0
Median	60.0	59.0	57.5	57.5
Lesion location ^c				
Olfactory cleft		98	38	37
Ethmoid sinus		20	1	1
Sphenoid sinus		35	1	1
Sphenoethmoidal recess		60	4	4
Nasal septum		13	7	7
Other nasal cavity		33	8	7
Other paranasal sinuses		5	1	1
Number of patients	1667	212	50	50
Patients with multiple ESS	303	10	7	7
Number of multiple ESS	398	13	7	7
Multiple ESS rate	303/1667 (18.2%)	10/212 (4.7%)	7/50 (14.0%)	7/50 (14.0%)

Abbreviations: ESS, endoscopic sinus surgery; REAH, respiratory epithelial adenomatoid hamartoma.

^aHamartoma of the entire area and lesions of the olfactory area were histologically reviewed.

^bNumber indicates cases with pathology accession and includes multiple ESS for one patient.

^cA case often has specimens from multiple sites. Therefore, the number of lesions is greater than the number of cases.

57.7 years (SD 15.0, median 59.0, range 13–89) and the male/female ratio was 170/55 (3.09).

Histological specimens of these 225 cases were reviewed. One to eight location-labeled pathological specimens were submitted from each case. Nineteen cases were defined as a focal hamartomatous lesion or doubtful lesion, 52 as definite REAH, 12 as seromucinous hamartoma, and 11 as Schneiderian papilloma. Of the 52 pathologically identified cases of REAH (52/225 (23.6%) of histologically reviewed cases; 52/2065 (2.6%) of all ESS cases), 27 (51.9%) were unilateral and 25 (48.1%) were bilateral. Ten (19.2%) were isolated cases (REAH_i) and 42 (80.8%) were cases associated with sinonasal inflammatory polyps (REAH_{np}). REAH_{np} was associated with eosinophilic infiltration (28/42, 66.7%).

Among the 52 REAH cases, five showed widespread glandular epithelial atrophy associated with marked

thickening of basement membranes (Figure 2d). These five cases were all male and the average age was 53.4 years (range 32–72). Four of five cases were associated with inflammatory polyp with distinct eosinophilic infiltration (eosinophil count ≥ 70 /hpf). Three cases were clinically diagnosed with eosinophilic sinusitis and two with chronic sinusitis. Focal glandular epithelial atrophy (10%–20% of the lesion) was noted in 23 cases, and there was no glandular epithelial atrophy in 24 cases. Of the 98 cases of olfactory cleft polyps among the 225 cases, REAH was found in 38 (38.8%), and of the 19 focal hamartomatous lesion or doubtful cases, 10 were located in the olfactory cleft (52.6%). The male/female ratio in REAH cases was significantly higher than that in all ESS cases (47/5, 9.40 vs. 1272/793, 1.60, $p = 0.000007$).

The above data refer to cases based on pathological diagnosis, but one patient may have multiple

surgeries (that is, multiple diagnoses). To decrease the bias due to multiple ESS, duplication was analyzed using ID data. Among the 2065 ESS cases, 398 pathological diagnoses were from multiple ESS and 303 patients underwent ESS two or more times. The overall rate of multiple ESS was 303/(2065–398) (18.2%). Among the 225 cases, 13 pathological diagnoses were from multiple ESS and 10 patients underwent ESS two or more times. Among the 52 REAH cases, seven patients underwent ESS twice, and among these seven cases, two patients had two REAH surgeries; thus, the final number of patients with REAH was 50 (Table 1). The average age of 52 cases was 58.5 year old (SD 13.3, median 57.5, range 32–84), and male/female ratio was 47/5 (9.40). Olfactory cleft was the most frequent site (38/52, 73.1%), followed by other nasal cavity (8/52), nasal septum (7/52), and sphenoidal recess (4/52). Sixty lesional locations were observed in 52 cases. Among eight cases with multiple locations, three cases showed a REAH lesion straddling multiple regions (lesions within olfactory area such as a combination of olfactory cleft and sphenoidal

recess), and five cases showed REAH lesions most probably developing from multiple sites (e.g., olfactory area and other nasal cavity). The average age of 50 patients was 58.9 years (SD 13.0, median 57.5, range 32–84) and the male/female ratio was 45/5 (9.00). The rate of multiple surgeries in REAH patients (7/50) was significantly lower than that for all ESS patients (303/1667) (Fisher's exact probability test, $p = 0.034$). Of the 50 patients with REAH, 14 were clinically diagnosed with eosinophilic sinusitis, 37 with chronic sinusitis, and three with both eosinophilic and chronic sinusitis, while two had no sinusitis.

The number and rate of pathological diagnoses of REAH were calculated each year and for the first and last 7 years in the 14-year study period (Table 2). Initial and definite diagnoses were examined. As the initial diagnosis included focal hamartomatous lesions or doubtful cases, the number of definite REAH cases was smaller than that for initial diagnosis. The yearly rate of REAH ranged from 0.0% to 5.1%. The rate in the last 7 years (2015–2021) was significantly higher than that in the first 7 years (2008–2014) (38/1200 (3.17%) versus 14/865 (1.62%), Fisher's exact

TABLE 2 Pathological diagnosis of REAH by year and related factors

Year	Total ESS procedures	Initial diagnosis of REAH	Definite REAH	Rate (%) of definite REAH	Comparison of early and late periods	Olfactory cleft specimen sampled	Polyps or sinusitis with eosinophilic infiltration ^c
2008 ^a	48	1	0	0.0	2008–2014 Definite REAH 14/865 (1.62%)*	0	0
2009	118	1	0	0.0		0	2
2010	109	1	0	0.0		1	4
2011	147	5	4	2.7		3	1
2012	153	3	2	1.3		0	0
2013	139	4	3	2.2		3	0
2014	151	2	5	3.3		11	10
(Subtotal)	(865)	(17)	(14)	(1.62)	(18)	(17)	
2015	183	2	1	0.5	2015–2021 Definite REAH 38/1200 (3.17%)*	6	9
2016	204	12	8	3.9		13	26
2017	163	9	7	4.3		8	31
2018	204	12	5	2.5		15	25
2019	179	4	5	2.8		9	29
2020	156	5	8	5.1		10	38
2021 ^b	111	4	4	3.6		8	24
(Subtotal)	(1200)	(48)	(38)	(3.17)	(69)	(182)	
Total	2065	65	52	2.5		87	199

Abbreviations: ESS, endoscopic sinus surgery; REAH, respiratory epithelial adenomatoid hamartoma.

^aApril–December.

^bJanuary–September.

^cEosinophil count in pathology report started in 2015.

* $p = 0.032$.

probability test, $p = 0.032$). The number of olfactory cleft specimens in the last 7 years was significantly higher than that in the first 7 years (69/1200 [5.75%] vs. 18/865 [2.08%], $p < 0.001$; Table 2). Eosinophil count in pathology reports started in 2015, and pathological diagnosis of inflammatory polyps or chronic sinusitis associated with eosinophilic infiltration in the last 7 years was significantly higher than that in the first 7 years (182/1200 [15.2%] vs. 17/865 [2.0%], $p < 0.001$; Table 2).

Histopathological findings were compared among cases with REAH, inverted Schneiderian papilloma and inflammatory polyp (Figures 2 and 3; Table 3). REAH cases ($n = 52$) showed no neutrophilic infiltration in the lesional epithelium, and mild intra-epithelial eosinophilic infiltration in 20/52 cases. The basement membrane

around the glands was thickened ($n = 52$, $9.56 \pm 2.38 \mu\text{m}$, range 2.78–14.99 μm), and was slightly thicker than that of inflammatory polyp ($n = 25$, $6.92 \pm 3.28 \mu\text{m}$, range 0.0–15.9 μm , $p = 0.001$) and significantly thicker than that of inverted papilloma ($n = 25$, $1.31 \pm 1.64 \mu\text{m}$, range 0.0–5.1 μm , $p < 0.001$). Thickness of the basement membrane did not show annual changes such as increased thickness in recent cases. Inverted Schneiderian papilloma (Figure 2g,h) showed inversions of the surface epithelium composed of squamous and/or respiratory epithelium. Infiltration of neutrophils into the epithelium was observed in all cases (25/25), and was prominent in squamous epithelium. Mild intra-epithelial eosinophilic infiltration was found in 4/25 cases. The basement membrane was not thickened in most cases. Inflammatory polyp (Figure 2i,j) showed a small number of inverted respiratory epithelium in the edematous stroma. Neutrophilic infiltration was not observed in the epithelium, and slight eosinophilic infiltration was noted in 5/25 cases. The basement membrane was thickened.

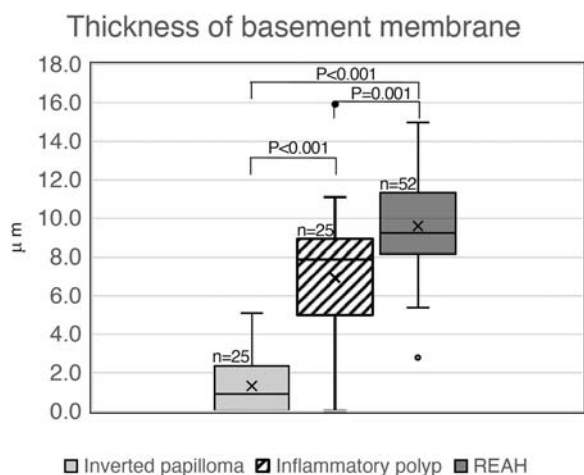


FIGURE 3 Thickness of the basement membrane in inverted Schneiderian papilloma, inflammatory polyp and respiratory epithelial hamartoma (REAH). Most inverted Schneiderian papillomas showed no thickening, but inflammatory polyp and REAH showed marked thickening of the basement membrane.

DISCUSSION

This study of 52 cases (50 patients) is among the largest scale studies of REAH. Safi et al.¹⁰ summarized a total of 441 REAH cases from 1995 to 2017, excluding single case reports, and among the studies included, only those of Vira et al.¹¹ and Lee et al.¹² had more than 50 REAH cases.

Pathological diagnosis of typical REAH is not difficult if the following criteria are applied:⁴ (i) polypoid lesions with a smooth surface and elastic firm consistency; (ii) proliferation of small to medium-sized glands in direct continuity with the surface epithelium; (iii) glands composed of ciliated respiratory epithelium often containing goblet cells; and (iv) thickening of the

TABLE 3 Histopathological characteristics of REAH and other lesions

Item	REAH	Inverted Schneiderian papilloma	Inflammatory polyp
Number of measured cases	52 (52) ^a	25 (43) ^a	25 (577) ^a
Age (mean \pm SD)	58.5 \pm 13.3 (58.5 \pm 13.3) ^a	63.7 \pm 10.8 (66.0 \pm 11.4) ^a	58.9 \pm 15.4 (55.0 \pm 15.5) ^a
Age range	32–84 (32–84) ^a	46–90 (43–90) ^a	15–89 (9–92) ^a
Male/Female	47/5 (47/5) ^a	16/9 (30/13) ^a	20/5 (424/153) ^a
Basement membrane thickness (μm)			
Mean \pm SD	9.56 \pm 2.38	1.31 \pm 1.64	6.92 \pm 3.28
Range	2.78–14.99	0–5.09	0–15.92
Intra-epithelial neutrophils	0/52	23/25	0/25
Intra-epithelial eosinophils	20/52	4/25	5/25

Abbreviation: REAH, respiratory epithelial adenomatoid hamartoma.

^aData of total cases are indicated in parentheses.

basement membrane. However, in the current study, there were many atypical cases that lacked goblet cells or thickening of the basement membrane. In addition, if the lesions were too small, they could not be identified as REAH. These focal or doubtful cases were finally excluded, but more than half of the excluded cases (10/19) were located in olfactory clefts, and thus, these atypical cases may also imply the presence of true REAH.

Inverted Schneiderian papilloma most frequently occurs in the nasal cavity and the maxillary sinus, showing a nontranslucent mulberry-like gross appearance. Histologically, multiple inversions of the surface epithelium composed of squamous and/or respiratory epithelium with infiltration of neutrophils into the epithelium are typical features of this lesion.¹³ The thickness of the basement membrane has not been mentioned in the literature. Our findings clearly showed that the basement membrane is not thickened in most cases of inverted papilloma.

In the first report of REAH, Wenig described locations in the posterior nasal septum, other nasal cavities, ethmoid sinus, and frontal sinus.² In subsequent studies, it became clear that the olfactory cleft is the most common site of origin,¹⁴ and a radiological study of REAH showed widening of olfactory clefts on computed tomography.¹⁵ The olfactory cleft was the most frequent site of REAH (37/50, 74%) in the current study, but there was also occurrence in other nasal cavities (7/50) and in the nasal septum (7/50) and sphenoidal recess (4/50). If the olfactory cleft, nasal septum and sphenoidal recess are collectively viewed as the "olfactory area," then the olfactory area is the predominant site of REAH.

In addition to REAH, hamartomatous lesions such as seromucinous hamartoma¹ and chondro-osseous hamartoma have been reported.^{16,17} Seromucinous hamartomas, but not chondro-osseous hamartoma, were found in this study. Kossai et al.¹⁸ introduced "olfactory epithelial hamartoma" as a new subtype of sinonasal hamartoma, which may have been included in REAH. In the definitions of respiratory and olfactory mucosa suggested by Kern,¹⁹ olfactory mucosa has no goblet cells, a thin basement membrane, irregular cilia, cellular lamina propria and numerous large nerve bundles. Kossai et al.¹⁸ found that some of the apical cells had small globular intraluminal protrusions at the luminal pole, probably representing an olfactory vesicle, which is also mentioned by Escada²⁰ based on an autopsy study of olfactory mucosa distribution. In the current study, we searched for olfactory epithelial components in hamartomatous lesions, but all hamartomas had numerous goblet cells, thickening of the basement membrane and evenly distributed cilia, and olfactory vesicles were not observed.

We found that the annual rate of REAH among all ESS cases increased from 1.62% to 3.25% from the

early to late 7-year periods of the current study, and we initially hypothesized that improved recognition of REAH by pathologists may be the main cause of this increase. However, as all the histopathological specimens of the olfactory area were microscopically reviewed in this study, the increase of pathological diagnosis of REAH seems not to be due to recognition of this lesion by pathologists, but to a true increase of the incidence of REAH.

Reasons for the increase of REAH were considered. We realized there was a modification of ESS procedure in our hospital. Until 2013, a microdebrider, which cuts and removes the tissue during ESS,²¹ was initially used to open the obstructed areas including olfactory clefts, and histopathological specimens were sampled later. Since 2014, if olfactory cleft lesions were clinically suspected, histopathological specimens were sampled before the use of a microdebrider. Since then, the number of olfactory cleft specimens has increased (2008–2014, 18 cases; 2015–2021, 69 cases). This seems to be the major factor of increased incidence of REAH. Lorentz et al.¹⁴ suggested that an increasing number of cases of REAH are being identified, mainly due to improved clinical recognition. Our present study supports their idea.

Eosinophilic chronic rhinosinusitis is a subgroup of chronic rhinosinusitis with nasal polyps. In Japan and East Asia, the incidence of eosinophilic chronic rhinosinusitis is increasing, but the reason is unknown.²² Dysosmia and olfactory cleft polyps are characteristics of eosinophilic chronic rhinosinusitis,²² which implies the link between REAH and eosinophilic chronic rhinosinusitis. In our study, pathological diagnosis of inflammatory polyps or chronic sinusitis associated with eosinophilic infiltration increased in recent years (2008–2014, 17 cases; 2015–2021, 182 cases), but these data may simply reflect the fact that eosinophil count in pathology reports has started since 2015 as a diagnostic criterion of eosinophilic chronic rhinosinusitis in Japan.⁸ Further studies are needed to clarify the true relationship between REAH and eosinophilic chronic rhinosinusitis.

Respiratory epithelial hamartoma is known to occur in association with sinonasal inflammatory polyps.^{4,15} In a systemic review of 441 patients with REAH by Safi et al.,¹⁰ the rate of isolated REAH (REAHi) was 34.9% and that of REAH with concurrent nasal polyposis (REAHnp) was 50.1%. In the current study, 84% of REAH cases were REAHnp, and 67% of REAHnp cases showed distinct eosinophilic infiltration (eosinophil count ≥ 70 /hpf). These data suggest that REAH is strongly linked to sinonasal inflammatory polyp with eosinophilic infiltration. The presence of numerous tissue eosinophils (≥ 70 /hpf) is associated with recurrence of chronic rhinosinusitis.⁸ The current study also indicated clinical diagnosis of eosinophilic sinusitis in 14/50 patients and chronic sinusitis in 37/50 patients. Thus, under-recognition of REAH in surgical pathology

may be due to the concurrent presence of typical sinonasal inflammatory polyps in specimens, which show similar thickening of the basement membrane to that found in REAH in this study.

Safi et al. found a recurrence rate of REAH of 4.1% in a follow-up period ranging from 4 months to 5 years.¹⁰ In the current study, repeated surgery in our hospital was analyzed. Among the 50 REAH patients, recurrence of REAH was observed in two patients (4.0%). This recurrent rate was similar to that of Safi et al.¹⁰

It is generally believed that hamartomas are benign lesions without malignant change, but there are some exceptions, such as carcinomas arising in the dermal nevus sebaceus of Jadassohn.²³ Ozolek and Hunt²⁴ showed that REAH has an intermediate fractional allelic loss of 31% compared with sinonasal adenocarcinoma (64%) and chronic sinusitis (2%), which suggests that REAH may have a neoplastic nature. Also, REAH and low-grade tubulopapillary adenocarcinoma share a similar immunohistochemical pattern of positive for CK7/MUC1 and SOX10.²⁵ A case of adenocarcinoma arising from seromucinous hamartoma was recently reported²⁶ and low-grade adenocarcinoma has also been associated with REAH.²⁷ In the current study, no malignant transformation was identified, but follow up of REAH is recommended.

Our clinicopathological data in Japanese patients were almost identical to those in overseas studies, including age, location, bilaterality, and association with inflammatory polyp. Male predominance was found in the first report of REAH by Wenig,² but many subsequent studies found no gender difference, as shown in Tables 2 and 3 of Safi et al.¹⁰ However, our study clearly showed male predominance (male/female = 45/5).

The incidence of REAH found in this study shows that it is a relatively common disease in Japan. A whitish rubbery firm appearance of gross specimens, thick basement membrane and the absence of intraepithelial neutrophilic infiltration are highly suggestive for a diagnosis of REAH. Recognition of this lesion and a clinical and pathological diagnosis are important for appropriate care of patients.

AUTHOR CONTRIBUTIONS

Study conception and design: Masamichi Goto and Mitsuharu Nomoto. *Clinical data collection and analysis:* Kengo Nishimoto and Tsutomu Matsuzaki. *Pathological data collection and analysis:* Masamichi Goto, Yasuyo Jougasaki and Mitsuharu Nomoto. *Drafting the manuscript and figures:* Masamichi Goto. *Reviewing and revising the manuscript:* Mitsuharu Nomoto, Kengo Nishimoto and Tsutomu Matsuzaki. *Final approval of the manuscript:* All authors.

CONFLICT OF INTEREST

None declared.

ORCID

Masamichi Goto  <http://orcid.org/0000-0003-0943-4115>

REFERENCES

1. Baillie EE, Batsakis J. Glandular (seromucinous) hamartoma of the nasopharynx. *Oral Surg Oral Med Oral Pathol.* 1974;38:760–2.
2. Wenig B, Heffner D. Respiratory epithelial adenomatoid hamartomas of the sinonasal tract and nasopharynx: a clinicopathologic study of 31 cases. *Ann Otol Rhinol Laryngol.* 1995;104:639–45.
3. Wenig B. Respiratory epithelial adenomatoid hamartoma. In: Barnes L, Eveson JW, Reichart P, Sidransky D, editors. *Pathology and genetics of head and neck tumours.* Lyon: IARC Press; 2005:33.
4. Wenig B, Franchi A, Ro J. Respiratory epithelial adenomatoid hamartoma. In: El-Naggar AK, Chan JKC, Grandis JR, Takata TSP, editors. *WHO classification of head and neck tumours.* Lyon: IARC Press; 2017. p. 31–2.
5. Akiyama K, Samukawa Y, Hoshikawa H. Olfactory cleft polypoid and respiratory epithelial adenomatoid hamartoma in eosinophilic chronic rhinosinusitis. *Int Forum Allergy Rhinol.* 2020;10:1337–9.
6. Endo R, Matsuda H, Takahashi M, Hara M, Inaba H, Tsukuda M. Respiratory epithelial adenomatoid hamartoma in the nasal cavity. *Acta Otolaryngol.* 2002;122:398–400.
7. Nomura K, Oshima T, Maki A, Suzuki T, Higashi K, Watanabe M, Kobayashi T. Recurrent chondro-osseous respiratory epithelial adenomatoid hamartoma of the nasal cavity in a child. *Ear Nose Throat J.* 2014;93:E29–31.
8. Tokunaga T, Sakashita M, Haruna T, Asaka D, Takeno S, Ikeda H, et al. Novel scoring system and algorithm for classifying chronic rhinosinusitis: The JESREC Study. *Allergy Eur J Allergy Clin Immunol.* 2015;70:995–1003.
9. Kanda Y. Investigation of the freely available easy-to-use software “EZR” for medical statistics. *Bone Marrow Transplant.* 2013;48:452–8.
10. Safi C, Li C, Tabaei A, Ramakrishna R, Riley CA. Outcomes and imaging findings of respiratory epithelial adenomatoid hamartoma: a systematic review. *Int Forum Allergy Rhinol.* 2019;9:674–80.
11. Vira D, Bhuta S, Wang MB. Respiratory epithelial adenomatoid hamartomas. *Laryngoscope.* 2011;121:2706–9.
12. Lee JT, Garg R, Brunworth J, Keschner DB, Thompson LDR. Sinonasal respiratory epithelial adenomatoid hamartomas: series of 51 cases and literature review. *Am J Rhinol Allergy.* 2013;27:322–8.
13. Hunt J, Bell D, Sarioglu S. Sinonasal papillomas. In: El-Naggar A, Chan J, Grandis J, Takata T, editors. *WHO classification of head and neck.* 2017. p. 28–31.
14. Lorentz C, Marie B, Vignaud JM, Jankowski R. Respiratory epithelial adenomatoid hamartomas of the olfactory clefts. *Eur Arch otorhinolaryngol.* 2012;269:847–52.
15. Hawley KA, Ahmed M, Sindwani R. CT findings of sinonasal respiratory epithelial adenomatoid hamartoma: A closer look at the olfactory clefts. *Am J Neuroradiol.* 2013;34:1086–90.
16. Fedda F, Boulos F, Sabri A. Chondro-osseous respiratory epithelial adenomatoid hamartoma of the nasal cavity. *Int Arch Otorhinolaryngol.* 2013;17:218–21.
17. Fleming KE, Perez-Ordoñez B, Nasser JG, Psooy B, Bullock MJ. Sinonasal seromucinous hamartoma: a review of the literature and a case report with focal myoepithelial cells. *Head Neck Pathol.* 2012;6:395–9.
18. Kossai M, El Zein S, Wassef M, Guichard J-P, Pouliquen C, Herman P, et al. Olfactory epithelial hamartoma: a new subtype of sinonasal hamartoma. *Am J Surg Pathol.* 2018;42:9–17.

19. Kern RC. Chronic sinusitis and anosmia: pathologic changes in the olfactory mucosa. *Laryngoscope*. 2000;110:1071–7.
20. Escada P. Localization and distribution of human olfactory mucosa in the nasal cavities. *Acta Med Port*. 2013;26:200–7.
21. Tang D, Lobo BC, D'Anza B, Woodard TD, Sindwani R. Advances in microdebrider technology: improving functionality and expanding utility. *Otolaryngol Clin North Am*. 2017;50:589–98.
22. Fujieda S, Imoto Y, Kato Y, Ninomiya T, Tokunaga T, Tsutsumiuchi T, et al. Eosinophilic chronic rhinosinusitis. *Allergol Int*. 2019;68:403–12.
23. Mitchell DC, Kuehn GJ, Scott GA, Doerr TD, Tausk F. A rare case of porocarcinoma and trichoblastoma arising in a nevus sebaceus of Jadassohn. *Case Rep Dermatol Med*. 2021;2021:3–5.
24. Ozolek JA, Hunt JL. Tumor suppressor gene alterations in respiratory epithelial adenomatoid hamartoma (REAH): comparison to sinonasal adenocarcinoma and inflamed sinonasal mucosa. *Am J Surg Pathol*. 2006;30:1576–80.
25. Baněčková M, Michal M, Laco J, Leivo I, Ptáková N, Horáková M, et al. Immunohistochemical and genetic analysis of respiratory epithelial adenomatoid hamartomas and seromucinous hamartomas: are they precursor lesions to sinonasal low-grade tubulopapillary adenocarcinomas? *Hum Pathol*. 2020;97:94–102.
26. Rengifo DA, Varadarajan VV, Lai J, Justice JM. Transformation from sinonasal seromucinous hamartoma to adenocarcinoma: a case report. *ORL*. 2021;83:478–80.
27. Jo VY, Mills SE, Cathro HP, Carlson DL, Stelow EB. Low-grade sinonasal adenocarcinomas: the association with and distinction from respiratory epithelial adenomatoid hamartomas and other glandular lesions. *Am J Surg Pathol*. 2009;33:401–8.

How to cite this article: Goto M, Nishimoto K, Jougasaki Y, Matsuzaki T, Nomoto M. Respiratory epithelial adenomatoid hamartomas of the sinonasal tract: a histopathological analysis of 50 patients. *Pathol. Int.* 2022;72:541–549.
<https://doi.org/10.1111/pin.13271>

LETTER TO THE EDITOR

BRAF N581S and NRAS Q61R-mutated malignant melanoma and sensitivity to BRAF/MEK inhibitors

Dear Editor,

A 65-year-old man was referred to our hospital for a 20-mm melanocytic lesion on the chest that developed approximately 1 year ago. Wide resection and sentinel lymph node biopsy revealed atypical melanin-containing large cells infiltrating the deep dermis with lymphatic invasion, a tumor thickness of 4.6 mm, and metastatic cells in all lymph nodes from both axillae (Figure 1a,b). Thus, the patient was diagnosed with malignant melanoma (stage IIID, pT4bN3cM0). Bilateral axillary lymph node metastases were observed after adjuvant therapy with pembrolizumab for 10 months. Thereafter, the patient underwent bilateral axillary lymph node dissection and postoperative radiation therapy and received systemically administered pembrolizumab plus local interferon-beta injection in accordance with safety tests.¹ However, the subcutaneous metastases extended, and the patient was administered a combination of ipilimumab and nivolumab twice. Subsequently, the patient developed

immune-related pneumonitis; thus, the treatment was discontinued. Cancer multigene panel testing was performed for the cutaneous metastatic lesion. The Tumor Mutation Burden was 5.04 Muts/Mbp, microsatellite instability was stable, and BRAF p.N581S and NRAS p.Q61R were actionable genetic abnormalities. Hence, BRAF/MEK inhibitors (dabrafenib plus trametinib) were prescribed off-label after discussions with the patient, specialist geneticists, and oncologists. After 2 months of treatment, the subcutaneous metastasis in the axilla shrunk, and the resectable frontal chest tumor was removed under general anesthesia. Stable disease was determined according to RECIST v1.1 (Figure 1c-f).

This is the first case of BRAF N581S mutation-positive melanoma with favorable results using BRAF/MEK inhibitors. Previously, one patient with BRAF N581S mutation-positive non-small cell lung cancer was reported to achieve 33-month partial response with BRAF/MEK inhibitors combination therapy² BRAF mutations have >200 alleles

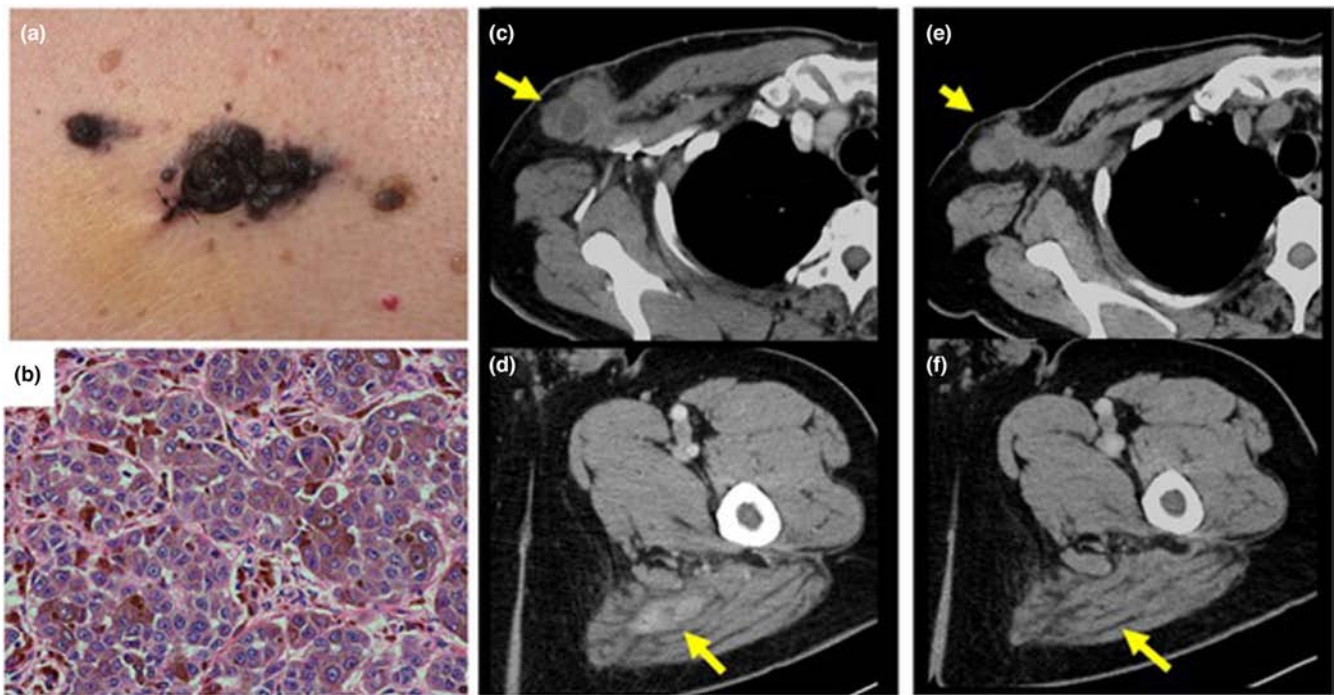


FIGURE 1 (a) Clinical features at initial examination. A dark brown nodule of approximately 20 mm in size, with an undefined border, and ulceration was visible on the chest. (b) Pathology. Atypical melanin-containing large cells infiltrating the deep dermis with lymphatic invasion. The tumor thickness was 4.6 mm and all lymph nodes from both axillae had metastatic cells. The magnification of figure is 200x. (c, d) computed tomography images obtained immediately before administration of the BRAF/MEK inhibitors. Enlarged metastases in the right axilla, which was adherent to the axillary artery, and in the femoral muscle were detected. (e, f) computed tomography images obtained 2 months after BRAF/MEK inhibitors administration. The axillary lymph nodes and femoral muscle metastases were smaller.

and are classified into three classes according to their mode of action: *BRAF* V600 mutations are classified as class 1, RAS-independent mutations are classified as class 2, and mutations enhancing binding to RAS and CRAF kinases and promoting Ras-dependent signaling are classified as class 3, including *BRAF* N581S mutation.³ A next-generation sequencing study of 446 melanoma cases reported *BRAF* mutations in 42% of cases; 77% were class 1, 7.4% were class 2, and 12% were class 3. Melanomas with class 3 mutations were often detected in the head, neck, or upper back and were chronic in elderly patients. Chronic sunlight exposure is assumed a contributing factor. Since *BRAF* inhibitors preferentially inhibit activated *BRAF* monomers (V600 mutants), they are unlikely to suppress ERK signaling in class 3 mutant-driven tumors. MEK inhibitors are believed to amplify ERK signaling in the tumor and inhibit tumor cell growth.⁴ Furthermore, class 3 *BRAF* mutations in melanomas are often associated with RAS mutations.⁴ Moreover, the MEK inhibitor binimetinib prolongs the progression free survival of malignant melanomas with *NRAS* and *BRAF* class 3 mutations with even greater efficiency than dacarbazine.⁵ Supported by the positive results obtained in our case, patients with malignant melanomas harboring class 3 *BRAF* mutations may benefit from the combination of *BRAF*/MEK inhibitors. Moreover, cancer multigene panel testing can be valuable for exploring alternative treatments for advanced melanoma following standard treatment failure.

CONFLICT OF INTEREST

The authors have no conflicts to declare.

Natsuko Sasaki-Saito^{1,2}

Kentaro Yamamura¹

Taiyo Hitaka¹

Yui Hirano¹

Katsuhiko Nishihara¹

Megumi Aoki¹

Shigeto Matsushita¹

¹Department of Dermato-Oncology/Dermatology, National Hospital Organization Kagoshima Medical Center, Kagoshima, Japan

²Department of Dermatology, University of Occupational and Environmental Health, Kitakyushu, Japan

Correspondence

Shigeto Matsushita, Department of Dermato-Oncology/Dermatology, National Hospital Organization Kagoshima Medical Center, 1-8, Shiroyama-cyo, Kagoshima 892-0853 Kagoshima, Japan.

Email: shigeto0302@gmail.com

ORCID

Natsuko Sasaki-Saito <https://orcid.org/0000-0001-6122-8429>

Kentaro Yamamura <https://orcid.org/0000-0003-1614-591X>

Katsuhiko Nishihara <https://orcid.org/0000-0002-3801-4278>

Shigeto Matsushita <https://orcid.org/0000-0003-2001-5341>

REFERENCES

1. Fujimura T, Hidaka T, Kambayashi Y, Furudate S, Kakizaki A, Tono H, et al. Phase I study of nivolumab combined with IFN- β for patients with advanced melanoma. *Oncotarget*. 2017;8:71181–7.
2. Liu Y, Zeng H, Wang K, Li Y, Tian P, Li W. Acquired *BRAF* N581S mutation mediated resistance to gefitinib and responded to dabrafenib plus trametinib. *Lung Cancer*. 2020;146:355–7.
3. Lokhandwala PM, Tseng LH, Rodriguez E, Zheng G, Pallavajjala A, Gocke CD, et al. Clinical mutational profiling and categorization of *BRAF* mutations in melanomas using next generation sequencing. *BMC Cancer*. 2019;19:665.
4. Yao Z, Yaeger R, Rodrik-Outmezguine VS, Tao A, Torres NM, Chang MT, et al. Tumours with class 3 *BRAF* mutants are sensitive to the inhibition of activated RAS. *Nature*. 2017;548:234–8.
5. Dummer R, Schadendorf D, Ascierto PA, Arance A, Dutriaux C, di Giacomo AM, et al. Binimetinib versus dacarbazine in patients with advanced *NRAS*-mutant melanoma (NEMO): a multicentre, open-label, randomised, phase 3 trial. *Lancet Oncol*. 2017;18:435–45.

CARDIOVASCULAR FLASHLIGHT

<https://doi.org/10.1093/eurheartj/ehac498>
 Online publish-ahead-of-print 14 September 2022

3D-rendered computed tomography imaging support the diagnosis and strategic decision-making: a rare case of acute pulmonary thromboembolism presenting with thrombus straddling a patent foramen ovale

Chika Matsushita *, Mahoto Inatsu, and Hideki Tanaka

Department of Emergency, National Hospital Organisation Kagoshima Medical Center: Kokuritsu Byoin Kiko Kagoshima Iryo Center, 8-1, Shiroyama-cho, Kagoshima-shi, Kagoshima 892-0853, Japan

*Corresponding author. Tel: +81 992231151, Email: sen.1826.hana@gmail.com

A 63-year-old man with hypertrophic cardiomyopathy was transferred to our hospital for investigation of swollen left lower limb and gradual development of dyspnoea in the last few days. Venous echography showed blood clots in the left femoral vein. Transthoracic echocardiography (TTE) showed dilated right heart cavities, pulmonary hypertension estimated at 50 mmHg and snake-shaped thrombus with flipping movement across atrioventricular valves with cardiac cycle in each individual left (Panel A, Supplementary material online, Video S1) and right atrium (Panel B, Supplementary material online, Video S2). As the reason for poor TTE-acoustic window, the spatial relationship and continuity of the both atrial thrombi were not clearly depicted. A spiral computed tomography (CT) scan showed bilateral intra-atrial filling defect (Panel C) as well as intramural filling defect in pulmonary arteries (Panel D). Prompt 3D-rendered imaging reconstruction revealed a long thrombus caught in transit across a patent foramen ovale (PFO; Panel E, Supplementary material online, Video S3). Urgent decision for open-chest surgery was made to prevent additional adverse effect to both pulmonary and systemic circulation. Surgical removal of clots in both atria and pulmonary arteries with direct suturing of a PFO was completed uneventfully (Panel F). This is the first report of informative assessment of a thrombus straddling a PFO by use of 3D-rendered CT imaging.

The data underlying this article are available in the article and in its Supplementary material online.

Supplementary material is available at *European Heart Journal* online.

The authors thank Hideaki Yamaguchi (Radiologist) for technical assistance with reconstruction of 3D-rendered CT imaging.

This research did not receive any specific grant from funding agencies in the public, commercial, or not-for-profit sectors.

The authors have submitted their declaration which can be found in Supplementary material online.

